

Thesis for the degree of MSc in Marine Technology in specialization of
Marine Engineering

A Digitised Exploration into the Design Space of Naval Power Plants

By

T.A.R. de van der Schueren

Performed at

Nevesbu

This thesis MT.21/22.014.M. is classified as confidential in accordance with
the general conditions performed by the TU Delft

January 24, 2022

Company Supervisor

Responsible Supervisor Ir. S.A.Los
E-mail S.A.Los@nevesbu

Thesis Exam Committee

Chair/Responsible Professor	Rear-Admiral (ret.) Ir. K. Visser	Faculty 3mE, TU Delft
Staff Member	Dr. Ir. P. de Vos	Faculty 3mE, TU Delft
Staff Member	Dr. B. Atasoy	Faculty 3mE, TU Delft
Staff Member	Dr. M. Lourenço Baptista	Faculty AE, TU Delft
Company Member	Ir. S.A. Los	Nevesbu

Author details

Study Number 4375823
E-mail Tom.Schueren@hotmail.com

Preface

My passion for optimisation can be traced back to when I was younger, playing board and computer games. My favourite games were always strategy games, figuring out the best ways to crush my opponents, which were usually my little sisters. At a later age, I came to realise that this desire to win stretched further than just games and also entailed a love for mathematics and applied physics, resulting in a study Marine Technology. Within this study, my attention was drawn to Marine Engineering for its tangibility and problem solving mindset. Combining optimisation problems and Marine Engineering in one thesis is thus the perfect combination. So without further ado, let's get started.

Before you lies the thesis "A Digitised Exploration into the Design Space of Naval Power Plants", part of the final assessment for the degree Master of Science in Marine Technology within the specialization Marine Engineering at Delft University of Technology. The subject is the exploration of the design space of naval surface vessels via a concept exploration tool.

This research has been performed at Nevesbu, in Alblasterdam, The Netherlands. Nevesbu is a naval architecture and marine engineering company with great expertise in naval vessels. I would like to thank Nevesbu and its employees for the opportunity to conduct my thesis with them. A special word of gratitude naturally goes to my supervisor Sven Los, not only for guiding me through this project, but also for being a sounding board for my frustration and a sparring partner for my ideas. Another word of gratitude must be given to Jitte van Dijk, for providing me with a foundation to build on and for brainstorming about the challenges and solutions found along the way.

Furthermore, I would like to extend my thankfulness to my exam committee, for taking the time to evaluate and grade my work. More specifically, I would like to thank Klaas Visser for his feedback during our sessions and, of course, Peter de Vos, for not only being my supervisor during this project, but also for being an employer, colleague and teacher during my studies. I remember a comment made by Peter during my board year, while discussing the legacy of Vulcanus:

"With some students you can see from a mile away that they will become marine engineers."

I don't know if I fitted that picture back then, but I like to think I do now.

Moreover, I would like to express my appreciation to everyone I met during my study period and that had a positive influence on the person I am today. Friends, former and current housemates, my board members, fellow students, colleagues, teachers, and all others: Thank you! Specifically, I am thankful for Patrick for helping me with the lay-out of this thesis and for nothing else, don't go feeling special now.

Finally, I am grateful to my parents and to Annika and Lotte. Pappa, mamma, thank you for all the love and support I have received from day one till now. Growing up, I have come to realise how fortunate I have been all my life, with you as my parents. Never having to worry about anything and knowing you will always be there for me. I hope I did not put too much stress on you during my studies, but worry no more, I have made it! An, Lot, thank you for sharing your childhood with me and for making some of the most amazing memories together. I am glad we have had our childish fights in the past and that we can laugh about them now. Luckily, we have held on to some of our sibling rivalries, even though I am no longer on the winning end of most of them (was I ever?). Thank you for being my little sisters and letting me your the big brother, but more importantly, thank you for letting me win a game from time to time...

Tom de van der Schueren

Delft, January 2022

Summary

The drive for more economical and sustainable sailing is widely known within commercial shipping, yet similar focus is not found in the development of naval surface vessel. Meanwhile, most countries, including The Netherlands, have put sustainability on the agenda for their armed forces. These recent emission policies in combination with the availability of new low emission components from commercial shipping will likely drive the application of state-of-the-art technologies in power plants on naval surface vessels. With the availability of new techniques comes the possibility to experiment with alternative and unique power plant configurations. A challenge that arises with all these possible configurations, is the number of concepts that can be considered. As a result, the contemplated design space has grown significantly, resulting in a design space too large for a human design team to evaluate.

A concept exploration tool is introduced as a possible solution. It facilitates the users in exploring the full design space, by generating and evaluating every concept within said space. In this context, a concept is defined as a unique set of components within a predefined topology, where only main components of a power plant are considered. The evaluation uses a mission profile in terms of power demand to simulate the performance of all components. A score is given to each configurations based on a multi criteria analysis. Key performance indicators of a concept are defined based on the operations of the power plant and preference of the client. All in all, it can be said that a concept exploration tool enables a new design philosophy, where constraints are kept to a minimum and decisions are based on quantified measurements of the concepts.

A concept exploration tool for commercial vessel has already been developed. This tool is not directly applicable to naval vessels, since the employed client preference are solely commercially focused and certain commonly utilised naval components are missing. Therefore, a new is tool developed where the signatures and the robustness of the power plant are added as naval preferences, along side the existing preferences for efficiency, emissions, volume and mass. Moreover, controllable pitch propellers, gas turbines and a solid-oxide fuel cells are included in the tool. Furthermore, the computational time is decreased significantly to increase the practical usability of the tool.

A brute force search algorithm is applied to explore the complete design space. This means that all possible solution must be generated and evaluated. Due to the complexity of a power plant, this would result in an unmanageable number of concepts. Therefore constraint are implemented, both in the generation phase, as well as in the evaluation phase. All considered configurations are generated with a building algorithm that ensure only feasible combinations of components are constructed. During the evaluation phase, the components are installed into a power plant, after which a mission is simulated to study the overall performance of the power plant. Lastly, a ranking of concepts and a visualisation of the design space is produced by the tool.

Three case studies have been conducted to analyse the workings of the concept exploration tool. The case studies are based on an existing frigate, offshore patrol vessel and fast offshore patrol vessel. The case study showed a significant preference for configurations with electric motors and solid-oxide fuel cells. This dominance is a result of the high efficiency of such configurations having a ripple effect on other key performance indicators. A similar notable result could be found in the combination of a controllable pitch propeller and an electric motor. A sensitivity analysis showed that the preferences of a client have a significant effect on the optimal concept. Furthermore, the computational time has been decreased with a factor 200 to 500 compared to the previous concept exploration tool. This shows the practical potential of this tool.

In conclusion, the concept exploration tool is able to generate and evaluate thousands of varying concepts and choose an optimal configuration based on the preference of the client. In addition, the tool can give an insight into the design space the design team is working in. This visualisation may be of added value

to the design team when searching for trends, outliers or comparable concepts. Moreover, the output on concept level gives a design team a starting point for the rest of the design process and facilitates the comparison between different configurations based on quantified calculations. This may empower the human design team in their decision making for the rest of the design process. However, this research also showed that, even though computers are utilised, the limits of a workable design space can quickly be reached, especially when the run time must be minimised for practical applications. All in all, it can be concluded that a concept exploration tool enables design teams to explore larger power plant design spaces within a practical time frame. However, constraints must still be implemented to keep the size of the design space manageable.

Improvements can be made to the model structures and optimisation algorithms, to further unconstrain the design space. As a result, more concepts could be explored. For example, the usefulness of the tool can be significantly increased by including sub-systems into the model. Furthermore, it is recommended to investigate various model structures that enable a certain level of plug-and-play coding, ensuring that new model parts can be added in the future. Specifically, attention could be paid to multi-stage exploration tool. Due to the dominance of the electric motor in combination with a solid-oxide fuel cell, additional feasibility studies into solid-oxide fuel cells are encouraged. The same applies to the combination of a controllable pitch propeller and an electric motor.

Contribution of this Thesis

This research succeeded in developing a concept exploration tool that is capable of exploring the design space of power plants of naval surface vessels within a practical time frame. The aim of this thesis was to find a way to help engineers choose the optimal naval power plant configuration in the concept design phase. This is necessary, as the design space of naval power plants has become too large to be evaluated by humans. As a result, sub-optimal and conservative concepts may be produced.

For this study, a bridge was constructed between Marine Engineering, optimisation theory and practical usability. In previous research, the gap between any two of these pillars was investigated. Various examples can be found of Marine Engineering optimisation tools that are not used by the industry, optimisation tools found in the industry that do not cover Marine Engineering or practical Marine Engineering models that do not involve optimisation theory. Thus, combining all three subjects into one solution is new. The result is a tool that takes the theoretical knowledge of optimisation theory and Marine Engineering and converts it to a usable product for the industry. This goes a step further than most research, as the practical usability was a key factor during the implementation of the model. Moreover, it goes a step deeper than most tools applied by the industry, as it does not just solve a problem, but it helps the designers in their design choices.

The developed tool is capable of generating and evaluating thousands of concepts within minutes. Since the practical usability was a key factor in this development, choice were made to ensure a manageable run time. This is a different approach compared to most research, where computational speed can be of minor importance. The main motivations behind this approach is that a unused tool serves no function. There is a wealth of knowledge and information in the scientific world that is left untouched by the marine industry, as the implementation is inconvenient or not user-friendly. This thesis shows that that gap can be bridge, when the focus is somewhat shifted to the practical applications of the theory. It is a next step in applying digitised optimisation models to the practical industry of Marine Engineering.

The scientific impact of this study is a model that can explore the design space of power plants of naval surface services vessels. Furthermore, a sizing and performance model is developed for gas turbines and solid oxide fuel cells. Moreover, an existing power management strategy has been improved and a robustness tool has been implemented into a broader model. Hopefully, this is the beginning of future research into digitised optimisation methods within the industry of Marine Engineering. The impact on the industry is the possibility to quickly explore thousands of concept and visualise the design space. This visualisation gives a new dimension to the design process, as it shows the designers the number and location of all other concepts within the design space. In addition, it enables the designers to quickly evaluate the effects of changes to the client preferences on a given design. The societal impact can be found in the actual optimisations of the power plants. Once tools like this are commonly applied, it may lead to more efficient and less polluting vessels and it may guide users in the exploration of alternative propulsion methods.

Despite the progress that has been made in this thesis, a significant amount of research can still be done. The explored design space is still fairly constrained, due to the limitations of the computation time. Better model structures and algorithms could be developed to explore the design space more efficiently, resulting a larger feasible design space that can be evaluated within a given time frame. Moreover, multiple similar tools could be linked to provide a more detailed image or the design tools could be expanded into following design phases.

List of Figures

1	Infrared image of an unsuppressed vessel	8
2	Capabilities over time as a result of a failure	8
3	Diagram of predefined topology	12
4	Example of a mission profile with propulsive and electrical power demand. The required power is given over time in constant mission elements	13
5	Overview of the total model. Within the dashed frames the main sub-models can be found.	16
6	Working principle of IDeA, resulting in a non-growth of concepts	18
7	Chapter location within model, based on Figure 5	21
8	Two generation methods for the same configuration vector. (a) Method 1 generates all possible concepts and applies constraint to filter out the unfeasible ones. (b) Method 2 builds the vectors, by only adding components that are feasible with the existing components.	22
9	Chapter location within model, based on Figure 5	27
10	One engine type	30
11	Two engine types	30
12	Three engine types	30
13	Extra engine	31
14	Direct drive	31
15	Random configuration	31
16	Example of the battery management for two mission elements	36
17	Chapter location within model, based on Figure 5	39
18	Specific dimensions (m/MW) versus rated power (MW) for a database of gas turbines	40
19	Specific dimensions (m/MW) by van Es, the model and Rolls-Royce MT-30	41
20	Tubular fuel cell stacking	43
21	Length- and weight factor for generators sets from Wärstilä	45
22	Chapter location within model, based on Figure 5	48
23	Schematic of a simple cycle twin-shaft gas turbine	48
24	T-s diagram of an ideal Brayton cycle without losses	49
25	NOx emission ratio for multiple engine types at different power fractions. Constructed by van Dijk and updated with the gas turbine.	51
26	Air mass flow as function of relative power fraction	52
27	Specific work at every stage of the gas turbine. Used as verification of the gas turbine model.	53
28	Specific fuel consumption of the Rolls-Royce MT-30 in red markers and the model output in blue	53
29	Exhaust gas temperature of the Rolls-Royce MT-30 in red markers and the model output in blue	53
30	Power output of a single cell at different operating pressures. $A_{cell} = 0.01m^2$ $T = 800^{\circ}C$	57
31	SOFC losses and resulting polarization curve for $P = 1 atm$ and $T = 800^{\circ}C$. Used for verification of the SOFC model	58
32	Polarization curve of MSU data (in blue) and model output (in red) for $P = 3 atm$ and $T = 900^{\circ}C$	58
33	Propeller load line of a fixed pitch propeller (in red) and a controllable pitch propeller (in blue)	61
34	Effect of a CPP on the fuel consumption of a diesel engine	63
35	Effect of a CPP on the efficiency of a electric motor	63
36	Effect of a CPP on the fuel consumption of a gas turbine	63
37	Calculated charge pressure over calculation loop. The starting pressure was set to 3.5 bar. The final pressure is 199277 Pa, which is reached after 19 iterations.	65
38	Verification of the new diesel engine model. The results match perfectly, thus the the lines of both models overlap. The given conditions are not representative of existing engines.	65
39	Validation of the new diesel engine model. The measurements are given as markers of the same colour.	66
40	Specific fuel consumption of different engines	66

41	Efficiency curve of the electric motor	67
42	Chapter location within model, based on Figure 5	69
43	Capabilities over time as a result of a disruption	69
44	Example of network representation of hybrid configuration	70
45	Operational profile of case study 1A and 1B.	76
46	Type and number of components used by the top 1000 configuration of case study 1A. Multiple components can be combined, resulting in a sum of components higher than 1000.	78
47	Type and number of components used by the top 100 configuration of case study 1B. Multiple components can be combined, resulting in a sum of components higher than 100.	78
48	Efficiency-versus-volume design space. All concepts of case study 1A, including the optimal configuration indicated with a star and the Pareto front indicated with a black line. The colour of a concept is based on the overall ranking of the concept from best (red) to worst (blue).	79
49	Efficiency-versus-volume design space. All concepts of case study 1B, including the optimal configuration indicated with a star and the Pareto front indicated with a black line. The color of a concept is based on the overall ranking of the concept from best (red) to worst (blue).	79
50	Operational profile of case study 2A and 2B.	80
51	Type and number of components used by the top 1000 configuration of case study 2A. Multiple components can be combined, resulting in a sum of components higher than 1000.	82
52	Type and number of components used by the top 1000 configuration of case study 2B. Multiple components can be combined, resulting in a sum of components higher than 100.	83
53	Efficiency-versus-robustness design space. All concepts of case study 2A, including the optimal configuration indicated with a star and the Pareto front indicated with a black line. The colour of a concept is based on the overall ranking of the concept from best (red) to worst (blue).	84
54	Efficiency-versus-robustness design space. All concepts of case study 2B, including the optimal configuration indicated with a star and the Pareto front indicated with a black line. The color of a concept is based on the overall ranking of the concept from best (red) to worst (blue).	84
55	Operational profile of case study 3A and 3B.	85
56	Type and number of components used by the top 1000 configuration of case study 3A. Multiple components can be combined, resulting in a sum of components higher than 1000	87
57	Type and number of components used by the top 100 configuration of case study 3B. Multiple components can be combined, resulting in a sum of components higher than 100	87
58	Efficiency-versus-volume design space. All concepts of case study 3A, including the optimal configuration indicated with a star and the Pareto front indicated with a black line. The colour of a concept is based on the overall ranking of the concept from best (red) to worst (blue).	89
59	Efficiency-versus-volume design space. All concepts of case study 3B, including the optimal configuration indicated with a star and the Pareto front indicated with a black line. The color of a concept is based on the overall ranking of the concept from best (red) to worst (blue).	89
60	The mass and gravimetric energy density of various main propulsion concepts versus the effective energy delivered to the propeller at 10 MW.	92
61	The volume and volumetric energy density of various main propulsion concepts versus the effective energy delivered to the propeller at 10 MW.	92
62	The mass and gravimetric energy density of various electric generation concepts versus the effective energy delivered to the electric grid at 1 MW.	94
63	The volume and volumetric energy density of various electric generation concepts versus the effective energy delivered to the electric grid at 1 MW.	94
64	Diagram of a multi-stage exploration tool	103
65	Efficiency-versus-robustness design space. All concepts of case study 1A, including the optimal configuration indicated with a star and the Pareto front indicated with a black line. The colour of a concept is based on the overall ranking of the concept from best (red) to worst (blue).	112
66	Efficiency-versus-robustness design space. All concepts of case study 1B, including the optimal configuration indicated with a star and the Pareto front indicated with a black line. The color of a concept is based on the overall ranking of the concept from best (red) to worst (blue).	113

67	Volume-versus-robustness design space. All concepts of case study 1A, including the optimal configuration indicated with a star and the Pareto front indicated with a black line. The colour of a concept is based on the overall ranking of the concept from best (red) to worst (blue).	114
68	Volume-versus-robustness design space. All concepts of case study 1B, including the optimal configuration indicated with a star and the Pareto front indicated with a black line. The color of a concept is based on the overall ranking of the concept from best (red) to worst (blue).	114
69	Efficiency-versus-volume design space. All concepts of case study 2A, including the optimal configuration indicated with a star and the Pareto front indicated with a black line. The colour of a concept is based on the overall ranking of the concept from best (red) to worst (blue).	115
70	Efficiency-versus-volume design space. All concepts of case study 2B, including the optimal configuration indicated with a star and the Pareto front indicated with a black line. The color of a concept is based on the overall ranking of the concept from best (red) to worst (blue).	116
71	Volume-versus-robustness design space. All concepts of case study 2A, including the optimal configuration indicated with a star and the Pareto front indicated with a black line. The colour of a concept is based on the overall ranking of the concept from best (red) to worst (blue).	116
72	Volume-versus-robustness design space. All concepts of case study 2B, including the optimal configuration indicated with a star and the Pareto front indicated with a black line. The color of a concept is based on the overall ranking of the concept from best (red) to worst (blue).	117
73	Efficiency-versus-robustness design space. All concepts of case study 3A, including the optimal configuration indicated with a star and the Pareto front indicated with a black line. The colour of a concept is based on the overall ranking of the concept from best (red) to worst (blue).	118
74	Efficiency-versus-robustness design space. All concepts of case study 3B, including the optimal configuration indicated with a star and the Pareto front indicated with a black line. The color of a concept is based on the overall ranking of the concept from best (red) to worst (blue).	118
75	Volume-versus-robustness design space. All concepts of case study 3A, including the optimal configuration indicated with a star and the Pareto front indicated with a black line. The colour of a concept is based on the overall ranking of the concept from best (red) to worst (blue).	119
76	Volume-versus-robustness design space. All concepts of case study 3B, including the optimal configuration indicated with a star and the Pareto front indicated with a black line. The color of a concept is based on the overall ranking of the concept from best (red) to worst (blue).	119

List of Tables

1	Scoring method scenario 1	9
2	Scoring method scenario 2	9
3	All applied components per category. An asterisk (*) indicates substantial changes to an existing evaluation sub-model.	11
4	Efficiencies found in the power plant network	14
5	Component list with all input parameters and their type of specification	21
6	Three examples of the distributions of engines over multiple geared shafts. The engines that need to be installed are mentioned, along with two options to allocate the engines among the shafts. Option 1 shows a simple distribution. Option 2 shows the most even distribution of engines possible. Option 2 is the option that is chosen.	23
7	Verification tests for concept generation model	25
8	Verification tests for constraints of concept generation model	25
9	Verification test for installed mechanical power	32
10	Verification tests for installed electric power	34
11	Verification tests for mechanical power usage	35
12	Verification tests for electrical power usage	37
13	Dimensions of the Rolls-Royce MT-30 gas turbine	40
14	Verification and validation tests for gas turbine sizing	41
15	Dimensions of a SOFC tube and overall SOFC factors.	42
16	Verification tests for SOFC sizing	43
17	Upper and lower limit engine speeds per engine type	44
18	Thermodynamical processes in a gas turbine	50
19	Parameters used in the gas turbine model	50
20	Gibbs free energy and maximal OCV for a hydrogen fueled SOFC at atmospheric pressure	54
21	Parameters used in the SOFC model at an operating pressure of 5 bar.	57
22	Network details	71
23	Verification tests of robustness model	72
24	Vessel characteristics and weight factors for case study 1A and 1B	75
25	Mission elements of case study 1A and 1B.	75
26	Operational profile of case study 1A and 1B.	75
27	Optimal configuration of case study 1A and 1B, including KPI values	77
28	Vessel characteristics and weight factors for case study 2A and 2B	81
29	Mission elements of case study 2A and 2B.	81
30	Operational profile of case study 2A and 2B.	81
31	Optimal configuration of case study 2A and 2B, including KPI values	81
32	Vessel characteristics and weight factors for case study 3A and 3B	85
33	Mission elements of case study 3A and 3B	85
34	Operational profile of case study 3A and 3B.	85
35	Optimal configuration of case study 3A and 3B, including KPI values	86
36	Mass, volume and power density of the various main propulsion configurations. The model was asked to install 10 MW with a shaft speed of 200 rpm. All configurations are optimized for mass and volume, resulting in the highest possible power density.	91
37	Mass, volume and power density of the various electricity generation systems. The model was asked to install 11 MW at 3300V. Configurations are optimised for volume and mass (V/M) and for efficiency (Eff).	91
38	Mass, volume and power density of the various electricity generation systems. The model was asked to install 1 MW at 690V. Configurations are optimised for volume and mass (V/M) and for efficiency (Eff).	93
39	Calculation example of a 2 MW SOFC producing 1 MW of electric power with different fuels.	95
40	Total absolute average deviations from the the base case studies.	96
41	Number of concepts, number of elements and run time in seconds per case study	97

42	Client preference sets of case study 1A and 1B.	120
43	Client preference sets of case study 2A and 2B.	121
44	Client preference sets of case study 3A and 3B	122
45	Sensitivity analysis of client preferences in case study 1A	123
46	Sensitivity analysis of client preferences in case study 1B	124
47	Sensitivity analysis of client preferences in case study 2A	125
48	Sensitivity analysis of client preferences in case study 2B	126
49	Sensitivity analysis of client preferences in case study 3A	127
50	Sensitivity analysis of client preferences in case study 3B	128

Acronyms

- CET** Concept exploration tool.
- CNG** Compressed natural gas.
- CPP** Controllable pitch propeller.
- DE2** 2-stroke diesel engine.
- DE4** 4-stroke diesel engine.
- DF4** 4-stroke dual-fuel engine.
- DoFC** Degree of fuel cells.
- EGS** Electricity generation systems.
- EM** Electric motor.
- ESS** Energy storage system.
- FPP** Fixed pitch propeller.
- GB** Gearbox.
- Gen** Generator-set.
- GT** Gas turbine.
- HFO** Heavy fuel oil.
- IDeA** Intermediate DEsign Algorithms.
- KPI** Key performance indicator.
- Li-ion** Lithium-ion.
- LNG** Liquefied natural gas.
- MCA** Multi criteria analysis.
- MDO** Marine diesel oil.
- MPE** Main propulsion engine.
- OCV** Open circuit voltage.
- OPV** Offshore patrol vessel.
- PEMFC** Proton exchange membrane fuel cell.
- PMS** Power management strategy.
- PTO** Power take off.
- SOFC** Solid oxide fuel cell.

Nomenclature

α	Charge transfer coefficient	–
\dot{m}	Mass flow rate	kg/s
\dot{n}	Molar flow rate	mol/s
\dot{Q}	Heat flow	J/s
η	Efficiency	–
η_C	Polytropic compressor efficiency	–
η_e	Engine efficiency	W
η_r	Relative rotative efficiency	–
η_T	Polytropic turbine efficiency	–
κ	Specific heat ratio	–
μ	Weighted average	–
π	Pressure ratio	–
ρ	Density	kg/m ³
σ	Variance	–
τ	Temperature ratio	–
A	Tafel constant	V
B	Concentration loss coefficient	V
c_p	Specific heat at constant pressure	J/kg K
CV	Coefficient of variance	–
D	Diameter	m
D_{prop}	Diameter of the propeller	m
$DoFC$	Degree of fuel cells	–
E	Energy	Wh
E	Voltage	V
E_0	Open circuit voltage at atmospheric pressure	V
E_{loss}	Fuel cell losses	V
η_{mech}	Mechanical efficiency	W
F	Faraday's constant	C/mol

G	Free Gibbs energy	kJ/mol
G_0	Gibbs free energy at atmospheric pressure	kJ/mol
H	Height	m
h	Specific enthalpy	J/kg
I	Current	A
I	Set of engines of a certain engine type	–
i	Current density	A/m ²
i	Index for engine of certain engine type	–
i_0	Exchange current density	A/m ²
i_l	Limit current density	A/m ²
i_n	Internal current density	A/m ²
I_s	Set of engines of a certain engine type installed on shaft s	–
K_Q	Torque coefficient	–
L	Length	m
LR	Load ratio	–
m	Mass	kg
N	Number	–
n	Number of electrons involved in the reaction	–
n_C	Polytropic index for compressor	–
n_T	Polytropic index for turbine	–
n_{prop}	Rotational propeller speed	RPS
P	Power	W
p	Pressure	Pa
P_b	Brake power	W
p_i	Pressure at stage i	Pa
P_s	Shaft power	W
P_{td}	Thermodynamic power	W
P_{comp}	Compressor power	W
P_{cycle}	Power produced in one cycle	W
P_{elec}	Electrical power	W
P_{hurt}	Power produced in hurt state	W
P_{mech}	Mechanical power	W

P_{nom}	Nominal power	W
P_{prop}	Propeller power	W
Q	Heat	J
q	Heat per unit mass	J/kg
R	Gas constant	J/kg K
R	Robustness	—
r	Area specific resistance	Ωm^2
S	Set of shafts in configuration	—
s	Index for shaft	—
S_i	Score of KPI i	—
<i>Score</i>	Final overall score of configuration	—
T	Temperature	K
T	Time	h
T_i	Temperature at stage i	K
U_f	Fuel utilisation	—
W	Weight	kg
W	Work	J
w	Specific work	J/kg
WF_i	Weight factor of KPI i	—
x	Power of an engine of a certain engine type	W

Contents

Preface	iii
Summary	iii
List of Figures	vi
List of Tables	ix
List of Acronyms	xi
Nomenclature	xii
Contents	xv
1 Introduction	1
1.1 Background	2
1.2 Problem definition	2
1.3 Gap analysis	2
1.4 Concept exploration tool	3
1.5 Scope	3
1.6 Research questions	4
1.7 Structure of report	4
Part 1 - Model Overview	5
2 Defining the Optimal	6
2.1 Key performance indicators	7
2.2 Calculation method	8
3 Shaping a Concept and the Mission	10
3.1 Components	11
3.2 Topology	11
3.3 Mission	13
4 Making Modelling Decisions	15
4.1 Global overview	16
4.2 Model algorithm	17
4.3 Quasi-static modelling	18
Part 2 - Model Description	19
5 Concept Generation	20
5.1 Input	21
5.2 Configuration vector	21
5.3 Adjacency matrix	22
5.4 Constraints	23
5.5 Verification	25
6 Power Management Strategy	26
6.1 Installed mechanical power	27
6.2 Installed electrical power	33
6.3 Mechanical power usage	34
6.4 Electrical power usage	35

7 Sizing	38
7.1 Gas turbine	39
7.2 Solid-oxide fuel cell	42
7.3 Modified components	44
8 Performance	47
8.1 Gas Turbine	48
8.2 Solid oxide fuel cell	54
8.3 Controllable pitch propeller	61
8.4 Modified components	64
9 Robustness	68
9.1 Quantified definition	69
9.2 Calculating hurt state power	70
9.3 Simulated failures	71
9.4 Determine robustness score	71
9.5 Verification	72
Part 3 - Model Output	73
10 Case Studies and Results	74
10.1 Case study 1: Frigate	75
10.2 Case study 2: Offshore Patrol Vessel	80
10.3 Case study 3: Fast Offshore Patrol Vessel	85
10.4 Overall trends	90
10.5 Electric motors and fuel cells	90
10.6 Sensitivity analysis client preference	96
10.7 Research results	97
11 Conclusion and Discussion	99
11.1 Conclusion	100
11.2 Discussion	102
12 Recommendations	106
12.1 Model structure	107
12.2 Model operation	107
12.3 Model output	108
References	109
A Design space analysis	112
A.1 Case study 1	112
A.2 Case study 2	113
A.3 Case study 3	115
B Client preferences	120

1

Introduction

1.1 Background

Currently a significant amount of research has been performed into ways to make marine transport more sustainable and less polluting. Main topics are alternative fuels [1, 2], alternative power plants [3, 4] and alternative propulsion methods [5, 6] for commercial vessels. Similar focus is not found in the development of naval vessels. Little research has been published on implementing new techniques in naval surface vessels. Meanwhile most countries, including The Netherlands, have put sustainability on the agenda for their armed forces [7, 8, 9]. These recent emission policies in combination with the availability of new low emission components from commercial shipping will likely drive the application of state-of-the-art technologies in power plants on naval surface vessels.

With the availability of new techniques comes the possibility to experiment with alternative and unique power plant configurations. Examples of this are hybrid propulsion systems or even full battery powered ships [10]. A challenge that arises with all these possible configurations, is the number of concepts that can be considered. Previously, there was less of a need to examine a large number of ideas, as there was a set number of working concepts. Nowadays, the needs of the armed forces are changing and, equally important, there are more possible solutions. As a result, the contemplated design space has grown significantly. Research has shown that the number of generated concepts can grow exponentially [11], resulting in a design space too large for a human design team to evaluate. Van Dijk [12] argued that a concept exploration tool (CET) is required to estimate and compare the performance of the various concepts during the concept design phase. Although the research of van Dijk focuses on commercial vessels, the same logic can be applied to military vessels.

The operational requirements (concept of operations) of a surface navy vessel vary significantly from those of a commercial vessel. This leads to different mission profiles, requirements for the power plant (e.g. robustness and signatures) and client preferences for optimisation. For this reason, the CET made by van Dijk cannot directly be used for exploration of power plant concepts for naval surface vessels. Furthermore, naval vessels may employ different components compared to commercial vessels. As a result, additional sub-models have to be developed to model these components.

1.2 Problem definition

The challenge that may be (unconsciously) faced by certain design teams nowadays, is the size of the design space. When the number of possible configurations becomes too large, it is no longer feasible for a team of humans to think of and evaluate all concepts. As a result of this limitation, designers will make important decisions at the start of the design process to constraint the design space and thus decrease the number of concepts that are deemed viable. These early decisions are often based on previous experience and little available information, while having a significant impact on the final design.

The chosen viable concepts can be partially altered and optimised in later stages of the design process, but they won't rigorously change. This means that the final concept may be an optimised version of the initial concepts, but it is still unknown if this concept would have been optimal when compared with all feasible concepts. Essentially, it is unknown if the found optimal solution is a local optimum or a global optimum. Furthermore, this design philosophy inhibits innovations, as new ideas are often filtered out by the early choices and constraints put in place by the design team. This is done because completely new concepts take longer to develop, have an increased risk of delays and have a higher level of uncertainty with respect to the feasibility. All things considered, it can be said that the problem is a design space that is too large for humans to fully explore, leading to potential sub-optimal and conservative concepts.

1.3 Gap analysis

A significant amount of research has been done on effectively defining design spaces and finding optimal solutions, as this problem is faced by many design teams dealing with a large number of potential designs. The theories developed by this research work very well when the characteristics of the varying solutions are known, but here lies the crux faced when designing a power plant for a naval vessel. The characteristics or performance of the different solutions is often not precisely known or quantifiable, since computing them is a time consuming process. If the performance of all power plant configurations was known, finding the optimal configuration should be feasible.

When looking at tools that can evaluate the performance of many different power plant configurations, little literature can be found. This seems logical, as it is quite a niche market so hardly any research has been published in this particular direction. De Vos [13] developed a tool that explores the design space of networks

on board of vessels. However, for this research the component choice is of interest and to a lesser extent the connection between them. A concept exploration tool developed by van Dijk [12] is used by Nevesbu to evaluate many different power plant configurations for commercial vessel. This tool is useful, but cannot be used for power plant configurations of naval vessels [14]. Main reasons are the lack of naval oriented client preferences, the absence of certain components and the low computational speed. The new CET developed in this research will need to fill these gaps.

1.4 Concept exploration tool

To solve the problem defined in the previous paragraphs, the general idea of a concept exploration tool is introduced in this paragraph. A CET facilitates the users in exploring the full concept space, by generating and evaluating all the concepts in the design space. Since this CET is a computer model, it can evaluate concepts faster than a human and can therefore explore more concepts in a given time. The evaluation is done on the basis of a Multi Criteria Analysis (MCA). Key performance indicators (KPIs) of a concept are defined based on the functions of the solutions and weight factors are introduced to take the preferences of the user into account. Since the KPIs are quantified measures of a concept, concepts can be ranked based on their performance and the client preferences. All in all, it can be said that a CET enables a new design philosophy, where constraints are kept to a minimum and decisions are based on quantified measurements of the concepts.

The CET is to be used in an early design phase; the concept phase, as the name would already suggest. In the concept design phase the level of detail of both the requirements and the concepts is limited. In later stages functional requirements may be elaborated or altered and the concepts will be given more detail. For the tool this means that it has to function on a limited amount of input, but also that the level of detail in the tool does not have to meet the highest standards. As a result, assumptions may be used in the tool to simplify working principles or decrease computational time.

The CET developed in this research generates different power plants concepts by varying components, within a predefined topology. A concept is defined as a unique set of components, so by changing the components new concepts will arise, as is further explained in Chapter 5. A number of constraint are employed to ensure feasible configurations. These constraints should be kept to an minimum to keep the design space as large as possible. All viable concepts are stored in a library, after which they are evaluated. The evaluation model focuses on the performance of the concepts in terms of the defined KPIs, which are elaborated in Chapter 2. The performance of the various components is assessed based on first order principles, if possible. Subsequently, all concepts are ranked per KPI according to the according to their performance. An overall ranking is established by including the client preferences, along with a visualisation of the design space.

1.5 Scope

When designing a ship, many different subsystems and parts must be developed. Each design has its own space and requires a unique method to evaluate the concepts. For this thesis the focus will be on the design space of a power plant of a naval surface vessel. The aim of this research is to make a concept exploration tool for this design space.

The input for this tool is a mission profile and client preferences. The ship types considered in the case study are an offshore patrol vessel (OPV) and a frigate. The mission profile consist of a time-based propulsive and electrical power demand. The client preferences will be discussed in Chapter 2. The client preferences will not include the costs of the concepts. The output of the model is a ranking of the different configurations, a detailed description of every concepts and a visualisation of the total design space.

A power plant configuration consists of main components that can be found in a power plant. Auxiliary systems will not be modelled but will be added as weight, size and power consumers. All physical connections between components (pipes, wires, etc.) are not considered in this thesis. The modelled flows between components are limited to electrical and mechanical power. Mass flows between components and/or the rest of the vessel will not be considered, this includes heating, ventilation, air conditioning and hydraulics. An exception to this is the fuel consumption of certain components. All different combination of components will be deemed feasible as long as they meet all feasibility constraints, meaning that design choices are kept to a minimum. The topology of the configurations is fixed, but components may be switched off in certain scenario's leading to semi different topologies. Nuclear components will not be studied in this research.

The physical boundaries of the tool include the power plant and the fuel tanks, which means that the size and weight of the required fuel will be calculated. Electric power consumers and the electrical grid are not modelled, only the total amount of electric power needed. Water, hull and propeller interactions are not within the scope of this thesis, this also includes propeller efficiency. Furthermore, the propeller is seen as a propulsive power consumer and is thus not modelled. The demanded propulsive power enters the power plant at the shaft.

1.6 Research questions

In order to develop a concept exploration tool, as defined in the previous paragraphs, the following research questions have been developed.

1.6.1 Main question

How can the optimal power plant configuration for a naval surface vessel be determined given the mission profile and client preferences?

1.6.2 Subquestions

What are the KPI's of naval vessels on which to evaluate power plant configuration concepts?

What are the mission profile and ship characteristics per naval vessel?

How can a controllable pitch propeller and a gas turbine be modelled?

What new alternative power plant components could be considered for a power plant of a naval vessel?

How can these alternative power plant components be modelled?

What model structures can be used to ensure limited computational time?

What is the optimal power plant configuration for a naval surface vessels given multiple ship types, multiple mission profiles and multiple client preferences?

1.7 Structure of report

The report is divided into three parts: model overview, model description and model output. The first part, model overview, discusses the input of the model, describes the concept and mission definitions and gives an overview of the total model. It lays a foundation for the model and the rest of the thesis. It starts in Chapter 2 with how an optimal configurations can be defined. Chapter 3 follows with an description of the possible concepts and the mission input. Lastly, Chapter 4 gives an overview of the model itself.

In the second part, model description, the actual functioning of the model will be discussed. The sub-models presented in Chapter 4 form the structure for this part. It describes how all concepts are generated, managed, dimensioned and evaluated. Chapter 5 starts with the description of the concept generation, after which the power management strategy is discussed in Chapter 6. The dimensioning of all components can be found in Chapter 7, followed by the performance evaluation in Chapter 8. Finally, Chapter 9 presents the robustness sub-model.

The last part, model output, focuses on the output of the model. It shows the potential of the CET and how the output can be used in the design process. Furthermore, it reflects on the model workings and research questions. Chapter 10 shows the results of the research, including case studies. Subsequently, the conclusion and discussion are presented in Chapter 11. Lastly, recommendations for future research are given in Chapter 12.

Part 1
Model overview

"All models are wrong, but some are useful"
George Box

2

Defining the Optimal

Optimal is a subjective term. Therefore, only clients can determine what is optimal to them. Finding an optimal design in terms of a CET is a process of evaluating all options and deciding which configuration fits best with the mission and the interests of the user. Since not all aspects of a design can be assessed, key performance indicators are defined. These KPIs are derived from the operations of a power plant and from what the user considers important [14]. Furthermore, the KPIs have to be quantifiable, as a computer will perform the assessment.

2.1 Key performance indicators

The focus of this research is on the power plants of naval surface vessels, so the defined KPIs should reflect the performance of the power plant. The performance of a power plant does not only influence the power generation, but also other operations on board of a vessel. An example of this is that a smaller power plant leaves more space within the vessel. This space can then be used for other functions. Therefore, it is important to contemplate the effect of power plant operations on the whole vessel, when defining KPIs

The KPIs employed for the evaluations are:

- Total efficiency
- Emissions
- Size
- Weight
- Signatures
- Robustness

Within marine engineering and power plant design, efficiency is generally considered important. It does not only affect the operational cost of a vessel, but also the endurance and range of the ship. Thus, increasing the total efficiency is both economically and strategically advantageous. Furthermore, higher efficiency leads to lower fuel consumption, leaving more space and weight on board of the vessel for other functions. The total efficiency is computed by dividing the total work of the mission profile by the fuel heat input to all components throughout the mission, as can be seen in equation 1.

$$\eta_{tot} = \frac{W_{mission}}{Q_{fuel}} \quad (1)$$

Power plants generally emit emissions when producing power. As an increasing number of clients express a desire for reduced emissions, this is a reflection of the performance of the power plant. Three emissions gases are distinguished: CO₂, NO_x and SO_x. These three gases are the main contributors to the pollution of a vessel, in terms of volume and harmfulness. The emissions are quantified as the number of tons discharged per gas. Emissions rates for the different components and fuels are utilised to calculate the total emissions [12].

The size and weight are KPIs for similar reasons. A decrease in power plant dimensions leaves more space and weight for other functionalities, such as mission equipment. Additionally, the overall dimensions of the vessel are dependent on the size and weight of the power plant. Therefore, the hull design is partially dependent on the dimensions of the power plant, which in turn influences operational requirements, such as speed and manoeuvrability. The size and weight of every component are computed separately, after which they are all added together. The size and weight of fuel is included in this figure, as well as the mass of fuel tank itself.

Signatures are of the utmost importance for naval vessels, as being undetected is the first line of defence. The main signature originating in the power plant is the infrared image of the exhaust gases [14], as can be seen in Figure 1. At first, it was considered to take the temperature of the exhaust gases as a measure for the infrared signature. However, upon further investigation it became clear that most reciprocating engines yield the same exhaust gas temperature, independent of the engine type or load ratio. Subsequently, discriminating between these engines would not be possible. Therefore, the heat flow of the exhaust gases is taken as a measure for the infrared signature, as this allows for differentiation between engines. Exhaust gas cooling is a possibility to suppress the infrared signature of the exhaust gases, but this will not be included



Figure 1: Infrared image of an unsuppressed vessel [15]

in this thesis. The heat flow of every component during every mission element will be computed, after which a weighted average is taken as a definitive measure.

Robustness refers to the ability of a vessel to continue operation after a failure has occurred. This is highly significant for naval vessels, as intentional failure by hostile parties should be considered. De Vos [13] and others [16, 17] have studied the way a systems capabilities are influenced over time after a failure, of which a general response curve is shown in Figure 2. In the context of power plants, the relevant capability is the power it can produce. The most interesting state in terms of continued operationality is the hurt state, since this represents the state of the vessel for the remainder of the mission. Hence, the quantified benchmark for robustness is the ratio between the nominal power of the mission profile and the power output in the hurt state.

2.2 Calculation method

The ranking of the configurations is based on the performance of the concepts and the preferences of the client. Every concept receives a score per KPI. These scores are combined with the weight factors and

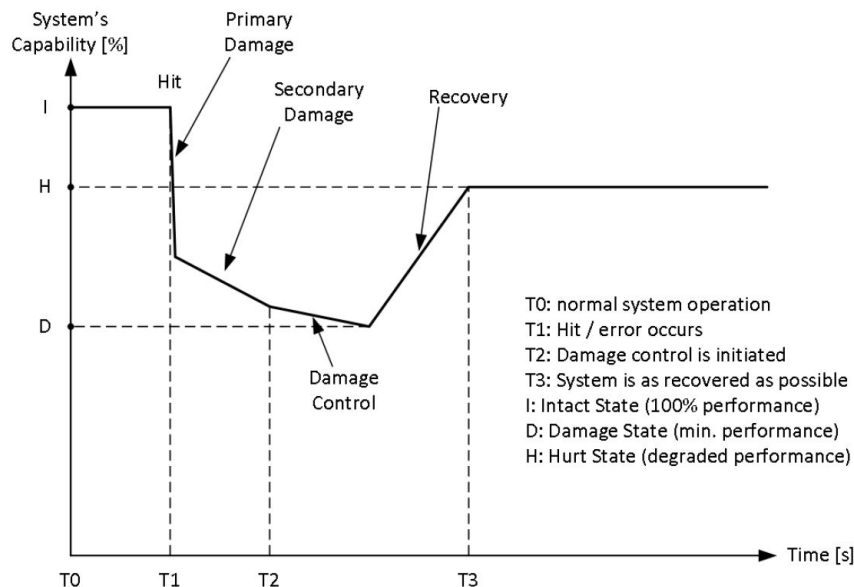


Figure 2: Capabilities over time as a result of a failure [13]

summed to compute the final score. The goal of the model is to minimize this score to obtain the optimal solution, as can be seen in the objective function in equation 2.

$$\text{Minimize}(\text{Score}) = \text{Minimize} \left(\sum_{i=1}^6 (WF_i \cdot S_i) \right) \quad (2)$$

The score per KPI is based on the performance of a concept compared to the other concepts. The number of points given to a concept per KPI range from 0 to 100. Since the objective function is a minimisation function, 0 is the best and 100 is the worst. The 0 points are set to absolute best that can be achieved within that KPI, even if that would be theoretically or practically impossible. Examples of this are 100% efficiency or 0 ton mass. The reasoning behind this is that a benchmark is required to scale all concepts to. The 100 points are rewarded to the worst concept within that KPI, e.g. the concept with the lowest efficiency or highest weight. All other concepts are placed linearly between these two extremes. Motivation for this method is that the relative differences between concepts is reflected in the score. For example, a concept that is three times as heavy receives three times the number of points.

This method is not without flaws, as will be demonstrated with an example. Table 1 presents a scenario, in which all concept are roughly of the same magnitude. In that case, the scoring method works nicely, reflecting the relative performances in the score. Concept 5 is punished for its significant mass, while the small gain in efficiency gives little extra value. The optimal configuration is concept 1, with a total score of 120. In scenario 2, presented in Table 2, one concept scores very poorly on one of the KPI. As a result, the relative performance of the other concepts has improved, while the actual performance stayed the same. Due to this, the score has become warped and the optimal configuration is now concept 4 with 96 points. It can be concluded that a poor concept makes that respective KPI partially irrelevant.

This problem proved most relevant for the volume and mass of the components, since overcapacitated components may be installed. As a result, the dimensions of the components may also increase. Therefore, a maximum power factor is introduced, to ensure that the components do not become oversized. The maximum installed power may only be a factor bigger than the required power. This guarantees that no extremely poor concepts are produced, which will warp the score of all other concepts. The value of the maximum power factor can be adjusted by the user of the CET.

Table 1: Scoring method scenario 1

Concept	Mass	Efficiency	Mass score	Efficiency score
Abs. Best	0	1.00	0	0
1	1	0.50	20	100
2	2	0.52	40	96
3	3	0.54	60	92
4	4	0.56	80	88
5	5	0.58	100	84

Table 2: Scoring method scenario 2

Concept	Mass	Efficiency	Mass score	Efficiency score
Abs. Best	0	1.00	0	0
1	1	0.50	2	100
2	2	0.52	4	96
3	3	0.54	6	92
4	4	0.56	8	88
5	50	0.58	100	84

3

Shaping a Concept and the Mission

For the CET to work, a concept must be defined. Similarly, the function of a concept, in this case the mission profile, must be determined. A concept is defined as a unique set of components with a subsequent topology. The applied components will be discussed in this chapter, along with the predefined topology. The mission profile is defined as a propulsive and electrical power demand over the duration of a mission, as can be read in this chapter.

3.1 Components

A configuration consists of a unique set of main components. A main component is a unit that works directly towards providing either propulsive or electrical power. Five types of main components can be distinguished: propellers, main propulsion engines (MPEs), electricity generation systems (EGSs), fuels and others. The considered parts can be found in Table 3. Most of the component sub-models are taken from previous performance evaluation models [12, 18], as is indicated with the citation. A number of these models is illustrated with an asterisk (*), which signals that the existing sub-model is substantially adjusted for the current CET. Components without a citation are completely new.

In comparison to the tool by van Dijk [12] and ten Hacken [18], three new components have been added: controllable pitch propeller (CPP), a gas turbine (GT) and a solid-oxide fuel cell (SOFC). The CPP and gas turbine are added, as they are main features on today's naval vessels, and a fair comparison between naval vessels would not be possible without these parts. In addition, the CET is supplemented with a SOFC to increase the number of possible alternatives in the power plant. The SOFC is chosen as it is seen as a promising technology that could be implemented on board of naval vessels [14].

Within one configuration, multiple identical components can be utilised. Moreover, multiple parts from one category can occur within one configuration. For example, a twin-shaft hybrid configuration with two 4-stroke diesel engines (DE4) and two electric motors (EM) can exist. In theory, the number of components within in a configuration is limitless, thus the number of concepts is infinite. In practice, a limit per component can be set by the user of the tool. For a standard complete run, the number of components will likely lie between the 40 and 45 components, resulting in roughly 10^{12} to 10^{13} different concepts. Most of these concepts are not feasible and will not be generated, as is explained in Chapter 5. Therefore, the actual design space will likely be between 50.000 to 200.000 concepts large, which is clearly too large for a human design team to evaluate.

In addition to the main components, a number of auxiliary components are present in the CET. These components are not used to define a concept, but are seen as essential for the operation of a power plant. These components are the electric grid, transformers, inverters and fuel tanks. They are generated as needed. The performance of these components is evaluated as if they are a separate component, meaning they have their own mass, volume and efficiency (if applicable). Furthermore, compressors and turbines are added as sub-components of main components. Their performance and dimensions are included within the main component they are attached to.

3.2 Topology

Components can be connected in multiple ways, resulting in multiple varying topologies. Every unique topology could form its own concept, resulting in a significant increase in the number of concepts. From a computational perspective, this is not feasible [12]. Therefore, a single predefined topology is applied to every concept. This topology is based on the physical connection between components and the logical flow of energy through a power plant. A basic diagram of the topology can be found in Figure 3. This basic diagram shows the topology with one part of every single component. In reality, the topology changes slightly per concept, as certain components are unused, while others are employed multiple times.

Table 3: All applied components per category. An asterisk (*) indicates substantial changes to an existing evaluation sub-model.

Propellers	MPE	EGS	Fuel	Others
Fixed pitch propeller [12]	2-stroke diesel engine [12]*	Generators [12]*	Marine diesel oil [12]	Li-ion batteries [18]
Controllable pitch propeller	4-stroke diesel engine [12]*	PEM fuel cell [18]*	Heavy fuel oil [12]	Gearbox [12]*
	4-stroke dual fuel engine [12]*	Solid-oxide fuel cell	Liquid natural gas [12]*	
	Electric motor [18]		Compressed natural gas [12]*	
	Gas turbine		Ammonia [12]	
			Hydrogen [12]	

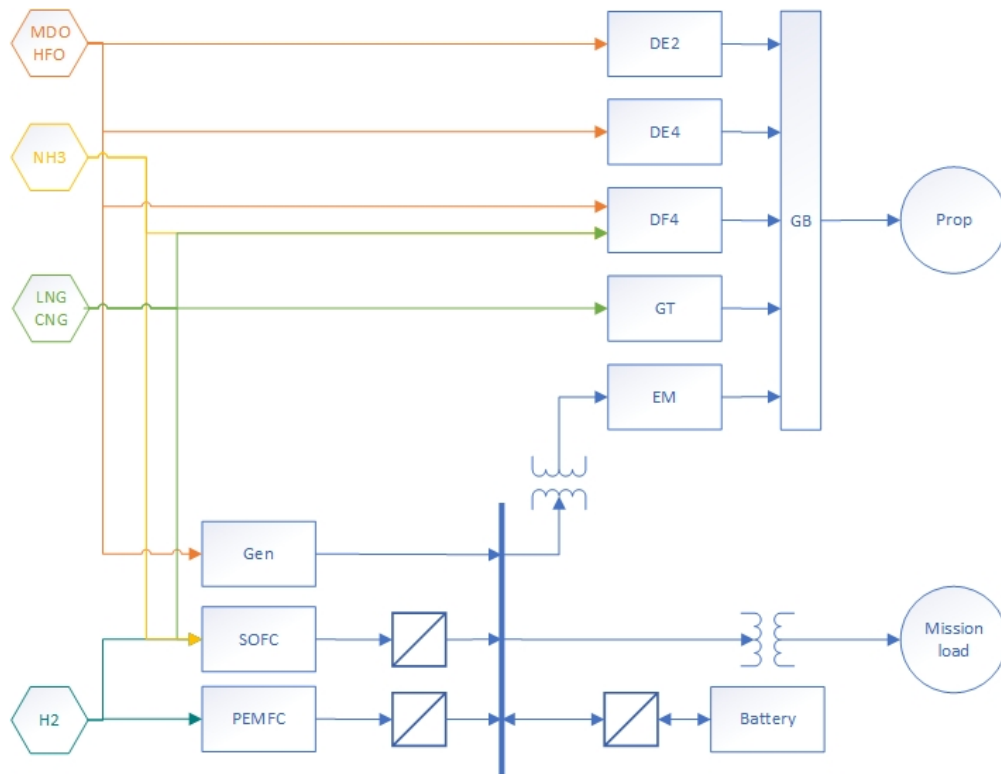


Figure 3: Diagram of predefined topology

The number of shafts and the presence of gearboxes have a significant effect on the topology, as they allow the adoption of multiple propulsive engines. This significantly enlarges the design space, as every combination of engines is a unique configuration and thus a concept. Furthermore, it complicates the engine allocation, since the engines must be distributed between the multiple shafts or gearboxes. This process is discussed in Chapter 5. In a multi-shaft configuration, the number and type of engines per shaft do not have to be equal. Better yet, a combination of direct drive on one shaft and a gearbox on the other is possible. This design choice is a result of the design philosophy, in which constraints are kept to a minimum. Though, it could be argued these configurations will most likely never be optimal or practical. In case of a direct drive, a single MPE is connected to the shaft. The possibility of a shaft motor/generator is not included in this CET, due to research time constraints.

The electric grid is greatly simplified into a single AC bus, to which all electric components are connected. The electric users may need varying voltages, depending on their power demand. Therefore, transformers are placed between the bus and the electric users. If the voltage of the device and the bus matches, no transformer is needed. The EGSs are designed to match the voltage of the grid, which eliminates the need for transformers. The batteries and fuel cells work on direct current, while the bus operates on alternating current. Accordingly, inverters are placed between the bus and these parts. The mission equipment is most likely connected to a secondary lower voltage bus. For this equipment more transformers and inverters may be needed. However, once the electric power leaves the power plant it is considered out of the scope of this research. Hence, the lower level electrical grids are not included in the topology.

The diagram in Figure 3 shows four fuel tanks, with occasionally two fuel types in a single tank. In practice, different fuel types do not share a single tank, which is also the case in the model. Although it is true that identical fuel for multiple components flows from one tank, the combined fuels are put together as they are comparable, which leads to a more orderly schematic. When a part is compatible with various fuel types, all combinations are generated as unique concepts and evaluated by the CET. The dual fuel engine (DF4) shows two fuel connections, due to the simultaneous need for pilot and dual fuel. All combinations between various pilot and dual fuels are also generated.

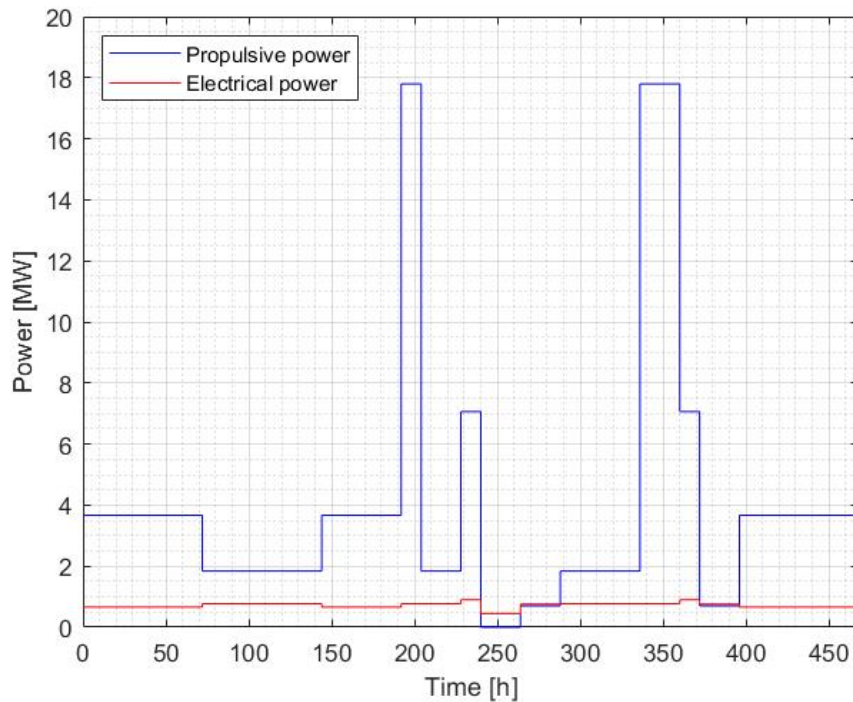


Figure 4: Example of a mission profile with propulsive and electrical power demand. The required power is given over time in constant mission elements

3.3 Mission

A mission is simulated to compute the performance of a concept. The mission profile is defined by the user of the tool and consists of the power required by the vessel over the duration of the mission. The power demand is subdivided into propulsive power and electrical power. For every stage of the mission the requested power is different. However, over the length of a mission stage, the power demand is assumed constant. This is not according to the reality, yet it is consistent with the level of detail of the CET and the design stage in which the tool is to be utilised. Figure 4 shows an example of the mission profile. It can be clearly seen that the required power is constant during a so called mission element. Consequently, the performance of the various components will also be constant during these mission elements. As a result, the dynamic behaviour of the different parts is not simulated, as will be discussed further in Chapter 4. If an electric motor is operated during a mission element, the electrical power needed by the electric motor is added to the electrical power demand of that mission element.

The propulsive power demand found in Figure 4 is defined at the propeller. This means that the power delivered by the MPEs must be greater, due to efficiency losses. Similarly, the electrical power is defined at the mission load, shown in Figure 3. Table 4 shows the efficiencies found in the network and the assumed values. If a component, such as a gearbox, is not present in a power flow, the efficiency is set to 100%. Internal component efficiencies are included in the performance of the part itself. In the case of the generator (Gen), the indicated efficiency is the efficiency of the actual generator. The attached diesel engine has its own internal efficiencies.

Table 4: Efficiencies found in the power plant network

Efficiency	Value
Shaft (direct drive)	99%
Shaft (gearbox)	97%
Reduction gearbox (per reduction step)	99%
Combinator gearbox	99%
Transformer	98%
Inverter	99%
Generator	95%

4

Making Modelling Decisions

The CET consists of multiple sub-models, each with a specific function. The sub-models can be divided into two main parts: the generation model and the evaluation model. All sub-models are run in sequence, with all concepts passing through the same sub-model at the same time. The choice has been made to apply a quasi-static modeling method, as this is consistent with the level of detail of the CET and will result in significantly higher computational speeds.

4.1 Global overview

Figure 5 shows the total CET, including input and output. The two main parts of the model can be found within the dashed frames. After the input is given to the CET, a run of the model is started at the top left, following the arrows, to end at the bottom right. The generation model generates all possible concepts based on the components list that is inputted. All feasible configurations are saved in the concept library to be used by the rest of the tool. Since the concepts are saved, multiple runs of the evaluation tool can be performed, without the need to run the generation model again. The power management can be seen as the brain of the CET, as it determines the required amount of installed power and controls the usage of the different components, based on the mission profile. It must be noted that the actual amount of installed power is determined by the sizing sub-model, as the amount of installed power may be larger than strictly necessary. The sizing sub-model sizes all components both in terms of power and dimensions. The client preferences are used to determine the optimal amount of power per component. The true installed power is communicated with the performance and robustness model. Next, the performance sub-model simulates the mission, based on the operational profile. It calculates the fuel consumption, emissions and signatures of all concepts. It can be seen that the performance sub-model also has an output towards the mission profile. This is a results of the operations of an electric motor, which adds a power demand to the electric mission profile. As a result, the performance of the MPEs is simulated first, after which all electric components are designed and simulated. Following, the robustness sub-model computes the robustness of the configurations. Lastly, all results are processed in the multi criteria analysis sub-model, which produces a ranking of all concepts and a visualisation of the design space.

The structure of the model, as seen in Figure 5, is not only the foundation of the CET, but also the foundation of part two of this thesis. In part two, the model is described by means of the sub-models found in the model structure. The sub-models are discussed in the order in which concepts flow through the model.

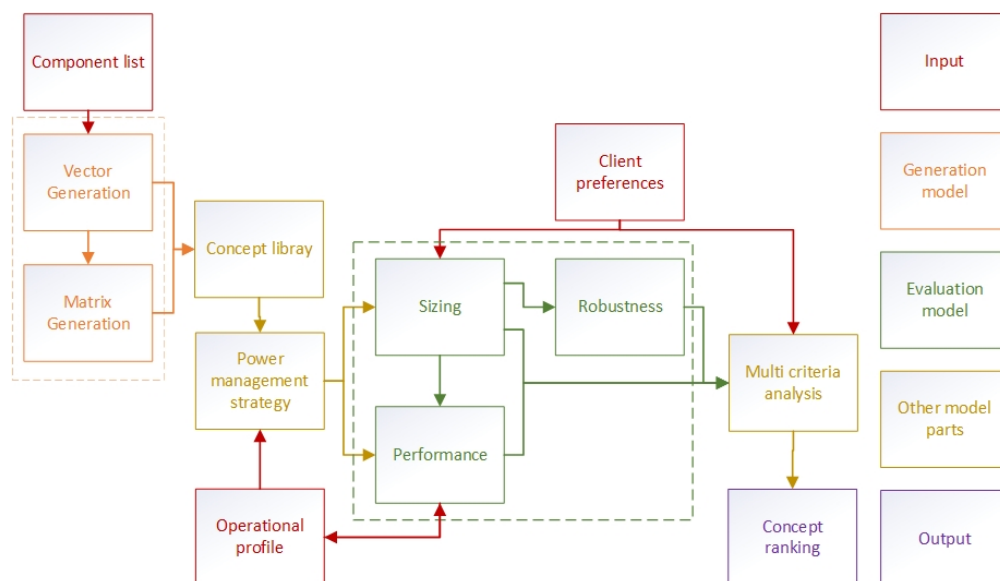


Figure 5: Overview of the total model. Within the dashed frames the main sub-models can be found.

As the given description may be a little abstract, a more step-by-step roadmap can be found below:

1. Load components list, operational profile, client preferences and model settings
2. Generate concept vector
3. Generate concept matrix
4. Save vector and matrix to concept library
5. Load concept library
6. Determine installed MPE power
7. Design shaft configuration
8. Design and size MPE components
9. Simulate mission for MPE components
10. Design electric grid
11. Determine electric mission profile
12. Determine installed EGS power
13. Design and size EGS components
14. Design and size ESS components
15. Simulate mission for EGS and ESS components
16. Simulate fuel usage and size tanks
17. Determine robustness
18. Combine results and determine final score
19. Present output

4.2 Model algorithm

The CET employs a modified brute force search algorithm to generate and evaluate all concepts. This means that all possible combinations are tried and compared to find the optimal solution. The choice is motivated by the fact that this algorithm offers one of the most exhaustive searches of the design space and is relatively easy to understand, program and use. The algorithm is modified, as trying every feasible and non-feasible concept would be computationally heavy, while not contributing to the useful exploration of the design space. Therefore, the choice is made to not generate all 10^{13} possible configurations and filter out the unfeasible ones, but instead only generate the feasible ones to start with. This process is explained further in Chapter 5.

Furthermore, intermediate design choices are resolved on the spot, rather than generating alternative concepts. During the design process, multiple design options are available on component level. Every option could be seen as a unique concept in and of itself, which would result in a vast expansion of the number of concepts. To guarantee a manageable computational time, Intermediate Design Algorithms (IDeAs) are used. This concept was developed by van Dijk [12] to limit the number of concepts within the CET. An IDeA designs every feasible option for a component and makes a first estimation of the performance of that component. The optimal design is chosen based on the client preferences, which explains the input of client preference into the sizing sub-model in Figure 5.

Figure 6 shows the working principles of the IDeAs and how it stops the growth of concepts. In situation A, every design option is developed into its own concept. With two options per type the situation stays relatively simple. However, in reality, there are often between 10 to 30 options per MPE or EGS component. This would result in a growth from 100,000 configurations to roughly 1 to 10 billion concepts, depending on the employed components. It is deemed infeasible to evaluate all these concepts within a reasonable time, even for a computer. Situation B shows a solution, by applying the IDeAs. It is noted that the use of the IDeAs goes against the design philosophy of the CET, as it essentially adds constraints and thus limits the design space. However, without these IDeAs the design space would not be explorable or design choices would not be optimised.

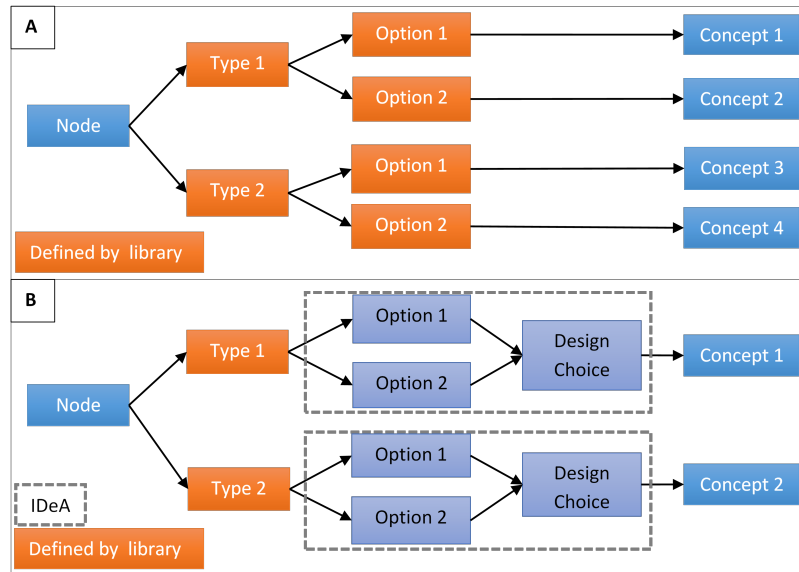


Figure 6: Working principle of IDeA, resulting in a non-growth of concepts [12].

The code of the model is run in Matlab. This choice was dictated by the author's affinity with this software and the fact that previous models had also been coded in Matlab. This allowed for a relatively easy transfer of code between the different models. Moreover, the code of the model is written in such a way that parallel computing is possible. Since the evaluation of one concept is completely independent of the evaluation of the other concepts, multiple concepts can be evaluated in parallel on multiple computer cores. Matlab has a build-in feature that facilitates the use of all cores, resulting in a significant decrease in computational time.

4.3 Quasi-static modelling

As mentioned before, the CET will employ a quasi-static performance model, instead of a dynamic one. The mission profile consist of multiple constant mission elements, as was shown in Figure 4. Consequently, the performance of the configurations is assumed constant during a mission element. Therefore, a single calculation suffices for the whole mission element. Consequently, the resulting simulated time step between calculation is greater than when a dynamic model is used. Accordingly, less computations are needed to simulate a given mission length, resulting in a decrease in computational time.

There are advantages and disadvantages to using a quasi-static performance model. The most significant advantage is the decrease in computational time, when compared to dynamic modelling. A disadvantage is that the dynamic behaviour of components can no longer be modelled. In reality, the mission profile of a vessel is not constant over a given period, but has fluctuations in the power demand. Components react to these fluctuations and this is reflected in their performance. Furthermore, ramping components up and down is not instantaneous, but has certain transitional period and corresponding component behaviour. Both these elements can not be modelled, since component behaviour is constant and instantaneous. As a result, a level of detail is lost in the CET. The significance of this detail level can be argued, as the fluctuations may only be a insignificant amount of the total power and the transitional period may be insignificantly short compared to the mission length. However, it is also important to remember the design phase, in which the CET is to be used. In the concept phase, more detailed mission profiles are often not available and estimations are sufficient to get a first idea about the design direction. More detailed simulation can be performed in later stages of the design process. Thus, the choice for quasi-static modelling is deemed acceptable for a CET.

Part 2
Model description

*"99 little bugs in my code
Take one down, patch it around
114 little bugs in my code!"*

5

Concept Generation

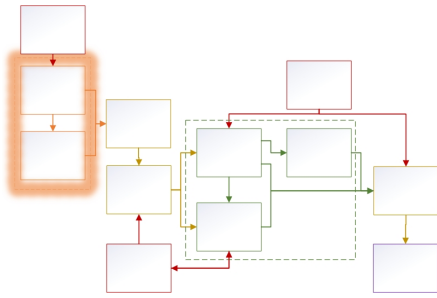


Figure 7: Chapter location within model, based on Figure 5

The first step the CET takes, is the generation of the feasible concepts. A concept is described by means of a configuration vector and an adjacency matrix, both of which are produced by the generation model. This process will be discussed in this chapter. A priori constraints are implemented to limit the design space to feasible concepts. Figure 7 shows the position of this chapter within the complete model structure. The input for this sub-model is a component list, provided by the user. The output of the generation model is passed on to the concept library where it will be saved, to be used later by the evaluation model.

5.1 Input

The input of the generation model is a component list, containing the type and specifications per component that is to be used during a run. These specification, including all input parameters, can be found in Table 5. For most components the specification is the maximal number of that component within one concept. By setting the maximal number to 0, a component is turned off and won't be include in the model run. For the fuels a maximal number does not make sense, so a simple on/off input is given. The maximal number of engines per gearbox and the maximal number of EGSs is also provided by the user. Lastly, for the batteries a maximum size in kWh is used as input.

5.2 Configuration vector

A vector is employed to describe the components present in a configuration. The vector has a length equal to the sum of the maximal number of all components. Since the length of the configuration vector is equal for all concepts and does not change during a run, every component can be assigned to a specific element in the vector. If a component is present in a concept, the corresponding element will be a '1'. Similarly, if the component is absent, the corresponding element will be a '0'.

Two methods were considered for the generation of the configuration vector. The first method generates all possible concepts and filters out the unfeasible ones. The second method build a vector, by only adding components that are feasible with the existing components. A simplified example of these methods is shown Figure 8. In the example a component list is used which defines a maximal number of 1 propeller, 1 gearbox (GB) and 2 engines. As a result, the length of the vector is equal to 4. The first element describes the state of the propeller, the second element the state of the GB and the last two elements the state of the diesel engines. Method 1 produces every possible combination of states, resulting in a majority of unfeasible configurations. Method 2 builds the vector by adding a category of components per step. In the first step,

Table 5: Component list with all input parameters and their type of specification

Input parameter	Specification	Input parameter	Specification
FPP	Max number	Li-ion	Max size
CPP	Max number	MDO	On/off
DE2	Max number	HFO	On/off
DE4	Max number	LNG	On/off
DF4	Max number	CNG	On/off
GT	Max number	NH ₃	On/off
EM	Max number	H ₂	On/off
PEMFC	Max number	GB	Max number
SOFC	Max number	Engines per GB	Max number
Gen	Max number	Total EGSs	Max number

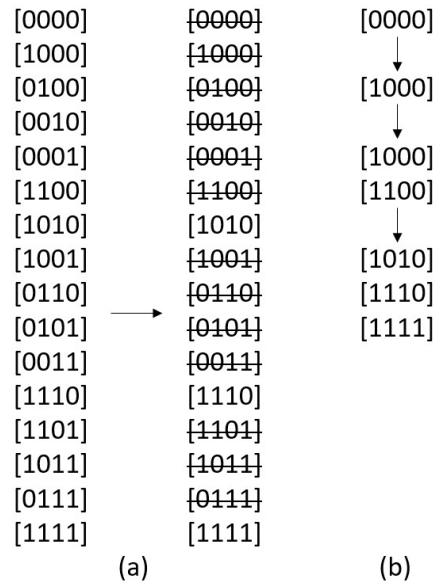


Figure 8: Two generation methods for the same configuration vector. (a) Method 1 generates all possible concepts and applies constraint to filter out the unfeasible ones. (b) Method 2 builds the vectors, by only adding components that are feasible with the existing components.

the propellers are added, followed by the gearboxes in the second step. It can be seen that after step two, two configuration arise, one without a gearbox and one with a gearbox. Both these configuration are feasible. The third step adds the engines. One engine is added to configuration without the gearbox, as two is deemed unfeasible. From the concept with a gearbox, two configurations arise, namely a single and double engine concept. Here it can be noted that a maximum per component is defined, so configurations with less of these components are also generated.

It may seem like method 1 would be faster, as it only includes one step. However, method 2 is significantly faster, since the number of involved concept is considerably smaller. It was mentioned that the total unfiltered design space is roughly 10^{12} to 10^{13} concepts large. It is unfeasible to test all configurations against the generation constraints, due to the sheer numbers. A quick calculation shows that at the rate of 1 million concepts per second, it would still take more than a day to filter every configuration. On the other hand, method 2 can produce all feasible concepts of a 40 component run in less than 30 seconds. Of course, this is only one example, yet it shows the significant difference in computational time. Even though method 2 does not filter the concepts with the help of constraints, constraints are still implemented to ensure only feasible concepts are constructed. These a priori constraint can be found in Paragraph 5.4.

5.3 Adjacency matrix

A matrix is applied to describe the connections between components. These connection are required for the robustness calculation, where the power flow through the configuration is computed. The topology is seen as a directed network, resulting in an asymmetric matrix. Connection between components are indicated with a '1', as is shown in equation 3. In this example the last vector of Figure 8 is taken, consisting of 1 propeller, 1 gearbox and 2 diesel engines. The connection flows from column to row, meaning that the connection from the GB (element 2) to the propeller (element 1), is found at position (1,2). Similarly, the connections from the engines to the gearbox can be found at position (2,3) and (2,4) respectively.

$$[1111] \rightarrow \begin{bmatrix} 0 & 1 & 0 & 0 \\ 0 & 0 & 1 & 1 \\ 0 & 0 & 0 & 0 \\ 0 & 0 & 0 & 0 \end{bmatrix} \quad (3)$$

The only component that does not have a directed power flow is the battery, since it can be charged and discharged. However, the bus, to which the battery is connected, is not seen as a main component, therefore it is not found in the configuration vector or adjacency matrix. The origin and destination of the battery

Table 6: Three examples of the distributions of engines over multiple geared shafts. The engines that need to be installed are mentioned, along with two options to allocate the engines among the shafts. Option 1 shows a simple distribution. Option 2 shows the most even distribution of engines possible. Option 2 is the option that is chosen.

	Shaft 1	Shaft 2	Shaft 1	Shaft 2	Shaft 1	Shaft 2
Engines	2 DE2 2 EM		3 DE2 3 EM		2 DE2 1 EM	
Option 1	2 DE2	2 EM	3 DE2	3 EM	2 DE2	1 EM
Option 2	1 DE2 1 EM	1 DE2 1 EM	2 DE2 1 EM	1 DE2 2 EM	1 DE2 1 EM	1 DE2

energy are main components and are never the same. This means a directed network can be established from the EGS through the battery to the electrical consumer, along with a direct connection between the EGS and the electrical consumer.

The generation of the adjacency matrix is relatively straightforward, as the topology is predefined. The only challenge is the allocation of engines in an multi-shaft geared configurations. The engines can be distributed among the shafts in several ways. The aim of the generation model is to distribute identical engines as evenly as possible over the multiple shaft, since this is desirable from a practical and power management perspective. Examples can be found in Table 6, where two distribution options are shown. In every example option 2 is chosen. In the first example, a symmetrical topology is achievable by evenly spreading the identical engines over the two shafts. However, this is not possible in example 2, resulting in an asymmetric configurations. Nonetheless, the identical engines are assigned as evenly as possible. Example 3 shows that an unequal number of engines per shaft can occur, even though identical engines are distributed as evenly as possible.

5.4 Constraints

The philosophy behind the CET is to minimize the amount of constraint, resulting in a design space that is as large as possible. Reality has proven that the design space explored in this research is too large for a computer to explore within reasonable time. Therefore, a number of constraints is introduced. The constraints find their origin either in practical objections or model simplifications.

- **One kind of propeller.** A configuration with both a FPP and a CPP is deemed infeasible. It is not impossible to have two different propellers, but in practice it does not occur. Furthermore, it simplifies the performance evaluation, as no distinction has to be made in propeller behaviour between multiple shafts.
- **High speed direct drive.** A configuration with a propeller directly driven by a high speed engine is regarded infeasible. The difference between the desired propeller speed and the engine speed is too large to consider such a configuration as feasible.
- **One kind of reciprocating propulsion engine.** One type of reciprocating propulsion engine can be used per configurations. For example, configurations with a high speed and a low speed diesel engine are deemed unfeasible. This choices is made as these types of configurations are hardly used and it simplifies the power management strategy significantly. This does not apply to the generator's diesel engine, so a low speed propulsion engine can be combined with a high speed generator engine.
- **Interchangeable fuels.** Certain fuels are interchangeable. Therefore, there is no added value in bunkering several such fuels, but it does take extra space, since separate tanks are required. As a results, configurations with comparable fuels are seen as undesired and thus infeasible. The interchangeable fuels are:

- MDO and HFO
- LNG, CNG and NH₃

The combination of NH_3 and natural gas might not seem interchangeable, but all components running on NH_3 are also compatible with natural gas.

- **One fuel per SOFC.** Despite the elimination of interchangeable fuels it can occur that the SOFC has two fuels available in a configuration, e.g. LNG and H_2 . In that case only one fuel is connected to the SOFC. The preference is given to either H_2 , as hydrogen is specifically installed for the fuel cells.
- **Symmetric topology.** When possible a symmetric topology is preferred over an asymmetric topology. This only affecting the allocation of the engines. If a symmetric allocation is possible it will be chosen.
- **Main electric motor.** The electric motor is seen as a main engine and not as a shaft engine. Consequently, when a directly driven propeller already has an engine, an EM cannot be added to this shaft. In reality, this would be possible. This choice is dictated by the fact that the power management strategy becomes significantly simpler and a power take off function is not available. The hybrid combination of EMs and internal combustion engines can be found in the CET, but this include a gearbox.
- **Electric bus connection.** It is assumed that all electrical components are connect via a central bus, yet this bus is not included as main component. As a result, all EGSs are directly connected to the electrical consumers in the adjacency matrix. When batteries are involved, another connection can be made from the EGSs, through the batteries, to the electrical consumers.

5.5 Verification

The concept generation model needs to be verified to ensure the model works and only feasible concepts are generated. In Table 7 the tests can be found that have been performed. The tests performed to check if constraints are applied correctly can be found in Table 8. A failed outcome means the model cannot work under the circumstances given in the test. At that point a warning is given to the user explaining why the model won't be able to run and what can be done to resolve the issue. A passed outcome means that the model was able to run and the expected results were obtained.

Table 7: Verification tests for concept generation model

Test	Outcome	Remark
Size of vector/matrix	Passed	Equal to amount of possible components
Component index in vector/matrix	Passed	
Single component per index	Passed	Element is either 1 or 0
Component is set 0	Passed	Done for every component
All propellers set to 0	Failed	Model cannot run, warning must be given
All GB set to 0	Passed	Only direct drive
All engines set to 0	Failed	Model cannot run, warning must be given
All EGS set to 0	Failed	Model cannot run, warning must be given
All fuels set to 0	Failed	Model cannot run, warning must be given
More props than engines available	Failed	Model cannot run, warning must be given
No fuel available for component	Passed	Component was not in configuration
Max amount of components	Passed	Done for every component
Max amount engine per GB	Passed	
Max amount of EGS	Passed	
Correct connection in matrix	Passed	Done for every type of connection
Engine division over prop/GB	Passed	

Table 8: Verification tests for constraints of concept generation model

Test	Outcome	Remark
One kind of propeller	Passed	
One kind of reciprocation engine	Passed	
High speed direct drive	Passed	Both in vector and matrix generation
Comparable fuels	Passed	
One fuel per SOFC	Passed	Preference also checked
Symmetric topology	Passed	
Main electric engine	Passed	
Electric bus connection	Passed	

6

Power Management Strategy

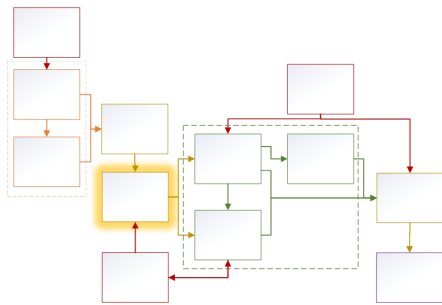


Figure 9: Chapter location within model, based on Figure 5

The power management (PMS) dictates how much power is installed and how much power is generated by the various components. Four PMSs can be distinguished: the installation of mechanical power, the installation of electrical power, the division of mechanical power generation and the division of electrical power generation. Figure 9 shows the position of this chapter within the complete model structure. The input for this sub-model is provided by the concept library and the operational profile. The required installed power per component is passed on to the sizing sub-tool, while the power usage per component is sent to the performance sub-model.

It must be noted that the minimum required power per component does not have to be equal to the actual installed power. The PMS computes how much installed power each component must have as a minimum, after which the sizing sub-model determines the actual installed power for that part. Larger components may be installed for robustness and/or efficiency reasons. Furthermore, the intended use of a component in the installation phase may not correspond with the actual use of that part in the performance phase. This is the result of two separate PMSs that need to optimise for varying situations and the sizing sub-model that may install larger components than dictate by the PMS. Moreover, no single correct PMS exists, as every concept and operational profile is slightly different. The chosen PMS must be applicable in every situation. As a result, global PMSs have been developed. These strategies are guaranteed to be suitable for every mission and configurations.

6.1 Installed mechanical power

For every configuration, the total installed mechanical power must be divided between the various engines. This division is controlled by a PMS, that dictates how much power gets installed per component, based on their intended usage. The applied PMS is a deterministic rule-based strategy. This type of PMS often will lead to robust and rigid strategies, however these strategies are often not totally optimised. The choice has been made to not use a flexible PMS, which would optimise the PMS for every situation, as this would require a lot of development time, computational time and a detailed mission profile.

The PMS must find a single unique solutions the division of power among the components. Therefore, rules are applied to constraint the optimisation of power division and ensure a single unique solution. Based on the stated rules, the PMS can be formulated as a set of equations that can be solved to compute the power output of the different engines. The stated rules are split into two categories: main rules, applicable to every concept and extra rules, applicable to certain configurations. For the set of equations the following variables and sets are used:

S	= set of shafts in configuration
s	= index for shaft
I, J, K	= set of engines of a certain engine type, I is the most common engine, followed by J and K
I_s, J_s, K_s	= set of engines of a certain engine type installed on shaft s
i, j, k	= index for engine of certain engine type
x, y, z	= power of an engine of a certain engine type, x is the most common engine, followed by y and z

6.1.1 Main rules

There are five rules that are applicable to every configurations, these main rules are:

1. **Minimize power.** Similar to other optimisation problems, an objective function is applied to come to a single unique solution. Here, the objective function aims to minimize the amount of installed power. As there is no constraint that limits the maximum amount of power per component, the problem is unbounded in that direction. The state objective function solves this challenge.

$$\text{Min} \left(\sum_{i \in I} x_i + \sum_{j \in J} y_j + \sum_{k \in K} z_k \right) \quad (4)$$

An exception is made for a so called 'extra engine'. An extra engine is an engine that is not needed in order to meet rule 2 or 3. This engine can thus be given any size, depending on what it will be used for. In this CET, extra engines will be employed as cruising engine and thus be given the power that is most often used in the mission profile. An example is shown in in Figure 13. The mathematical formulation is slightly changed to accommodate this exception.

$$\begin{aligned} \text{Min} \left(\sum_{i \in I - \{i_{extra}\}} x_i + \sum_{j \in J - \{j_{extra}\}} y_j + \sum_{k \in K - \{k_{extra}\}} z_k \right) \\ x_{i_{extra}} = P_{cruise} \\ y_{j_{extra}} = P_{cruise} \\ z_{k_{extra}} = P_{cruise} \end{aligned} \quad (5)$$

2. **Total power.** The total installed power must be equal or greater than the maximal required power. This rule originates from the fact that vessel should be able to fulfill its mission, stated in the operational profile. In some cases more power can be installed than needed to fulfill the mission.

$$P_{required} \leq \sum_{i \in I} x_i + \sum_{j \in J} y_j + \sum_{k \in K} z_k \quad (6)$$

3. **Shaft power.** The installed power per shaft must be equal or greater than maximal required power divided by the number of shafts. This rules arises from the desire to sail at full speed without using the rudder, which would lead to extra resistance. In order to accomplish this every shaft should be able to deliver its equal part of the total needed power. This rule is essentially a more specific version of rule 2, rendering rule 2 unnecessary. However, rule 2 will apply to the installation of electrical power and is thus retained.

$$\begin{aligned} P_s &= P_{total} / n(S) & \forall s \in S \\ P_s &\leq \sum_{i \in I_s} x_i + \sum_{j \in J_s} y_j + \sum_{k \in K_s} z_k & \forall s \in S \end{aligned} \quad (7)$$

4. **Similar engines.** Engines of the same type should have the same installed power. This rules emanates from the easy of use, maintenance and reduced cost that comes with using the same engines compared to using different size engines. Furthermore, this rule will lead to symmetric configurations where possible. However, this rule eliminates the possibility of a father-son configuration. This option is not included in the CET, as it would introduce a new degree of freedom in the PMS. For this degree of freedom a new constraint would have to be written, to ensure a unique solutions will be found. The limited research time prevented the development of such a new constraint.

$$\begin{aligned} x_i &= x_i & \forall i \in I \\ y_j &= y_j & \forall j \in J \\ z_k &= z_k & \forall k \in K \end{aligned} \quad (8)$$

An exemption to the rule is made in the case of a configurations with multiple shafts, where at least one shaft is directly driven and one shaft has a gearbox. The engines on the directly driven shaft and on the geared shaft do not have to be of the same size as this could lead to multiple big engines on the gearbox shaft. An example of this can be found in Figure 14. For this exception the formulation of the rule is slightly changed to exclude direct drive engines.

$$\begin{aligned}
x_i &= x_i \quad \forall i \in I - \{i_{direct}\} \\
y_j &= y_j \quad \forall j \in J - \{j_{direct}\} \\
z_k &= z_k \quad \forall k \in K - \{k_{direct}\}
\end{aligned} \tag{9}$$

5. **Real positive power.** Every installed component should get an amount of installed power. A component with no installed power can be seen as a nonexistent component, which would result in the configuration no longer being unique. Furthermore, a component cannot have negative or imaginary installed power, which is a statement purely for mathematical correctness.

$$\begin{aligned}
x_i &> 0 \text{ and } x_i \in \mathbb{R} \quad \forall i \in I \\
y_j &> 0 \text{ and } y_j \in \mathbb{R} \quad \forall j \in J \\
z_k &> 0 \text{ and } z_k \in \mathbb{R} \quad \forall k \in K
\end{aligned} \tag{10}$$

6.1.2 Extra rules

After the application of the main rules, a single unique solution may not be found. For example, when multiple engine types are connected to the same shaft. Therefore, extra rules are imposed to ensure a single unique solution. The extra rules are linked to the number of engine types within a configuration, as that is the number of extra degrees of freedom. As mentioned in Paragraph 5.4, only one type of reciprocating engine can be installed per configuration. Therefore, there are three possible engine types per concept.

One engine type

With one engine type, no extra degree of freedom is introduced. Therefore, the main rules suffice. It must be noted that in this case the sets J and K are empty, as there is only one type of engine.

Two engine types

With two engine types in a configuration, an extra degree of freedom may be introduced, resulting in no unique solution. An example can be found in Figure 11. In the case of no unique solution, a new rule is implemented. This rule can also be used to make the PMS more efficient. The chosen approach is that the most common engines are given the amount of power that meets the power demand for the majority of the mission. This majority is given as a percentage of total mission time, where the percentage can be changed by the user of the tool. The other engine type can then be seen as booster engines, which are only employed in case maximal speed must be reached. When both engine types have an equal number of engines installed, the preference is given to reciprocating engines, then electric motors and then gas turbines.

$$\sum_{i \in I - \{i_{direct}\}} x_i = P_{majority} \tag{11}$$

Three engine types

With three engine types in a configuration, another degree of freedom may be introduced. The two-engine-types rule is applied, and in the case of no unique solution, an additional rule is implemented. An example can be found in Figure 12. The second most common engines are used as manoeuvring engines, meaning the installed power is equal to the lowest power demand found in the mission profile. It should be noted that in this case every engine has full manoeuvring power. This is a result of the fact that during manoeuvring every propeller should be able to produce the full manoeuvring power. When there is no one type of common engine, the same preference as with two engine types is used.

$$y_j = P_{manoeuvring} \quad \forall j \in J - \{j_{direct}\} \tag{12}$$

6.1.3 Examples

Some calculation examples have been added to clarify the power management strategy. The total needed power in all examples is set to 10 MW. The majority power is set to 6 MW, the cruising power to 2 MW, while the manoeuvring power has been set to 1 MW.

One engine type

Figure 10 shows a configurations with one engine type. With one engine type installed, only the main rules apply. The minimal shaft power is 5 MW (rule 3), both engines must deliver the same amount of power (rule 4) and a minimal amount of power must be installed (rule 1). This leads to both diesel engine having 5 MW of installed power.

$$P_{total} = 10MW$$

$$P_s = 5MW$$

$$P_{DE} = 5MW$$

$$P_{installed} = 10MW$$

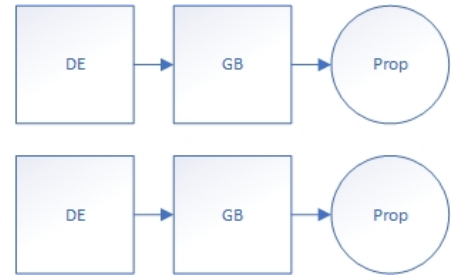


Figure 10: One engine type

Two engine types

Figure 11 shows a configurations with two engine types. If only the main rules would apply, the installed power of the diesel engines and electric motors cannot be determined, as their installed power is interchangeable. Therefore, a new rule is introduced, as discussed previously. Since both engine types have two engine types installed, the preference is given to the diesel engines to produce the majority power of 6 MW. This 6 MW is divided equally over the diesel engines, as dictated by rule 4. The remaining amount of power (4MW) is divided equally over the electric motors.

$$P_{total} = 10MW$$

$$P_s = 5MW$$

$$P_{majority} = 6MW$$

$$P_{DE} = 3MW$$

$$P_{EM} = 2MW$$

$$P_{installed} = 13MW$$

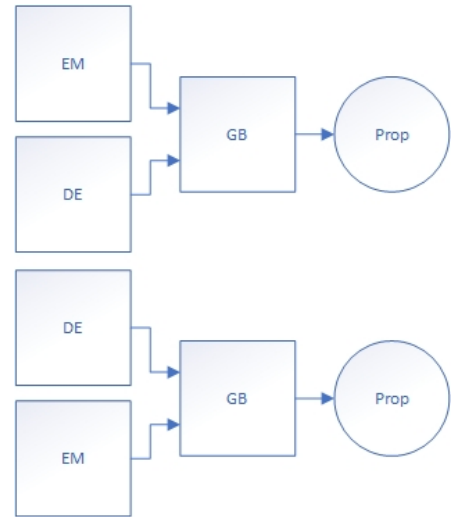


Figure 11: Two engine types

Three engine types

Figure 12 shows a configurations with three engine types. Again, a new rule is introduced, as previously discussed. The majority power is divided between the diesel engines. Every electric motor is give the manoeuvrability power. The remaining power is divided between the gas turbines.

$$P_{total} = 10MW$$

$$P_s = 5MW$$

$$P_{majority} = 6MW$$

$$P_{manoeuvring} = 1MW$$

$$P_{DE} = 3MW$$

$$P_{EM} = 1MW$$

$$P_{GT} = 1MW$$

$$P_{installed} = 10MW$$

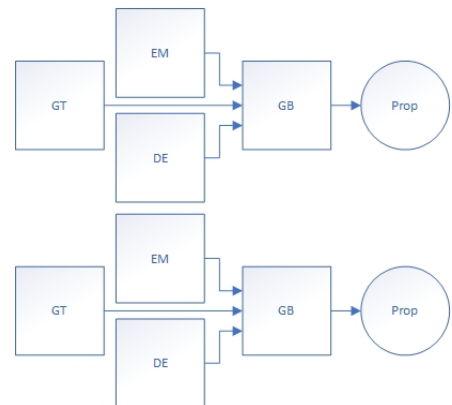


Figure 12: Three engine types

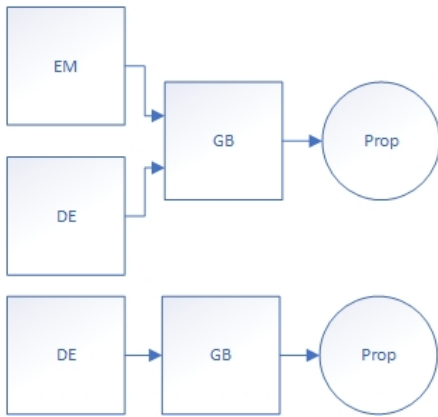


Figure 13: Extra engine

Extra engine

Figure 13 shows a configurations with an extra engine. The shaft power is still 5 MW (rule 3), so the diesel engine on the second shaft must deliver 5 MW. Rule 4 dictates that the identical diesel engine on the other shaft must also has 5 MW installed. Therefore, the electric motor is not needed to obtain the needed shaft or total power. This engine is seen as an extra engine and thus given the cruise power.

$$P_{total} = 10MW$$

$$P_s = 5MW$$

$$P_{cruise} = 2MW$$

$$P_{DE} = 5MW$$

$$P_{EM} = 2MW$$

$$P_{installed} = 12MW$$

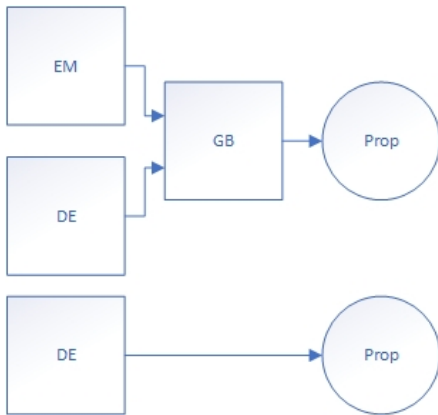


Figure 14: Direct drive

Direct drive

Figure 14 shows a configurations with a direct drive and gearbox drive. The direct drive is given as an exception on rule 4, meaning that the diesel engines don't have to have the same amount of installed power. The diesel engine on the direct drive is given 5 MW, due to rule 3. On the other shaft two engine types are installed, resulting in an extra degree of freedom. The diesel engine on this shaft is given majority power, making the electric motor an extra motor and thus a cruising engine. It can be argued that this strategy does not make sense, but this is a result of the atypical configuration. Most probably this configuration will not score high in the evaluation, but that is a results in and of itself.

$$P_{total} = 10MW$$

$$P_s = 5MW$$

$$P_{DE,Direct} = 5MW$$

$$P_{DE,GB} = 6MW$$

$$P_{EM} = 2MW$$

$$P_{installed} = 13MW$$

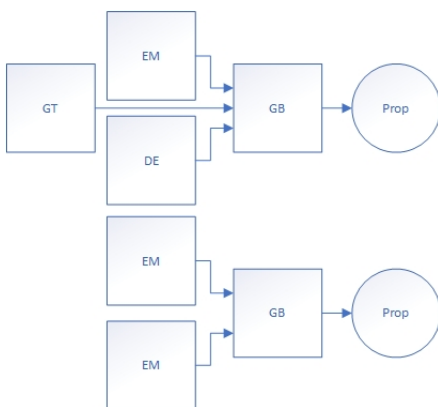


Figure 15: Random configuration

Random configuration

Figure 15 shows a random configuration added as a last calculation example. First the main rules are applied. The shaft power is 5 MW, which the two electric motor on the second shaft need to produce together and equally, meaning they both have 2.5 MW installed. On the first shaft there are now 2 unknown engine types, leading to the introduction of the majority rule. The majority power of 6 MW is given to the diesel engine, making the gas turbine an extra (and thus cruising) engine. Again, it can be argued that this strategy makes no sense, but for the same argument given in the previous example, this is accepted.

$$P_{total} = 10MW$$

$$P_s = 5MW$$

$$P_{EM} = 2.5MW$$

$$P_{DE} = 6MW$$

$$P_{GT} = 2MW$$

$$P_{installed} = 15.5MW$$

6.1.4 Robustness, extra power and the degree of hybridisation

The application of extra engines enables the possibility to install extra power not deemed necessary to fulfill the mission. Examples of this can be found in the previous paragraph. It can be argued that since these extra engines are not required, they should not be added to the configuration, as it will most likely not lead to an optimised design. However, omitting an engine will lead to a different configuration, one similar to a configuration that is already in the configuration library. This fact can be guaranteed by the way the various configurations are generated, where every feasible solution is produced. Therefore, a configuration with an extra engine can be seen as a regular configuration plus the extra engine. This extra engine does serve a purpose as it introduces a higher level of robustness in comparison with the regular configuration it stems from. In this way the difference in robustness between different configurations can be seen.

It may be noticed that the term 'degree of hybridisation' is not found in the description of the PMS, even though hybrid configurations are possible. The degree of hybridisation defines which part of the total power is produced by electrical engines. This degree is often provided as input to power division problems, such as the one above. However, in this case, the degree of hybridisation is a consequence of the power division strategy. The PMS divides the power, based on the operational profile. Therefore, the power of the EMs is also dependent on the operational profile. Consequently, the degree of hybridisation is a result of the operational profile.

6.1.5 Verification

The PMS for installed mechanical power is verified with the test found in table 9.

Table 9: Verification test for installed mechanical power

Test	Outcome	Remark
Total power	Passed	
Shaft power	Passed	
Similar engine	Passed	
Minimal power	Passed	
Positive real power	Passed	
One engine type	Passed	
Two engine types	Passed	Most common engine and correct power
Three engine types	Passed	Most common engine and correct power
Extra engine	Passed	Cruise power is installed
Direct drive	Passed	Difference between similar engines
Majority power	Passed	Majority power is calculated
Cruise power	Passed	Cruise power is calculated
Manoeuvring power	Passed	Manoeuvring power is calculated

6.2 Installed electrical power

Similar to the mechanical components, a PMS is needed to determine the minimal required installed power per component. Again, a deterministic rule-based strategy is applied, where the rules can be formulated as equations. Comparable to the previous PMS, the rules are divided into main rules and extra rules.

6.2.1 Main rules

The electrical PMS is almost identical to the mechanical PMS. Therefore, the same five main rules are applied to the electrical PMS, apart from one change. Since the electrical grid does not contain a shaft and is significantly simplified, rule 3 is no longer implemented. As a result, rule 2 becomes relevant again and 'extra components' are no longer possible. Thus, the four applied main rules are:

1. **Minimize power**
2. **Total power**
3. **Identical components**
4. **Real positive power**

6.2.2 Extra rules

Again, extra degrees of freedom are introduced, if there are multiple components types within one concept. Since there are three EGS components, two extra degrees of freedom could be present. Therefore, two extra rules must be developed to ensure a single unique solution.

Generator and a fuel cell

When there are generators and fuel cells within a concept, a distinction can be made between the two category. This discrimination is made as the fuel cells do not necessarily consume fossil fuel and therefore have a distinctive fuel consumption- and emission profile. Thus, a client may wish to promote these alternative components. A Degree of Fuel Cells (DoFC) is introduced to accomplish the differentiation between fuel cells and generators. The DoFC can be seen as the electrical counterpart of the degree of hybridisation. Unlike the degree of hybridisation, the DoFC is determined by the user and given directly as input to the PMS. The effect of the DoFC on the power division can be found in equation 13.

$$\begin{aligned} P_{Fuelcells} &= DoFC \cdot P_{total} \\ P_{Generators} &= (1 - DoFC) \cdot P_{total} \end{aligned} \quad (13)$$

PEMFC and SOFC

When both PEMFCs and SOFCs occur in a configuration another division has to be made. Due to the poor dynamical load behaviour of the SOFC, it is desirable to keep the load on the SOFC as constant as possible. Therefore, the total power of the SOFCs is equal to the base load found in the electrical mission profile, as shown in equation 14. The PEMFCs make up the difference between the fuel cell power and the base electrical power. If the minimal electrical power is greater than the fuel cell power, the fuel cell power is evenly divided over all fuel cells.

$$P_{SOFC,total} = P_{elec,min} \quad (14)$$

6.2.3 Batteries

Electrical power can be produced by the batteries, yet the power delivered by the batteries does not count towards the total power production. This means that the components of the EGS must be able to provide all the electrical power, without the assistance of the battery. This design choice is based on the desire to always be able to perform every mission type at any moment, independent of the state of charge of the batteries. If the battery would be included in the maximal power production, the missions capabilities of the vessel would be reduced when the battery is empty. Thus, the batteries are not included in the installation PMS. The size of the batteries is determined by the sizing tool.

6.2.4 Verification

The PMS for installed electrical power is verified with the tests found in Table 10.

Table 10: Verification tests for installed electric power

Test	Outcome	Remark
Total power	Passed	
Similar power	Passed	
Minimal power	Passed	
Positive real power	Passed	
DoFC	Passed	
Constant power SOFC	Passed	Minimal value is calculated and assigned
Low fuel cell power	Passed	Load is shared between PEMFC and SOFC

6.3 Mechanical power usage

During the mission, the usage PMS has to determine which engines is producing power during a certain mission element. Not every engine may be needed to provide the required power and having multiple engines work at low power may not result in the most efficient operation. Therefore, the usage PMS determines the optimal combination of engines for every mission element. A simple algorithm is employed that composes every combination of engines and their combined optimal power. The optimal power of an engine is defined as the power at continuous services rating. The engine combination closest to, but higher than, the required power is chosen and utilised.

The efficiency curves of the various engine types differ, enabling the optimisation of load ratios between the engines. The efficiency of an internal combustion engine decreases significantly at low load ratios, while the efficiency of an electric motor remains relatively high at reduced load ratios. Therefore, an chosen engine combination containing both engine types can gain efficiency by differentiating between the respective load ratios. In such a case, the internal combustion engines operate at their nominal working point and the electrical engines provide the remaining required power. For this situation, the respective load ratios of all engine types can be calculated with equation 15.

$$\begin{aligned}
 LR_{ICE} &= 1 \\
 LR_{EM} &= \frac{P_{mission} - P_{ICE,total}}{P_{EM,total}}
 \end{aligned} \tag{15}$$

6.3.1 Torque check

A reciprocating engine can produce limited torque at low engine speed. Therefore, it may occur that the chosen engines are not able to deliver enough torque and thus power. Accordingly, a torque check is introduced in the usage PMS, which compares the generated torque with the required torque. When the developed torque is insufficient, the next engine combination in terms of optimal power is selected. This process continues until sufficient torque can be supplied. Rule 2 of the installation PMS guarantees that there is always a combination of engines that can provide the needed torque and power.

6.3.2 Verification

The PMS for used mechanical power is verified with the tests found in Table 11.

Table 11: Verification tests for mechanical power usage

Test	Outcome	Remark
All combinations	Passed	
Optimal combination	Passed	
Load ratio	Passed	Hybrid strategy included
Power per engine	Passed	
Torque check	Passed	Next engine combination is chosen

6.4 Electrical power usage

The PMS for electrical power usage is more complex than the above mentioned mechanical usage PMS, due to the addition of batteries. The battery can charge and discharge during a mission element, leading to an increase or decrease in the electrical power demanded from the other components. Whether the battery is charged or discharged depends on the state of charge of the battery, the required electrical power and the available electrical power generation.

6.4.1 Battery management

The aim of the battery management is to optimise every mission element by charging or discharging the battery. Similar to the MPEs, each EGS type has an optimal operating point. For the generators this is at nominal load, while for fuel cells this is set at 10% load (which can be changed by the user). The difference between the actual working point and the optimal working point can be covered by the batteries, either by charging or discharging.

Figure 16 shows an example of the steps the battery management takes. This values used in this example are not based on actual values. The electrical power demand is displayed along with all combination of optimal power. Moreover, the current battery energy is found in orange on the right axis. The accompanying equation can be found below. (a) The PMS starts with computing the available discharge power of the battery over a mission element by looking at the available battery energy end the element duration (equation 16). The maximal discharge power of the battery is taken into account. The resultant power demand is equal to the power of the element minus the available discharge power (equation 17). This power demand is utilised to find the optimal EGS combination (equation 18). In this case that would be 150 kW, meaning that a component can be switched off compared to the power production of 300 kW. (b) Next, the actual discharged power and consumed energy are calculated (equation 19) and the current energy of the battery is updated. (c) It may occur that the available discharge power is not enough to reach a lower optimal combination. (d) In that case, the battery is charged, resulting in an increase in current battery energy. Again, an optimal working point is achieved. The maximal charge power is limited by the capacity of the battery to prevent overcharging of the battery (equation 20).

$$P_{avail,discharge} = \min \left(P_{max,discharge}, \frac{E_{battery}}{T_{element}} \right) \quad (16)$$

$$P_{demand} = P_{element} - P_{avail,discharge} \quad (17)$$

$$P_{optimal} \geq P_{demand} \quad (18)$$

$$P_{battery} = P_{element} - P_{optimal} \quad (19)$$

$$P_{max,charge} = \min \left(P_{optimal} - P_{element}, \frac{E_{max,battery} - E_{battery}}{T_{element}} \right) \quad (20)$$

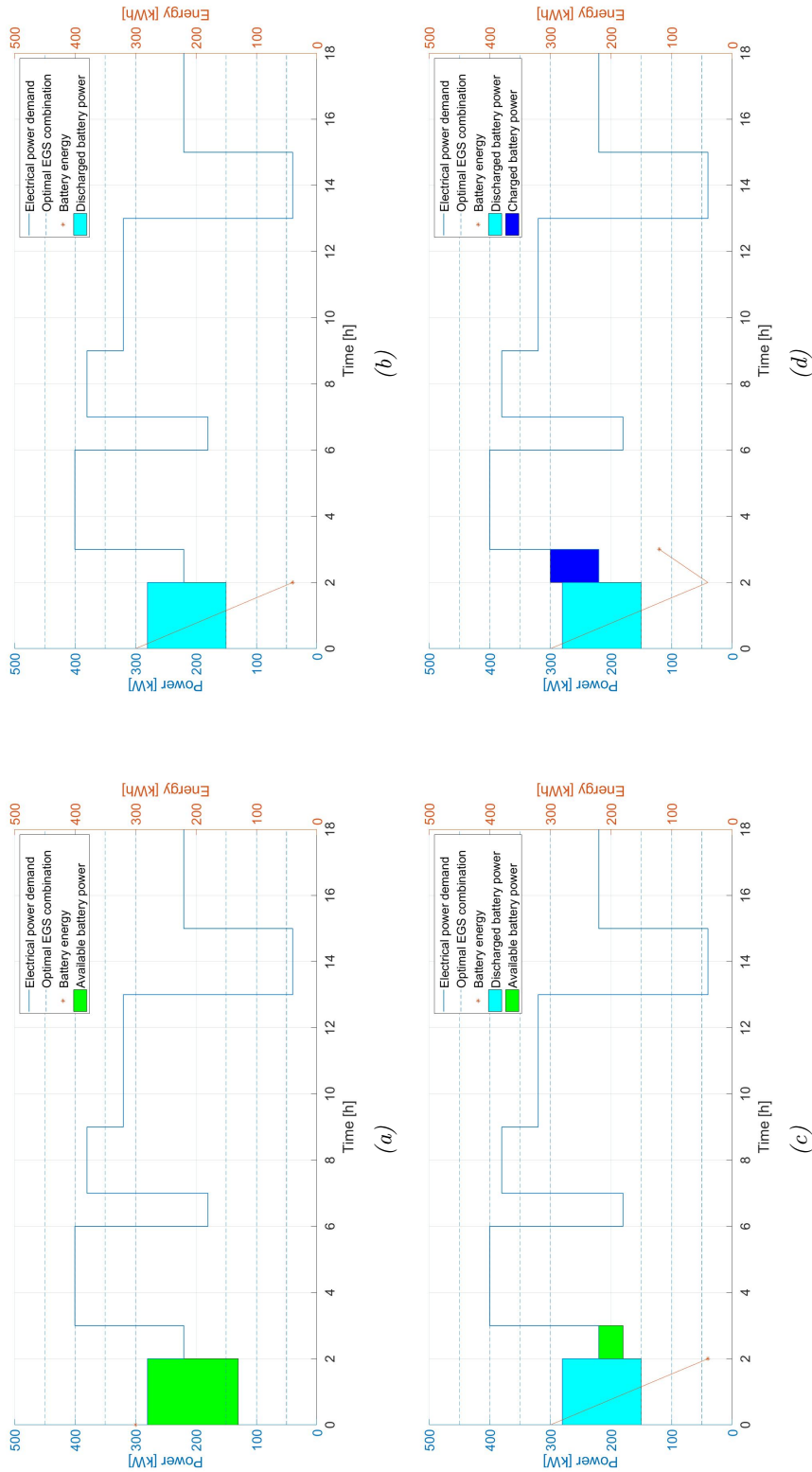


Figure 16: Example of the battery management for two mission elements

6.4.2 EGS management

Similar to the mechanical usage PMS, the electrical usage PMS has to decide which components provide power during a mission element. The same simple algorithm is employed to produce every combination of components and their resulting power. As mentioned in the previous paragraph, the optimal EGS combination is chosen based on the power demand after the batteries have been applied.

The optimal load point of the fuel cells is set to 10% load. In theory, the highest efficiency of a fuel cell can be found at 0% load. However, this would mean that fuel cells are not included in the optimal combination. A balance must be struck between the theoretical optimal point and the practical application of the fuel cells. Since the optimal and nominal working point are not the same for fuel cells, a situation may arise where the combined optimal power is insufficient. In this case, the load ratio of any generator is set to '1', while the remaining power is distributed equally between the fuel cells, as shown in equation 21. This is similar to the hybrid strategy of the mechanical usage PMS, found in equation 15

$$\begin{aligned} LR_{Gen} &= 1 \\ LR_{FC} &= \frac{P_{mission} - P_{Gen,total}}{P_{FC,total}} \end{aligned} \quad (21)$$

6.4.3 Verification

The PMS for used electrical power is verified with the tests found in Table 10.

Table 12: Verification tests for electrical power usage

Test	Outcome	Remark
Battery capacity	Passed	Checked after every mission element
Available discharge power	Passed	
Used battery power	Passed	
Max charge power	Passed	
All combination	Passed	
Optimal combination	Passed	
Load ratio	Passed	Hybrid strategy included
Power per component	Passed	

7

Sizing

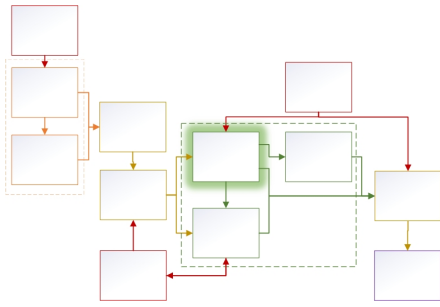


Figure 17: Chapter location within model, based on Figure 5

The sizing sub-model has three functions. It determines the actual installed power of every component, computes the corresponding size and weight and designs the components in detail. Figure 17 shows the position of this chapter within the complete model structure. The sub-model uses the required installed power per components and the client preferences as input. The actual installed power is passed on to the performance and robustness tool. Furthermore, the component details are also given to the performance sub-model. Lastly, the size and weight of the component is sent to the MCA to convert to a score.

The sizing of a gas turbine and a SOFC will be discussed in detail, as these are new components. The size of the CPP is not included in the CET. Every model taken from van Dijk [12] or ten Hacken [18] has been re-verified (and re-validated if possible). Modification made to these existing models will be described briefly. If the sizing of a component has not changed compared to the version made by

van Dijk or ten Hacken, the component will not be discussed.

The introduction of robustness may lead to a desire the install components with a certain amount of reserve power capacity. Therefore, the option to install more power is included for all MPE and EGS components. Essentially, multiple variations at different power outputs are designed, after which the IDeA is applied to determine the optimal design. As discussed, the client preference are applied within the IDeA to define what optimal is. Paragraph 2.2 showed that the MCA employed within the IDeA might not function properly when enormous designs are considered. Therefore, the maximum power factor is applied within the sizing tool.

7.1 Gas turbine

Gas turbines are energy converters, converting chemical energy to mechanical energy via thermal energy. Gas turbines are known for there high specific power, which makes them ideal for high speed, low weight application. In the CET, a simple cycle twin-shaft turbine is modelled, as this this is the type of gas turbine that is installed in the newest frigates of the British Navy [19] and the destroyers of the US Navy [20]. The type installed in both these vessels is the Rolls-Royce MT-30, on which parameters of the model will be based.

7.1.1 Sizing a gas turbine

The sizing of a gas turbine is less obvious than the sizing of for instance a diesel engine. This is because the relation between the dimensions and the performance of a gas turbine is less specific. Therefore, trends found between actual gas turbine are used to determine a relation between power output and dimensions. Van Es [21] argued that the width and height are proportional to the diameter of the compressor and turbine, which in turn is proportional to the square root of the power of a gas turbine, as can be seen in equation 22. He also argued that the length of the turbine is dependent on the number of compressor stage. This number is linked to the power of the gas turbine, so a relation between the power output and the length of the gas turbine would be expected.

$$W \text{ and } H \propto D \propto \sqrt{P} \quad (22)$$

When looking for trends in existing gas turbines, van ES found the relations shown in Figure 18. These equations do not quite show the proportionality as expected in equation 22. The figure shows that the trendlines fit quite well with a standard deviation of 0.081, 0.018 and 0.030 for the length, width and height respectively. A disadvantage of the method used by van Es is that it does not differentiate between different cycle types. When implementing a simple cycle gas turbine in the CET, the trendlines may give a slightly distorted image, due to the other cycles on which the figure is based. Van Es mentioned this himself. For example, an inter-cooled regenerative cycle is 1.5 times higher than a simple cycle, due to the heat exchanger on top of the turbine.

Since the simulated gas turbine is modelled after the Rolls-Royce MT-30, which is a simple cycle gas turbine, the relations of van Es can be corrected for the specific dimensions of this gas turbine. These dimensions can be found in Table 13. In this manner, the dependency found by van Es still applies, while also considering the specific type of simulated gas turbine. Figure 19 shows both the specific dimensions according to van

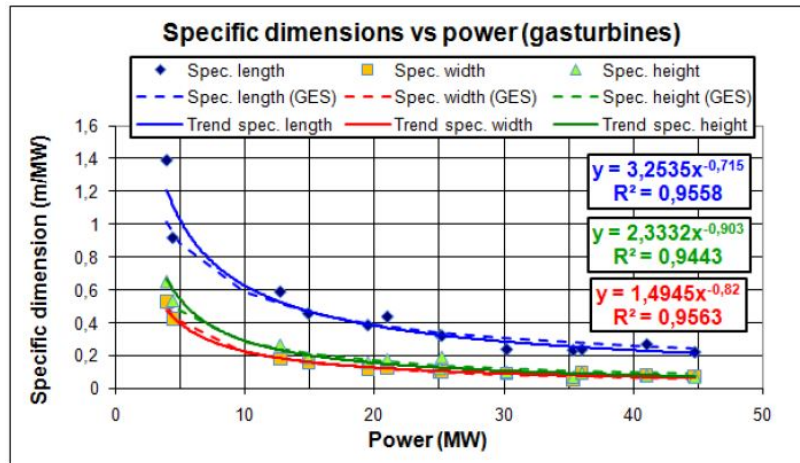


Figure 18: Specific dimensions (m/MW) versus rated power (MW) for a database of gas turbines [21].

Es, as well as the corrected functions used in the model and the dimensions of the Rolls-Royce MT-30. The functions applied in the model can be found in equation 23. The mass of the gas turbine is scaled linearly with the volume of the gas turbine with the use of the density of the MT-30. The density is derived from the dimensions and mass as presented in Table 13.

$$\begin{aligned}
 L &= (3.04 \cdot P_B^{-0.72}) \cdot P_B \\
 W &= (1.39 \cdot P_B^{-0.82}) \cdot P_B \\
 H &= (2.45 \cdot P_B^{-0.90}) \cdot P_B
 \end{aligned} \tag{23}$$

The dimensions presented in equation 23 are the dimensions of the actual gas turbine itself and the auxiliary equipment attached to it. Since gas turbines have a relatively large air consumption, a large air mass flow is required. As a result the inlet and outflow duct of a gas turbine can be of substantial size, especially considering that these ducts will likely run over the complete height of the vessel. Nevertheless, the dimensions of the air ducts is not included in the model for two reasons. Firstly, the air ducts of other equipment, though significantly smaller, are also not included in the model. Secondly, the actual dimensions of the air ducts are a function of the location of the gas turbines within the general arrangements, which lies beyond the scope of this research.

7.1.2 Optimising the gas turbine design

As mentioned in the introduction of this chapter, multiple variations of the gas turbine are designed, each with a different power output. To enable the IDeA to choose an optimal design, the gas turbine should be evaluated on all KPIs. Therefore, the expected performance of every design is computed, based on the method discussed in Paragraph 8.1. The evaluation looks at the performance of the gas turbine at the load defined by the PMS, as this is the intended application of the gas turbine. An example is given. The PMS defines that a gas turbine has to develop 10 MW. Designs from 10 MW up to 30 MW are produced.

Table 13: Dimensions of the Rolls-Royce MT-30 gas turbine [22].

Parameter	Unit	Value
Power	MW	40
Length	m	8.70
Width	m	2.70
Height	m	3.55
Mass	ton	32
Density	ton/m ³	0.38

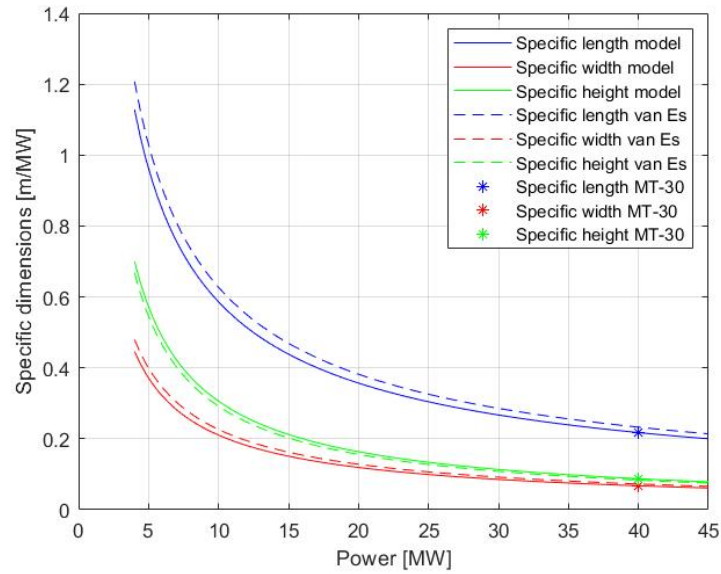


Figure 19: Specific dimensions (m/MW) by van Es, the model and Rolls-Royce MT-30

The efficiency, emissions and signatures of all designs is computed for an output of 10 MW. Moreover, the robustness of all designs is calculated. Next, all designs are scored per KPI and the client preference are introduced as weight factors. Lastly, the optimal design is chosen.

7.1.3 Verification

The sizing of the gas turbine is verified and validated with the tests found in Table 14.

Table 14: Verification and validation tests for gas turbine sizing

Test	Outcome	Remark
Length	Passed	Validated with Rolls-Royce data
Width	Passed	Validated with Rolls-Royce data
Height	Passed	Validated with Rolls-Royce data
Weight	Passed	Validated with Rolls-Royce data
Performance	Passed	Validated in Paragraph 8.1
IDeA	Passed	Verified for this sub-model

7.2 Solid-oxide fuel cell

Solid oxide fuel cells directly convert chemical energy into electrical energy, without the need for thermal energy. Due to the lack of combustion, a fuel cell is often seen as an important step towards emission-free power generation. There are multiple SOFC types, the most common ones being a planar, micro-tubular or tubular design [23]. The tubular SOFC is simulated in the CET, as they have been shown to work in larger configuration, have the possibility to internal reforming and have relatively good dynamic behaviour [14]. A disadvantage of this design is the lower power density, due to the way the tubes are stacked, leaving space in between them.

7.2.1 Sizing a SOFC

The surface area of a cell and the number of cells are the main factors when sizing a SOFC. The surface area dictates the current a cell can produce, as is explained in Paragraph 8.2. Since a tubular design is used, the surface area can be changed by varying the length or diameter of the tube. In the CET, the diameter is kept constant, while the length is varied. The dimensions of a tube can be found in Table 15. The length of a single cell does not influence the internal losses and achieved cell voltage [24]. The number of cells is a function of the voltage and power a single tube can produce. In order to meet the grid voltage, multiple cells are connected in series. The power of a stack is equal the total voltage times the cell current. By installing multiple stacks the total power can be increased to match the required installed power. The mathematical expression for this process can be found in equation 24. Since the number of cells and stacks is discreet, a ceiling function is utilised to ensure enough power is developed. As a result, it may occur that a design can produce more power than intended. The cell voltage is obtained with the use of a polarisation curve, which is further explained in Paragraph 8.2

$$\begin{aligned}
 N_{cell} &= \left\lceil \frac{E_{grid}}{E_{cell}} \right\rceil N_{stack} \\
 N_{stack} &= \left\lceil \frac{P_{req}}{P_{stack}} \right\rceil = \left\lceil \frac{P_{req}}{E_{stack} I_{cell}} \right\rceil
 \end{aligned} \tag{24}$$

Figure 20 shows a stacking arrangement of a tubular SOFC. It can be seen that the tubes are stacked right on top of each other, due to their interconnection. This makes calculating the total dimensions of all the tubes relatively straightforward. The tubes are seen as a rectangular cuboid, with a height and width equal to the diameter plus double the thickness. The figure also shows that the SOFC consists of more than just tubes. Accordingly, the cuboid volume is multiplied by a volume factor to achieve the volume of the actual SOFC. Little information is published about the total dimensions of a SOFC versus the volume of the cells. As a result, no volume factor specific to a SOFC could be calculated. Therefore, the volume factor applied to the the SOFC is copied of the PEMFC. This volume factor is most likely not accurate for a SOFC, but at least to a limited extent the additional volume is taken into account. Similarly, the density of SOFC could not be computed and the value of the PEMFC is taken. The density of a SOFC is most likely lower, due to the relatively large quantity of air between the tubes. Both the volume factor and the density can be found in Table 15.

In addition to the actual SOFC, other subsystems are required to operate the fuel cell and provide electricity to the electrical grid. The main subsystems are compressors, turbines, heat exchangers and inverters. The heat exchangers are not modelled in the CET for two reasons. Firstly, the heat exchangers of other main components are also not modelled. Secondly, in order to accurately model a heat exchangers significantly more details have to be known. Since the SOFC is turbocharged, a turbine is needed to power the compressor.

Table 15: Dimensions of a SOFC tube and overall SOFC factors.

Dimension	Unit	Value	Source
Length	m	1.0 - 1.8	[23, 24, 25]
Diameter	mm	22	[23, 25]
Thickness	mm	2.2	[23, 25]
Volume factor	-	2.1	[18]
Density	ton/m ³	1.51	[18]

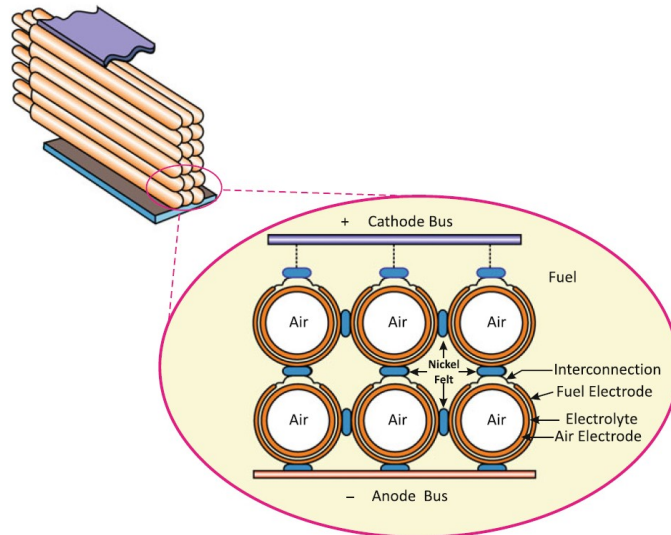


Figure 20: Tubular fuel cell stacking [25].

The sizing of the compressor done according to the method applied by van Dijk [12]. It is assumed that the turbine has the same dimensions as the compressor. The inverter will be discussed separately later on in the chapter.

7.2.2 Optimising the SOFC design

When designing the optimal SOFC, there are two variables that can be optimised, namely the total power output and the surface area of a cell. The latter mainly affects the number of cells and stacks and to a lesser extent the performance of the fuel cell. Therefore, the surface area of a cell is optimised first for every power output, after which the optimal power output is chosen by the IDeA. However, the first step the tool has to take is determining the optimal current density. Figure 30 in Paragraph 8.2 shows that the maximal cell power is achieved at various current densities, depending on the operating conditions of the fuel cell. This does not only depend pressure, but also on temperature and fuel composition, among other things. Thus, the optimal current density is established to ensure maximal cell power and overall power density. Once the optimal current density is computed, the CET constructs multiple tubes of different length and calculates the according number of cells, stacks and overall dimensions. The tube length with the lowest total fuel cell volume is chosen for that power output. Similarly to the gas turbine, the performance of the designs with various power outputs is evaluated. The IDeA chooses the optimal design based on the client preferences.

7.2.3 Verification

The sizing of the gas turbine is verified with the tests found in Table 14.

Table 16: Verification tests for SOFC sizing

Test	Outcome	Remark
Current density	Passed	Optimal found
Surface area	Passed	Optimal found
Number of cells	Passed	Grid voltages matched
Total volume	Passed	
Sufficient power output	Passed	
IDeA	Passed	Verified for this sub-model

7.3 Modified components

Every model taken from van Dijk [12] or ten Hacken [18] has been re-verified (and re-validated if possible). Certain modifications have been made to a number of sub-models to fit these models into the current CET. Only the adjustments made to these sizing sub-tools will be discussed in this paragraph.

7.3.1 Gearbox

During the verification of the gearbox, two inaccuracies were discovered. Firstly, it appeared that the gearboxes were fairly small. It turned out that a mistake was made in the unit of the tooth shear stress in the source paper used by van Dijk. The shear stress was a factor 1000 too large, resulting in tiny pinion wheels. Secondly, the sizing of multi-stage gearboxes was not implemented correctly. The tool correctly identified multi-stage gearboxes, yet sized them as a single-stage gearbox. Therefore, the relatively large gear ratio was applied to a singular stage, resulting in an excessive main wheel. Consequently, the overall width and height were massive. The calculation is changed, so the gear ratio per stage is computed, resulting in smaller main wheels. The core length of the gearbox increases, as multiple wheels have to be placed in series. However, the overall length is not altered significantly, since the specific length is different for multi-stage gearboxes [26].

Lastly, the table with the upper and lower limit for the engine speeds was updated with the gas turbine. The updated table can be found in Table 17. The nominal engine speed of the gas turbine is set at 3300 RPM, equal to the Rolls-Royce MT-30. Lower engine speeds may be advantageous for the size of the gearbox, yet these were not found in conventional designs. Increasing the engine speed does affect the performance of the gas turbine within the CET, as the gas turbine has a free turbine. However, the size of the gearbox will increase significantly. Therefore, 3300 RPM is seen as the optimal engine speed and the engine limits are set as such.

7.3.2 Electric motor

The electric motor was originally modelled as a submarine engine, meaning the dimension were based the cylinder shape of the submarine. In a surface vessel, the negative space of the EM can also be considered occupied. This means the EM must be seen as an rectangular box in terms of effective volume usage. The weight of the EM is still calculated with the actual volume of the engine, as the negative space has no mass. Furthermore, the parameters of the EM were change to better simulated an EM intended for a surface vessel. The high torque load in combination with the absence of a gearbox in a submarine result in an EM that is capable of producing a significant amount of torque at very low RPM. In terms of dimensions, this manifests itself in a large diameter and a small length. For EMs in surface vessels, the nominal RPM is most likely higher, while the produced torque can be lower. Therefore, the shape factor and the stator/rotor ratio have been adjusted to better reflect this in the dimensions. The new values are based on Stapersma and de Vos [26]. Moreover, the correction factor for length and diameter have been updated accordingly. In total, the volume of the EM did not change significantly.

7.3.3 Batteries

A new model was implemented to determine the capacity of the batteries. This capacity is determined by designing multiple variations and letting the IDeA select the optimal one. The IDeA needs an estimation of the operations of the component to come to a decision. The performance of a battery is indirect, as it has a constant efficiency, no emissions and no signatures. Therefore, the effect of the batteries on the complete electric generation is evaluated.

The efficiency of the batteries is related to the number of mission elements that can be optimised. A mission element is defined as optimised if all employed components operate at their optimal load point. Figure

Table 17: Upper and lower limit engine speeds per engine type [12]

Engine type	Lower limit	Upper limit	Unit
2-stroke diesel	60	250	RPM
4-stroke diesel	400	2000	RPM
4- stroke dual fuel	400	1200	RPM
Electric motor	60	2000	RPM
Gas turbine	3300	3300	RPM

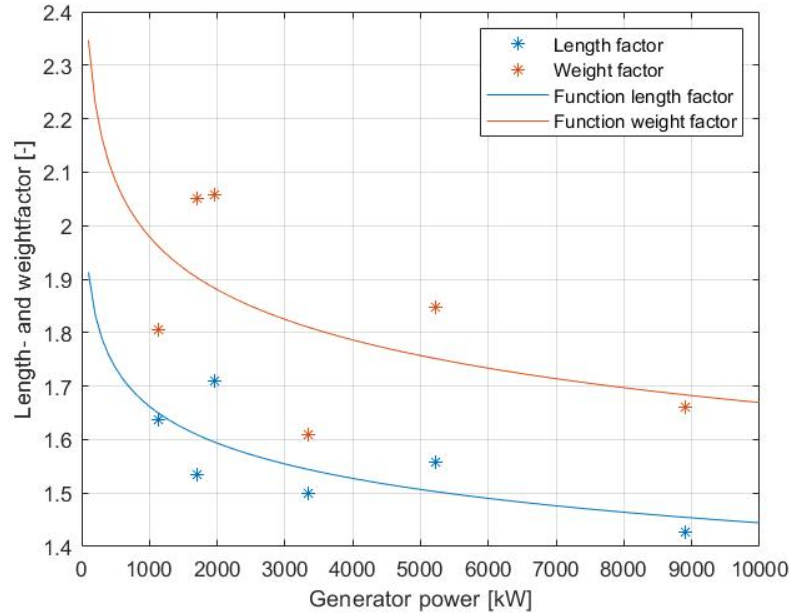


Figure 21: Length- and weight factor for generators sets from Wärstilä [29, 30, 31]

16(a) shows an example where there is enough capacity to optimise that mission element. The assessment of whether there is enough capacity assumes a full battery. The effect of batteries on the emissions and signatures of the EGS is expressed as the number of diesel generators that can be shut off, since these are the main contributors within the EGS. The algorithm examines in which mission elements a generator can be switched off, by supplying the power by the batteries. Figure 16(b) shows an example where a generator can be switched off. The maximum number of generators that can be turned off during a single mission element is equal to the number of generator in that configuration, meaning that a configuration without generators will not benefit from an emissions or signatures reduction. The batteries are not counted towards the robustness of a configuration, as a battery will not be able to replace a EGS component for a sustained period of time. It could be argued that the batteries can be used to provided emergency power to mission equipment. However, an emergency mode is not included in the robustness evaluation.

When the optimal battery capacity is determined, the design method by van Dijk [12] is applied. The specific energy of the batteries was updated to 200 Wh/kg [27, 28]. In addition to the capacity of the battery, the discharge power is computed by the sub-model. The discharge power is dependent on the state of charge of the battery and the C-rating. For lithium-ion batteries a C-rating of one is recommended for continuous use. Furthermore, the available discharge power decreases with a decreasing state of charge. To guarantee that the required discharge power can always be met, the batteries are designed to achieve this power at a 20% state of charge. A state of charge below 20% is undesirable as the cell can be damaged and the available power is sharply decreased. Thus, the functional capacity lies between 20% and 100% state of charge. This conservative approach will lead to batteries that are larger than optimal, but it has an advantageous effect on the lifetime of the batteries and calculation speed of the model.

7.3.4 Generators

The generators-sets operated in the CET are 4-stroke medium or high speed engines attached to the actual generators. The same design algorithm as for the diesel engines is applied to the generators. The size of the actual generator is calculated as a factor of the size of the engine. The same is done for the weight of the generators. These factors are based on generator-sets from Wärstilä [29, 30, 31]. The data can be found in Figure 21. A trend line is applied to find the length and weight factor for every generator power. The functions can be found in equation 25.

$$\begin{aligned} L_{factor} &= 2.53P_{gen}^{-0.061} \\ M_{factor} &= 3.30P_{gen}^{-0.074} \end{aligned} \quad (25)$$

The choice in engine speeds for a generator set is limited, due to the dependency on the frequency of the electrical grid. Subsequently, the engines are designed to run at either 750, 1000 or 1800 rpm. All three options are designed within the algorithm, the optimal being selected by the IDeA. Corresponding to the engine speed, the specific fuel consumption is set to 175, 190, 205 g/kWh respectively [29, 30, 31].

7.3.5 Proton exchange membrane fuel cell

Similarly to the SOFC, an algorithm is used to find the optimal current density for the PEMFC. Due to changes in the performance model of the PEMFC, the optimal current density is no longer equal to the maximal current density. The optimal current density will most likely not differ between various PEMFC, as the operating conditions are equal for every design. However, if in the future changes would be made to the operation conditions, the optimal current density will be automatically determined by the sizing model.

7.3.6 Inverters

The inverters are sized based on the power flowing through them. A trend function based on data by ABB [32]. A small inaccuracy was made in this method, as the trend function was not tested for very large amount of power flowing through them. As a result, inverters could be assigned a negative size and weight at high power levels. This issue was resolved by limiting the power flowing through a single inverter to 1 MW, based on the data by ABB. When larger power flows are required, multiple inverters will be installed, as is done in reality.

8

Performance

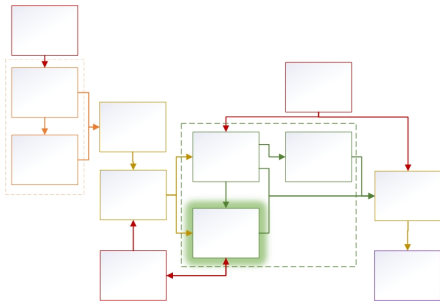


Figure 22: Chapter location within model, based on Figure 5

The performance sub-model evaluates the fuel consumption, emissions and signatures of the configurations during a missions. Figure 22 shows the position of this chapter within the complete model structure. The actual installed power and the components details are provided by the sizing tool, while the operational profile is given by the user as input. The output is sent to the MCA. If an electric motor is employed during a mission element, the electrical power demand of that mission element is updated, for which output is passed on to the operational profile.

Similar to the previous chapter, the gas turbine, SOFC and CPP will be discussed in detail, as they are new components in the CET. The performance of the diesel engine is also described in more detail, as it is based on a model of the Delft University of Technology [33]. The models taken from van Dijk [12] and ten Hacken [18] are re-verified (and re-validate if possible). Modification made to these existing models will be described briefly. If the performance evaluation of a component has not changed compared to the version made by van Dijk or ten Hacken, the component will not be discussed.

8.1 Gas Turbine

The performance of the modelled gas turbine is evaluated by studying its thermodynamical principles. First the inner workings, followed by the implementation of the principles into the model. Next, the used parameters are described, after which the model is verified and validated.

8.1.1 Working principle

A schematic of a simple cycle gas turbine can be found in Figure 23. Air enters the gas turbines through an air inlet (1). This air gets compressed to a higher pressure by the compressor (2). The power needed to compress this air is delivered by the compressor turbine. Once the air is compressed, fuel is added and combustion takes place in the combustion chamber (CC). This process happens at a constant pressure. The heated pressurised air (3) enters the compressor turbine where it expands and cools down, to provide power to the compressor. The air gets expanded again in the power turbine, which powers the load. The exhaust gas (4) leaves the system and enters back into the environment.

The thermodynamical principles of a gas turbine are applied to model the performance of the gas turbine. These principles can be described via the ideal Brayton cycle, found in Figure 24. The numbers found in Figure 23 correspond with the numbers of Figure 24. In a later stage losses are introduced, making the the cycle no longer ideal. The following assumption are made in the model:

- There are no pressure losses in any component, apart from the compressor and turbine.
- The change of kinetic energy in the air is taken into account by using total temperature and pressure throughout.
- The air is a perfect gas with constant specific heat and does not change in the process.

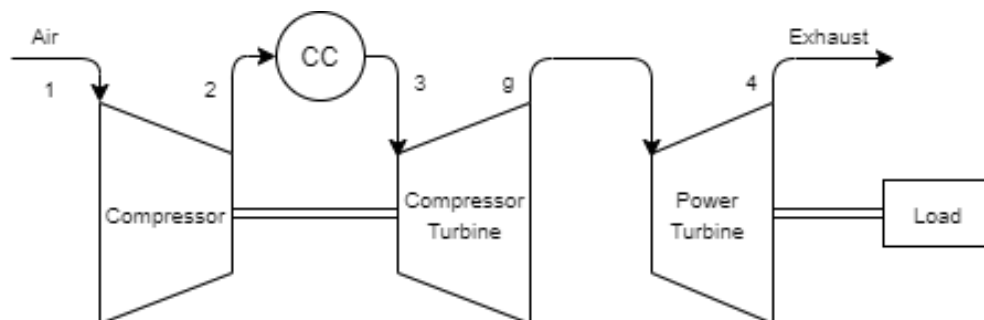


Figure 23: Schematic of a simple cycle twin-shaft gas turbine

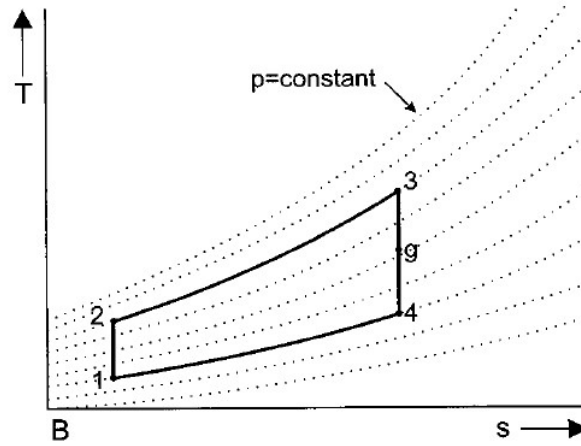


Figure 24: T - s diagram of an ideal Brayton cycle without losses [34]

- Heat is added to the air by an external source instead of internal combustion.
- Heat is extracted from the air with a heat sink, instead of discharging the exhaust gasses into the environment.
- The mass flow is constant throughout the cycle, so the mass of the added fuel is neglected.

The brake power of a gas turbine is equal to the air mass flow times the net work of the Brayton whole cycle, as can be seen in equation 26. By calculating the work added or subtracted at every stage, the net work of the gas turbine can be computed. Similarly, by calculating the heat addition and subtraction at every stage, the fuel consumption and heat loss can be computed. The work and heat changes per stage can be calculated with equation 27 and 28 respectively. It can be seen that the temperatures at every stage are dictating the performance of the gas turbine, so the model should calculate these.

$$P_b = P_{cycle} = \dot{m} \cdot w_{cycle} \quad (26)$$

$$w = \frac{|P|}{\dot{m}} = (h_{in} - h_{out}) = c_p(T_{in} - T_{out}) \quad (27)$$

$$q = \frac{|\dot{Q}|}{\dot{m}} = (h_{out} - h_{in}) = c_p(T_{out} - T_{in}) \quad (28)$$

Two ratios are defined to determine the temperature of the air at every stage, namely the pressure ratio (equation 29) and the temperature ratio (equations 30 and 31)[34]. The compression and expansion of the air is assumed to be polytropic, and not isentropic as is assumed in an ideal cycle. This means that the process is still adiabatic, but no longer reversible, due to friction. As a result, the polytropic efficiency is introduced to relate pressure ratios to temperature ratios, as is shown in equations 30 and 31.

$$\pi = \pi_C = \frac{p_2}{p_1} = \frac{p_3}{p_4} = \pi_T \quad (29)$$

$$\tau_C = \frac{T_2}{T_1} = \left(\frac{p_2}{p_1}\right)^{\frac{n_C-1}{n_C}} = \pi^{\frac{n_C-1}{n_C}} = \pi^{\frac{1}{\eta_C} \frac{\kappa-1}{\kappa}} \quad (30)$$

$$\tau_T = \frac{T_3}{T_4} = \left(\frac{p_3}{p_4}\right)^{\frac{n_T-1}{n_T}} = \pi^{\frac{n_T-1}{n_T}} = \pi^{\eta_T \frac{\kappa-1}{\kappa}} \quad (31)$$

Table 18: Thermodynamical processes in a gas turbine

Stage	T_{out}	Work	Heat	Process
1 → 2	$T_2 = T_1 \pi^{\frac{1}{\eta_C} \frac{\kappa-1}{\kappa}}$	$c_p(T_1 - T_2)$	-	Air compression
2 → 3	$T_3 = T_2 + \frac{q_{fuel}}{c_p}$	-	$c_p(T_3 - T_2)$	Fuel combustion
3 → g	$T_g = \frac{T_3}{\pi^{\eta_T \frac{\kappa-1}{\kappa}}}$	$c_p(T_3 - T_g)$	-	Air expansion
g → 4	$T_4 = \frac{T_g}{\pi^{\eta_T \frac{\kappa-1}{\kappa}}}$	$c_p(T_g - T_4)$	-	Air expansion
4 → 1	-	-	$c_p(T_1 - T_g)$	Heat losses

All thermodynamical processes per stage are displayed in Table 18. The total work of the cycle can be found by summing the work of every stage. The work of stage 1 → 2 is negative, meaning work is added to the air. This work is needed to compress the air. Similarly, the heat of stage 4 → 1 is negative, as this is the heat loss of the exhaust flow. The fuel addition can be found in stage 2 → 3, in the form of q_{fuel} .

The heat loss of the exhaust flow is not the only loss in the gas turbine. Mechanical losses and power take off (PTO), for example in the bearings and fuel pumps, can be responsible for up to 5% of the total power [38]. This loss should be subtracted from the thermodynamical power computed by the equations in Table 18. It is assumed that part of the mechanical losses are independent of the working point of the gas turbine, and thus constant. The other part is assumed to be dependent on the rotational speed of the gas turbine.

8.1.2 Model implementation

The model starts its calculation at the nominal working point of the gas turbine, as the output power, engine efficiency and air mass flow of the Rolls-Royce MT-30 are known at this point. The heat input is computed with equation 32. All stages of Table 18 can be followed to derive the exhaust losses and the thermodynamic power. Next, the mechanical losses during nominal operations are determined with equation 33.

$$q_{fuel} = \frac{\dot{Q}_{fuel}}{\dot{m}_{air}} = \frac{P_b}{\eta_e \dot{m}_{air}} \quad (32)$$

$$\begin{aligned} \dot{Q}_{fuel} + \dot{Q}_{exhaust} &= P_b + P_{mech} \\ P_{mech} &= \frac{P_b}{\eta_e} - P_b + \dot{Q}_{exhaust} \end{aligned} \quad (33)$$

Equation 33 should be applied with care, since there is a dependency between the engine efficiency and the exhaust heat flow, that is not directly visible from the given equations. As equation 34 shows, the engine efficiency is a function of multiple other efficiencies, including the polytropic compressor and turbine efficiency. This dependency is not programmed into the model, since the influence of the polytropic efficiencies on the engine efficiency is highly complex. As a result, a situation may occur where the exhaust heat flow is greater than the difference between the fuel heat flow and the brake power, which is thermodynamically

Table 19: Parameters used in the gas turbine model

Parameter	Unit	Value	Reference
π	-	18	[35]
η_e	-	0.39	[36]
η_c	-	0.92	Fitted, based on [37]
η_t	-	0.85	Fitted, based on [37]
X	-	0.70	Fitted
T_1	K	288	[36]
m_{air}	kg/s	33-120	[36]

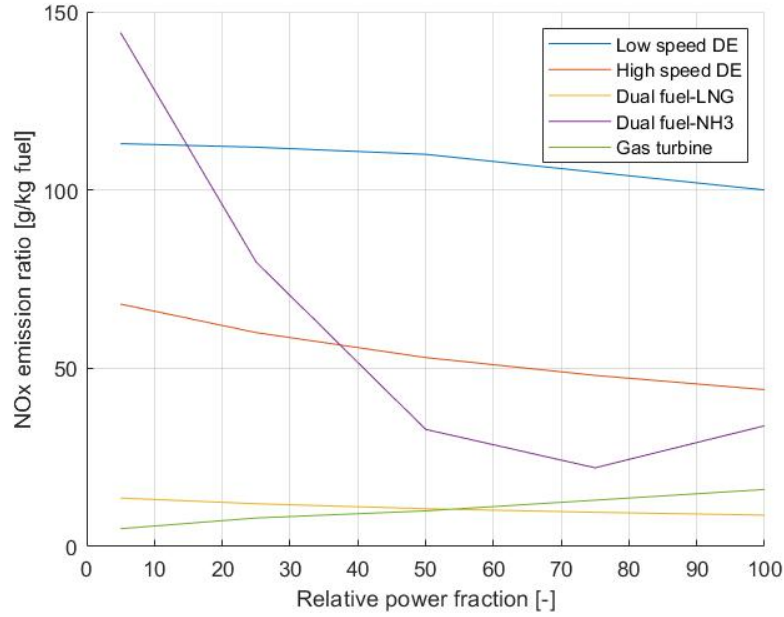


Figure 25: NOx emission ratio for multiple engine types at different power fractions. Constructed by van Dijk [12] and updated with the gas turbine.

impossible. Therefore, there should always be a balance between the input of the engine efficiency and polytropic efficiencies.

$$\eta_e = f(\eta_C, \eta_T, \eta_{mech}, \dots) \quad (34)$$

Once the nominal properties are known, the part load conditions can be evaluated. The air mass flow of the Rolls-Royce MT-30 at every part load conditions is known. Therefore, equation 32 can also be employed at part load conditions. As a result, the processes in Table 18 can be applied to a range of fuel heat flow inputs. From the resulting range of thermodynamical powers the mechanical power losses are subtracted to calculate a range of brake powers, as is shown in equation 35. The brake power closest to, but higher than, the demanded power output is taken as the true brake power, along with its corresponding fuel input.

$$P_b = P_{td} - X \cdot P_{mech} - (1 - X) \cdot P_{mech} \frac{n_{eng}}{n_{nom}} \quad (35)$$

As mentioned previously, the mechanical losses are assumed to be partially constant and partially dependent on the rotational speed of the gas turbines. The fraction (X) is a variable that can be used to fit performance curves to practical data. It must be noted that the rotational speed is the speed of the power turbine. Since a twin-shaft gas turbine is used, the compressor and first turbine turn independent of the power turbine. Therefore, the mechanical losses of the first two components of the gas turbines are captured in the constant part of the mechanical losses, while the mechanical losses of the power turbine are captured in the variable part.

The emission of the gas turbine is computed with the use of emission rates. These rates describe how much emission is produced per kilogram fuel. The emissions rates of CO₂ and SO_x are completely dependent on the fuel composition. Therefore, the same emissions calculation can be applied as for diesel engines [12]. It should be noted that it is assumed that the consumed natural gas does not contain sulfur, so there is no SO_x emission from a gas turbine. The NO_x emission rate is component and load ratio dependent. Figure 25 shows the NO_x emission rate for multiple diesel engines as well as for a simple cycle gas turbine [34].

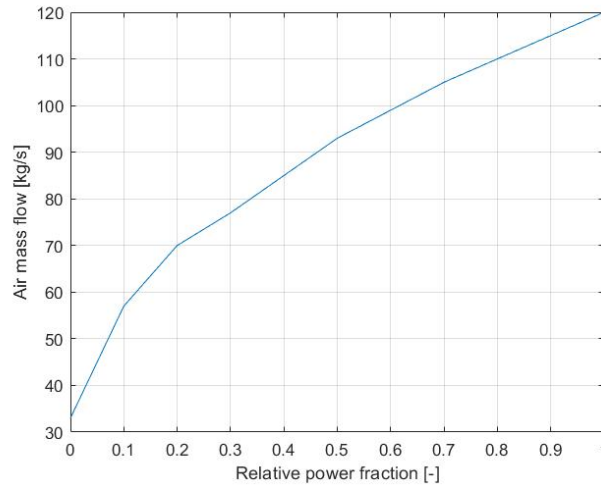


Figure 26: Air mass flow as function of relative power fraction [36].

8.1.3 Parameters

The parameters used in the model can be found in Table 19. These parameters can be adjusted by the user if desirable. The pressure ratio of the Rolls-Royce MT-30 could not be found, so the pressure ratio is taken from a similar aeroderivative simple cycle twin-shaft gas turbine. The fitted values are based on the given references and fitted to the curves found in Figures 28 and 29. The air mass flow is given as a range, since the value is dependent on the load ratio. Figure 26 shows the relation between the air mass flow and the relative power fraction.

8.1.4 Verification and validation

The gas turbine model is verified by studying the specific work performed at every stage, as is shown in Figure 27. The output work goes to zero as the power fraction goes to zero. Furthermore, the work delivered by the power turbine is equal to sum of the mechanical losses and the output work. Moreover, the compressor and the power turbine together form the work of the combined turbines. Lastly, the specific work of the mechanical losses decreases as the power fraction increases. This is logical, since the air mass flow increases more rapidly than the mechanical losses do, leading to a smaller mechanical loss per kilogram air. All in all, the model performs as expected.

The gas turbine model is validated in terms of specific fuel consumption (Figure 28) and exhaust gas temperature (Figure 29). The Rolls-Royce data is taken from Herdzyk and Cwilewicz [36]. The specific fuel consumption matches decent, especially at higher power fractions. Similarly, the exhaust gas temperature fits acceptable at higher power fraction. However, at lower power fractions the exhaust gas temperature does not seem to fit quite as well. This is probably due to the constant pressure ratio and polytropic efficiencies. In practice, these variables are likely a function of the working point of the gas turbine, yet in the model they are kept constant trough out the operational range. It can be argued that gas turbines should not be used at such low power fraction and therefore these exhaust gas temperature are not relevant. On the whole, the model output is deemed acceptable and usable.

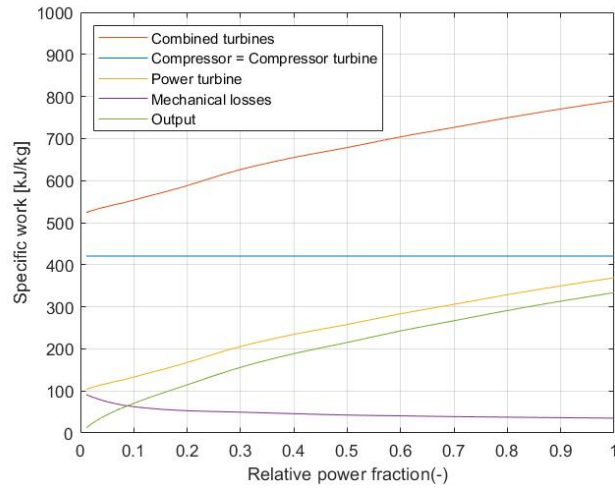


Figure 27: Specific work at every stage of the gas turbine. Used as verification of the gas turbine model.

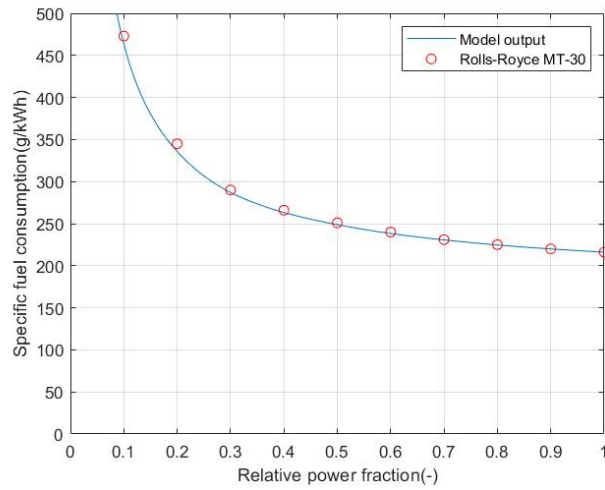


Figure 28: Specific fuel consumption of the Rolls-Royce MT-30 in red markers and the model output in blue

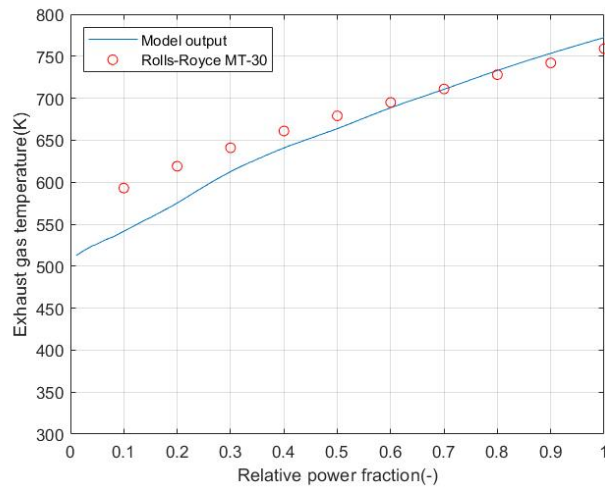


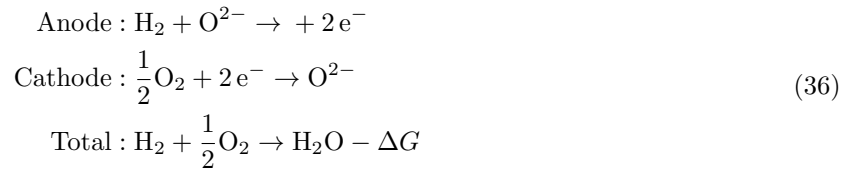
Figure 29: Exhaust gas temperature of the Rolls-Royce MT-30 in red markers and the model output in blue

8.2 Solid oxide fuel cell

The performance of the solid oxide fuel cell is simulated with the use of a polarization curve. The curve shows the obtained voltage at a given current density. With the obtained voltage and current the electric power output of the fuel cell can be determined. The choice for using a polarization curve a modelling method is based on the minimal computational requirement, acceptable level of detail and the non-interest of the inner workings of a fuel cell.

8.2.1 Working principle

A fuel cell consists of three parts: the anode, the cathode and the electrolyte. In a SOFC negatively charged ions move from the cathode to the anode through the electrolyte. The electrons cannot move through the electrolyte and move to an external circuit, creating a current and thus electrical power. The total reaction can be found in equation 36. In the total reaction, an amount of Gibbs free energy is released, since energy release is defined as negative Gibbs energy. This Gibbs energy is temperature and pressure dependent and can be converted to electric energy.



As mentioned, the electric energy produced by a fuel cell is a function of the Gibbs free energy of a reaction. The reversible voltage of the fuel cell is dictated by the amount of Gibbs free energy, as is shown in the Nernst equation 37 [39, 40]. This reversible voltage is also known as the open circuit voltage (OCV). For performance at atmospheric pressure, the Gibbs free energy and the corresponding OCV can be found in Table 20. Equation 37 also shows a dependency on the operation pressure and concentration of the reactants. This will be discussed later on in this paragraph.

$$\begin{aligned}
 E &= -\frac{\Delta G_0}{2F} + \frac{RT}{2F} \ln \left(\frac{p_{\text{H}} p_{\text{O}_2}^{\frac{1}{2}}}{p_{\text{H}_2\text{O}}} \right) \\
 E &= E_0 + \frac{RT}{2F} \ln \left(\frac{\alpha \beta^{\frac{1}{2}}}{\delta} \right) + \frac{RT}{4F} \ln(P)
 \end{aligned} \tag{37}$$

Activation losses

Activation losses represent the slowness of the reaction. Some energy is spent on driving the chemical reaction. The higher the temperature of the fuel cell, gets the lower this loss will be [42]. This effect was discovered by Tafel and can be described with the Tafel equation, see formula 38 [43, 44]. The activation losses are present in both the anode and cathode side of the fuel cell. The losses on both sides of the fuel cell don't have to be equal, so the equation has to be solved for the anode and cathode separately. The Tafel constant (A) is often experimentally determined. This constant is temperature dependent and causes the activation losses to decrease at increased operating temperature.

Table 20: Gibbs free energy and maximal OCV for a hydrogen fueled SOFC at atmospheric pressure [39, 41]

$T[^\circ\text{C}]$	$\Delta G_0[\text{kJmol}^{-1}]$	$E_0[\text{V}]$
100	-225.2	1.17
200	-220.4	1.14
400	-210.3	1.09
600	-199.6	1.04
800	-188.6	0.98
1000	-177.4	0.92

$$E_{loss,act} = \frac{RT}{\alpha nF} \sinh^{-1} \left(\frac{i}{2i_0} \right) = A \sinh^{-1} \left(\frac{i}{2i_0} \right) \quad (38)$$

Ohmic losses

The resistive losses occur due to the resistance the electrons encounter in the electrodes and the ions encounter in the electrolyte. This resistance can be described with Ohm's law, as is shown in equation 39. These losses are the cause of the linear middle part of the polarization curve. The resistance experienced by the fuel cell is a function of the operating temperature.

$$E_{loss,res} = ir \quad (39)$$

Concentration losses

When a fuel cell is producing electricity it consumes fuel and oxygen. At the electrodes the concentration of fuel and oxygen will drop as it takes time to transport new fuel and oxygen to the electrodes. When a lower concentration of fuel or oxygen is available the reaction will slow down and less energy can be produced. At higher currents, more fuel is consumed and consequently the transport losses will increase. There is no analytical description for this loss, so a numerical formula is used to model this loss, see formula 40 [42]. The current that a fuel cell can produce is limited by a limit current density, modelling the current density at which fuel and oxygen cannot be supplied fast enough for the reaction to happen. This loss is predominant in high temperature fuel cells, such as SOFC's. Similarly to the Tafel constant, the concentration loss coefficient (B) is experimentally determined and dependent on the operating temperature

$$E_{loss,trans} = -\frac{RT}{nF} \ln \left(1 - \frac{i}{i_l} \right) = -B \ln \left(1 - \frac{i}{i_l} \right) \quad (40)$$

Cross-over losses

The electrolyte of a fuel cell is designed to only transport ions, however some leakage of fuel and electrons always occurs [42]. This means that for instance hydrogen molecule diffuse through the electrolyte and react with the oxygen on the other side. The electrons in this reaction don't go through the external circuit, so no usable current arises. The same goes for electrons passing through the electrolyte instead of the external circuit. The fuel and electrons crossing over can be seen as an internal current that is produced by the fuel cell, even when the external circuit is open. A result of this is that the measured OCV of a fuel cell is not equal to the theoretical OCV as described in equation 37. This loss can be modelled by adding a constant internal current density to the actual current density in all the losses mentioned above, as can be seen in formula 41. The cross-over losses are relatively low for high temperature fuel cells.

$$i \rightarrow i + i_n \quad (41)$$

When the OCV and all losses are combined, the function of the polarization curve is found, as is shown in equation 42.

$$E = E_0 + \frac{RT}{2F} \ln \left(\frac{\alpha \beta^{\frac{1}{2}}}{\delta} \right) + \frac{RT}{4F} \ln(P) - A \cdot \sinh^{-1} \left(\frac{i + i_n}{i_0} \right) - (i + i_n)r + B \cdot \ln \left(1 - \frac{i + i_n}{i_l} \right) \quad (42)$$

8.2.2 Operating temperature

A SOFC can operate at temperatures ranging from 600 °C to 1000 °C [25, 27, 45, 46]. Due to this high temperature, the possible efficiency is high, internal reforming is possible and the fuel cell is less sensitive to pollution in the fuel. A major disadvantage of these temperatures is the dynamic behaviour of the fuel cell. The start-up time as well as the reaction to load changes are sub-optimal. Both these characteristics are not included in the CET, since a quasi-static modelling method is used. As a result, the SOFC is not penalised for its disadvantages. A solution can be found in changing the design operating temperature, depending on the intended usage of the SOFC. When the electric mission profile is highly dynamic, the design operating temperature can be decreased. At lower operating temperatures (roughly 600°C) the dynamic behaviour

of a SOFC is acceptable for transport purposes [47], yet the efficiency will be worse. When the electric mission profile is more constant, increased operating temperatures can be applied, resulting in an increased efficiency. In this way, the SOFC is penalized by the lower efficiency when the operational profile shows dynamic behaviour.

The level of dynamic behaviour of the mission profile can be quantified with the coefficient of variation of the profile, for which the formula can be found in equation 43. The choice is made to use the coefficient of variance, instead of the variance itself, as the electric mission profile can greatly differ between configurations. When an electric motor is used, the electric mission profile includes significantly higher power demands than when no electric motor is used. The coefficient of variance normalizes this difference, resulting in a fair comparison between different configurations. The configurations with the highest coefficient will have SOFCs with a design temperature of 600 °C, while the smallest coefficient will lead to SOFCs with a design temperature of 1000 °C.

$$CV = \frac{\sigma}{\mu} \quad (43)$$

The characteristics of the polarization curve, and thus the performance of the fuel cell, are a function of the operating temperature of the SOFC. At higher temperatures the activation losses decrease, while the concentration losses and Ohmic losses increase [39, 48]. Furthermore, as was also shown in Table 20, the open circuit voltage decreases at higher temperatures.

8.2.3 Operating pressure

As mentioned previously and shown in equation 37, the operating pressure of a fuel cell effects the voltage output. An increase in pressure results in an increase in voltage, yet the power output might not follow the same logic, depending on how the air is compressed. Figure 30 shows the effect of different operating pressures and compression methods on the power output of a fuel cell stack. When compression is free, no power is needed to compress the air, the expected increase in output power can be found. An example of free compression is the usage of compressed air tanks, as can be done on submarines [18]. However, when the air needs to be compressed by a compressor, a negative effect of increased pressure on the total output power of the stack can be seen. The required compression power, as shown in equation 44, is thus higher than the benefit of a higher operating pressure.

Despite the effect shown in Figure 30, examples can be found of SOFCs with compressor applied to them. Often, these compressors are powered by a turbine running on the exhaust gasses of the SOFC. The power captured from the exhaust gasses can be seen as free power, leading to free compression. The electrical power produced by the SOFC is no longer used to power a compressor, resulting in increased output power at increased operating pressure. The choice has been made to model a turbocharged SOFC operating at 5 bar, as this configurations has an improved power output. A SOFC operating at 10 bar was considered. However, it was feared that a fair comparison with a PEMFC would no longer be possible. The user of the tool may change the operating pressure to any desired value.

$$P_{comp} = Q_{air} \frac{\kappa P_1}{\kappa - 1} \left[\left(\frac{P_2}{P_1} \right)^{\frac{\kappa-1}{\kappa}} - 1 \right] \quad (44)$$

8.2.4 Parameters

The parameters used in the model can be found in Table 21. These parameters can be adjusted by the user if desirable. The fitted values are based on the given reference and fitted to the curve found in Figure 32. The values of the parameters have been given for four different temperatures. For temperatures in between the given values, interpolation is used to determine the value.

8.2.5 Verification and validation

The polarisation curve of the SOFC model is verified by studying the losses occurring in the fuel cell, as is shown in Figure 31. The activation losses are the predominant losses at low current density, while at high current density the concentration losses are the biggest. Furthermore, the activation losses are significantly smaller at the anode than at the cathode. This is as anticipated as the anode is characterized by fast reaction kinetics, while the cathode has relatively slow reaction kinetics [25]. Lastly, the polarization curve

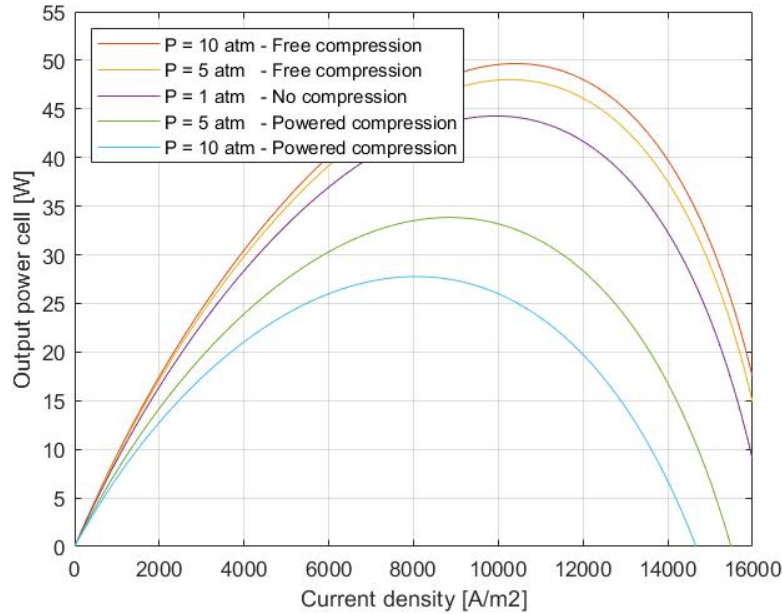


Figure 30: Power output of a single cell at different operating pressures. $A_{cell} = 0.01m^2$ $T = 800^\circ C$.

is the result of the summation of all the losses and the OCV, as expected. All in all, the model performs as predicted.

The polarisation curve of the SOFC model is validated with the use of a SOFC data of the Montreal State University (MSU) [44, 50]. The data and the corresponding model output can be found in Figure 32. The data of MSU is based on a fuel cell with an inlet pressure of 3 atm. As this solely effects the OCV, the model can easily be corrected for this. The parameters of the model at $900^\circ C$ are fitted to the given data. The model output fits almost perfectly with the data, resulting in an acceptable SOFC model.

8.2.6 Fuel consumption, utilisation and reforming

The fuel consumption of a fuel cell is directly related to the current produced by the fuel cell. The derivation can be found in equation 45. Since there is a continuous flow of fuel through the fuel cell, not all fuel will be used. This results in a higher practical fuel consumption than the theoretically needed, as can be seen in equation 46 [51]. A fuel utilisation of 90% is being used in the CET [25, 52].

Table 21: Parameters used in the SOFC model at an operating pressure of 5 bar.

Parameter	Unit	Value at operating temperature [$^\circ C$]				Reference
		600	800	900	1000	
E_0	V	1.07	1.02	0.99	0.96	[39, 41]
$i_{0,a}$	A/m^2	100000	100000	100000	100000	[25]
$i_{0,c}$	A/m^2	1000	1000	1000	1000	[25]
i_n	A/m^2	100	100	100	100	[25]
i_l	A/m^2	18000	18000	18000	18000	Fitted, based on [25, 49],
A_A	V	0.16	0.13	0.10	0.07	Fitted, based on [49]
A_C	V	0.55	0.40	0.30	0.15	Fitted, based on [49]
B	V	0.18	0.20	0.22	0.24	Fitted, based on [25]
r	Ωm^2	6.0e-06	5.0e-06	4.0e-06	3.0e-06	Fitted, based on [25, 49]

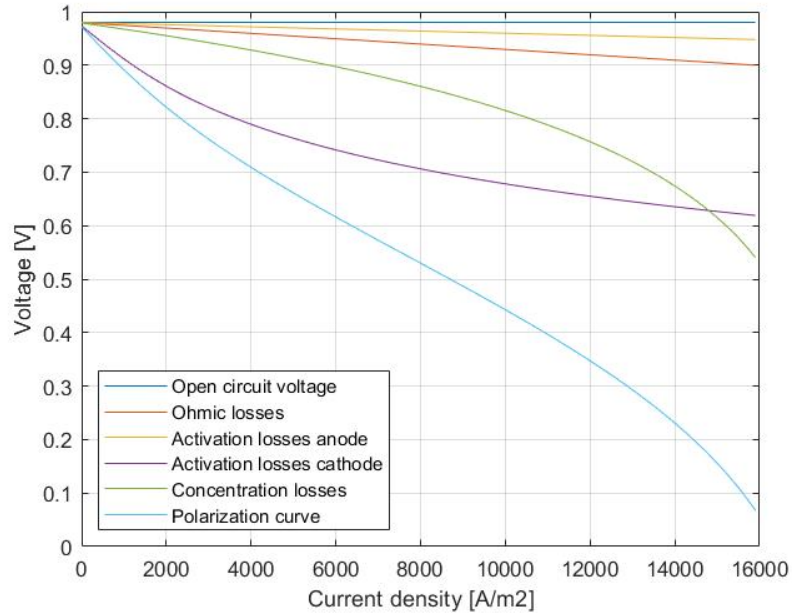


Figure 31: SOFC losses and resulting polarization curve for $P = 1 \text{ atm}$ and $T = 800^\circ\text{C}$. Used for verification of the SOFC model

$$I_{\text{cell}} = \frac{[C]}{[s]} = \frac{[C]}{[\text{mol}_e]} \cdot \frac{[\text{mol}_e]}{[s]} = F\dot{n}_e \quad (45)$$

$$\dot{n}_{\text{H}_2, \text{cell}} = \frac{\dot{n}_e}{2} = \frac{I_{\text{cell}}}{2F}$$

$$\dot{n}_{\text{H}_2, \text{total}} = \dot{n}_{\text{H}_2, \text{cell}} \cdot N_{\text{cell}} \cdot N_{\text{stack}}$$

$$\dot{n}_{\text{H}_2, \text{practical}} = \frac{\dot{n}_{\text{H}_2, \text{theoretical}}}{U_f} \quad (46)$$

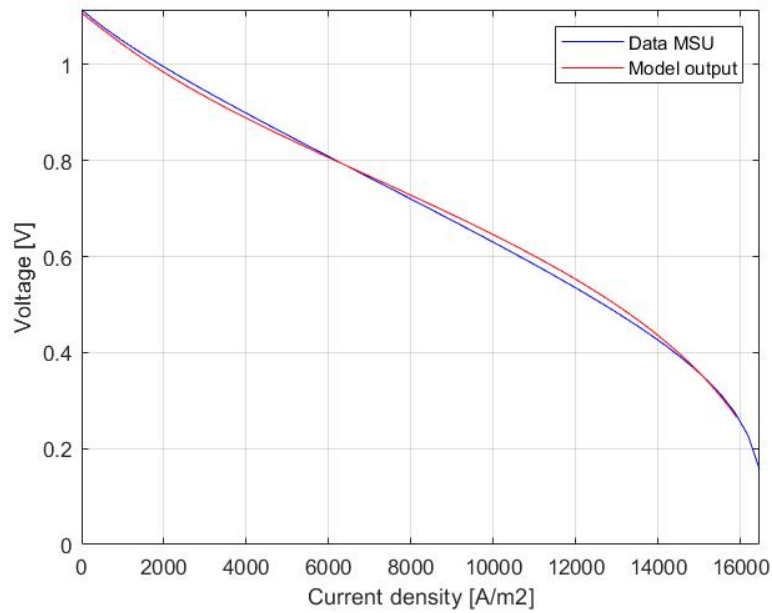
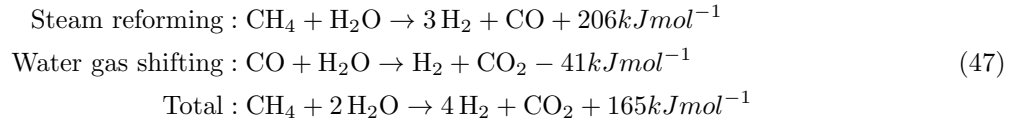


Figure 32: Polarization curve of MSU data (in blue) and model output (in red) for $P = 3 \text{ atm}$ and $T = 900^\circ\text{C}$.

Another phenomenon seen in fuel cells is the change of partial pressure, due to fuel being consumed. When hydrogen is being consumed and steam is being formed, the pressure balance shifts. Equation 37 shows that when the partial pressure of hydrogen decreases and the partial pressure increases, the OCV becomes lower. As a result, the voltage at the end of a fuel cell can be substantially lower than at the beginning [25]. This is especially true for SOFCs, as they operate at high temperatures and the steam is being formed at the anode side, mixing with the fuel. This aspect is highly complex to model when only looking at the polarization curve of a fuel cell. The challenge is solved by fitting the polarization curve to experimental data, whereby this effect is indirectly captured in the polarization parameters.

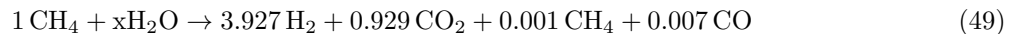
Apart from hydrogen, other fuels can be used in a SOFC, due to internal reforming. There is no need for an external reformer as the temperature at the anode is high enough to cause the reformation reaction to happen [42, 45]. The reformation of methane (natural gas) can be found in equation 47 [25, 53] and the reforming of ammonia can be found in equation 48 [25, 54].



Methane is reformed in a process called steam reforming, where steam is added to create carbon monoxide and hydrogen. The carbon monoxide then reacts again with steam to create carbon dioxide and more hydrogen in a process called water gas shifting. The total reaction is endothermic, meaning energy has to be added in order for the reaction to occur. This energy comes from the heat of the SOFC. The water needed can be externally added, but also the product water of reaction 36 can be used. In practice the steam to carbon ratio lies in the range of 2 to 3 [25].

Similarly to the fuel utilisation, not all methane will be converted to hydrogen. The conversion ratio is a function of the fuel utilisation, as when more fuel is being consumed the chemical equilibrium of reaction 47 will ensure more methane is being reformed. From experimental data [52] it is determined that at 90% fuel utilisation 99.9% of the methane is converted and 93.0% of the carbon monoxide is converted, resulting in equation 49. Since the fuel is a mixture instead of pure hydrogen, the partial pressure of the hydrogen decrease. As a result the voltage of the fuel cell will also decrease, as can be seen in equation 37. The voltage drop can be found in equation 50, where $\alpha_0 = 1$ for pure hydrogen. The assumption is made that the perfect amount of water is used in reaction 49. Otherwise, the partial pressure of hydrogen will decrease further, due to the presence of extra water at the anode.

Since carbon monoxide and dioxide is being formed in the reforming process of methane, and some methane leakage is possible, the SOFC is no longer emission free. The resultant methane is often combusted to prevent leakage into the environment and to provide heat for the heat exchangers. The carbon monoxide has a relatively small global warming potential and is created in insignificant amounts, so is therefore ignored as an emission. The carbon dioxide emission is included in the CET as a percentage of the consumed methane.



$$\begin{aligned} \Delta E &= \frac{RT}{2F} \ln \left(\frac{\alpha}{\alpha_0} \right) \\ \alpha &= \frac{3.927}{4.894} = 0.81 \end{aligned} \quad (50)$$

Ammonia is reformed in a decomposition process. This process is endothermic, getting its energy from the heat of the SOFC. No additional reactants are needed to reform ammonia. The conversion rate of ammonia is 99% [54, 55], resulting in equation 51. Again a mixture is formed, leading to a reduced partial pressure of hydrogen. The resulting voltage drop can be found in equation 52. Nitrogen gas is produced in the reforming process of ammonia, but is not seen as an emissions, since 80% of the air consists of nitrogen gas.

The leakage of ammonia does not contribute to global warming, yet may have other harmful impacts on the environment. For this reason, the ammonia might have to be captured in a later stage, but this won't be included in the CET.



$$\Delta E = \frac{RT}{2F} \ln \left(\frac{\alpha}{\alpha_0} \right) \quad (52)$$

$$\alpha = \frac{1.495}{1.99} = 0.75$$

8.2.7 Nominal current density

The maximal power of a SOFC is often not found at the maximal current density, due to internal losses. Figure 30 shows an example of this influence. Increasing the current density beyond the nominal current density will result in a lower output power and higher heat production. When sizing the SOFC it is important to know at which current density the maximal power is reached, as this effects the voltage and power of a cell, and thus the number of needed cells and stacks. Furthermore, the algorithm deciding the needed current density assumes that an increase in current density leads to an increase in power, which is only true for current densities below the nominal density.

As the nominal current density varies between designs and operating temperatures, an algorithm is used to determine the nominal current density. The algorithm simply calculates the expected power of a cell for every current density and then finds the maximal value. This solution is not computational taxing, but does ensure a more optimal SOFC design.

8.2.8 Exhaust heat

As the SOFC operates at a significant temperature and emits gasses, heat signatures become important. The heat signature of a SOFC is calculated in the same way as the heat signatures of an internal combustion engines, as can be seen in equation 53. Just like with internal combustion engines only the heat of the exhaust air is considered, and not the heat of the fuel remains. This is done to keep a fair comparison.

$$\dot{Q}_{exhaust} = \dot{m}_{air} c_p (T_{amb} - T_{ope}) \quad (53)$$

8.3 Controllable pitch propeller

More and more naval ships are using controllable pitch propellers, including the frigates and OPV's of the Dutch Navy and the destroyers of the US Navy. Advantages of a CPP are increased manoeuvrability, better acceleration at low speed and the ability to have backward thrust without reversing the engine. Furthermore, CPP's allow for the use of a power take off, since the rotational speed of the shaft can be kept relatively stable.

8.3.1 Working principle

Higher pitch leads to higher torque on the propeller and lower rotational speed, while lower pitch does the opposite, assuming the delivered power remains constant. The efficiency of both the propeller and the engine is dependent on the pitch setting. Thus, the pitch setting has a direct relation on the fuel consumption of the vessel. Furthermore, since the load on the propeller can be controlled by changing the pitch, the pitch setting also plays an important role in minimizing cavitation.

In the CET made by van Dijk [12], the needed propeller rotational speed is calculated with the propeller law, as shown in equation 54. The value of C_4 is assumed constant by van Dijk, to simplify calculations. This is a reasonable assumption for a fixed pitch propeller in a first design phase, yet for a CPP this is not true. The value of C_4 is dependent on the torque coefficient, as can be seen in equation 55 [34]. As discussed before, the torque changes as the pitch of the propeller changes and so does the torque coefficient, and thus the value of C_4 .

$$P_p = C_4 \cdot n_{prop}^3 \quad (54)$$

$$C_4 = \frac{2\pi \cdot \rho \cdot D_{prop}^5}{\eta_r} \cdot K_Q \quad (55)$$

The correct way to find the value of C_4 is finding the value of K_Q for every pitch setting with the help of an open water diagram. However, this would require the ship- and propeller characteristics to be known, which is not necessarily the case. An easier way, which does not require an open water diagram, is to make a combinator curve with C_4 values instead of pitch values. This method is deemed viable, as there is no interest in the actual pitch angle, but only in the influence that changing the pitch has on the engine's operating point.

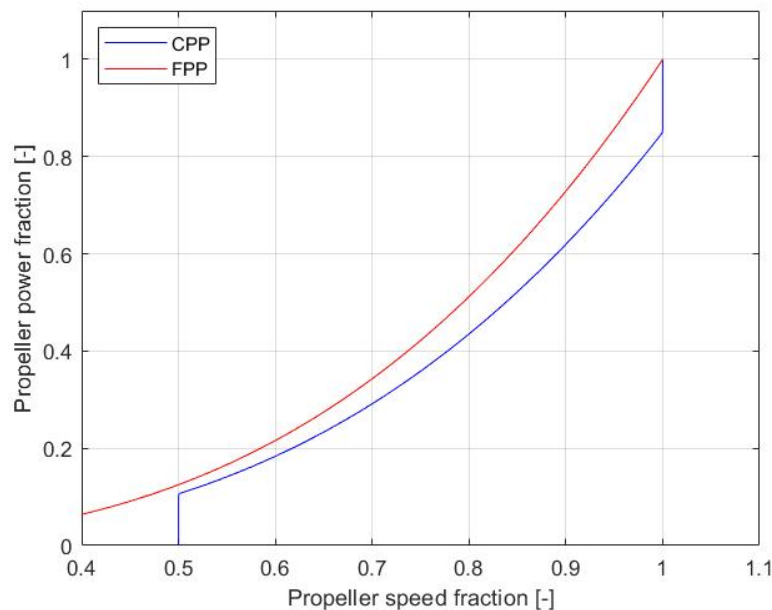


Figure 33: Propeller load line of a fixed pitch propeller (in red) and a controllable pitch propeller (in blue)

8.3.2 Model implementation

Looking at the literature, there does not seem to be a single combinator curve used by all ships, but rather a unique combinator curve per vessel [56, 57, 58, 59]. This combinator curve is optimized based on the vessel type, power plant and use of the vessel. In the case of the CET, the combinator curve is automatically generated by the model, so optimization based on the power plant is limited. As a result a general combinator curve is applied, of which the resulting propeller load line can be found in Figure 33.

At maximal power the C_4 value of the CPP is the same as for a FPP. As power decreases, the value of C_4 decreases instead of the propeller speed. Next, at a certain percentage of the total power, the value of C_4 is kept constant, resulting in a decrease in propeller speed. In the shown example, this is at 85% of the total power, but this can be adjusted by the user. Lastly, when the propeller speed reaches a certain percentage, the propeller speed is kept constant again and the value of C_4 is decreased again. In the shown example, this is at 50% of the propeller speed, but this can be adjusted by the user.

The maximal value of C_4 is determined, by rewriting equation 54, as can be seen in equation 56. The maximal propeller speed is often a more well known characteristic of a vessel type than the value of C_4 , so this fact is used to compute the maximum value of C_4 . Similarly, the constant value of C_4 is calculated with the same equation, but with a percentage of the maximal power.

$$C_{4,max} = \frac{P_{max}}{n_{prop,max}^3} \quad (56)$$

8.3.3 Effect on engines

As mentioned previously, the pitch setting has an effect on the operating point of the engines. Studying Figure 33 shows that similar power is now achieved at a higher rotational speed. The effect this has on a diesel engine, electric motor and gas turbine can be found in Figure 34, 35 and 36 respectively. Figure 34 shows that the fuel consumption of a diesel engine is worst with the applied combinator curve. The load torque is lower, due to the higher rotational speed. However, the mechanical torque loss is higher, as this is a function of the engine speed. The extra torque loss is higher than the reduction in load torque, leading to an increase in overall torque and thus fuel consumption. A similar phenomenon can be observed with the gas turbine in Figure 36. The relative mechanical loss in a gas turbine is significantly smaller than in a diesel engine, resulting in an insignificant effect of the increase of rotational speed. Figure 35 shows that an increase in rotational speed has a positive effect on the efficiency of the electric motor. The modelled efficiency curve of the electric motor is a function of the rotational speed of the motor. Since the highest efficiencies are found at the highest rotational speeds, an increase of in rotational speed thus has a positive effect on the efficiency.

The mentioned effects of the CPP are logical from a modelling perspective, yet from a practical point of view a different conclusion may be drawn. CPPs are often employed in combination with a internal combustion engine and seldom in combination with an electric engine. This is due to their advantages in manoeuvrability, their increased capabilities at low rotational speed and their ability to keep the shaft speed constant for a PTO. All of these advantages are not included in the CET, culminating in the previously described effects. There is no way of compensating for the modelled behaviour of a CPP as was done for the SOFC. Therefore, the results of the configurations with a CPP should be evaluated carefully. On the other hand, the CET shows the potential of combining a CPP with an EM. From an operational perspective such a configuration could be very interesting, as it combines the adaptability of the CPP with the large engine envelope of the EM. As a result, a significant amount of torque can be produced at almost every rotational speed and the efficiency of the EM over the total load range is outstanding. This makes this combination of components suitable for vessels with an irregular and highly dynamic operational profile.

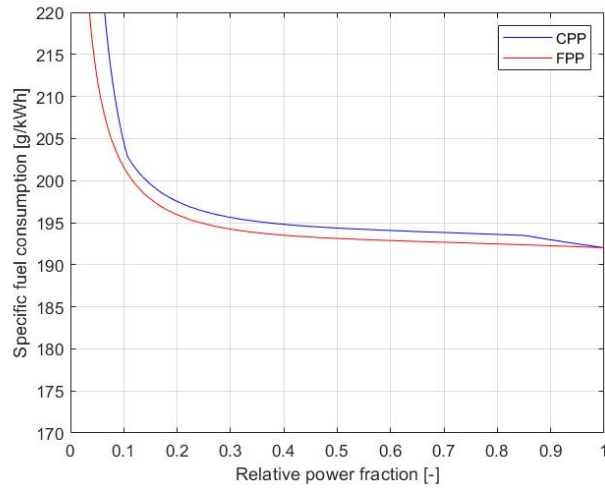


Figure 34: Effect of a CPP on the fuel consumption of a diesel engine

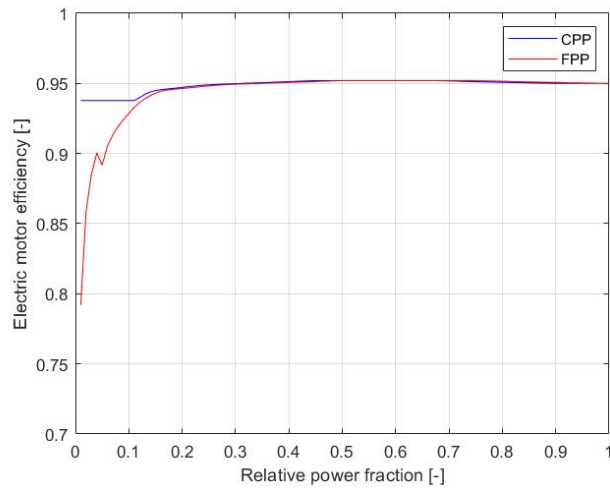


Figure 35: Effect of a CPP on the efficiency of a electric motor

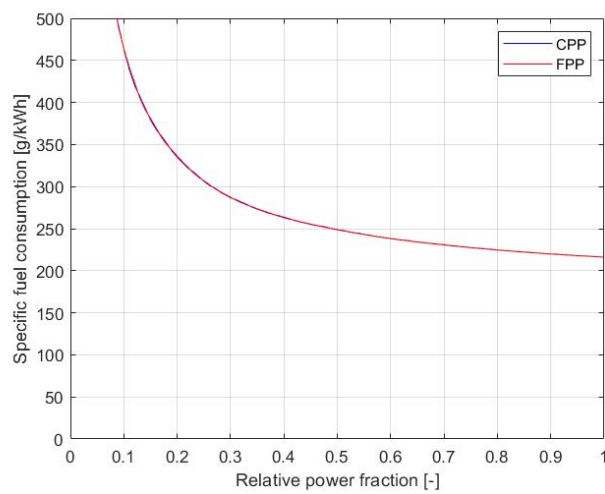


Figure 36: Effect of a CPP on the fuel consumption of a gas turbine

8.4 Modified components

Every model taken from van Dijk [12] or ten Hacken [18] has been re-verified (and re-validated if possible). Certain modifications have been made to a number of sub-models to fit these models into the current CET. Only the adjustments made to these performance sub-tools will be discussed in this paragraph. The performance of the diesel engines is described in a little more detail, as it is based on a model of the Delft University of Technology.

8.4.1 Diesel and dual fuel engines

The performance model of the diesel and dual fuel engine is based on a diesel model of the Delft University of Technology [33]. The main modification is to replace the dynamic model for a quasi-static model. The model follows the thermodynamical principles of a Seiliger cycle. It assumes known performance at the nominal working point after which the performance at part load can be calculated.

Working principles and model implementation

The working principles are based around the Seiliger cycle. Per stage the amount of work and heat can be calculated, resulting in a total fuel input and power output [34]. Similar to the gas turbine, first the performance at nominal power output is computed. The heat input efficiency, nominal torque loss and combustion characteristics of the nominal operation point are used for the calculation of part load conditions. The torque loss at part load conditions is a function of the nominal torque loss and the engine speed at that operation point, similar to equation 35.

To determine the fuel input needed at part load conditions, a range of fuel inputs is given to the model. The resulting torque is compared to the required torque. The torque closest to, but higher than, the required torque is selected as the output torque, along with its corresponding fuel input. It can occur that not enough torque can be delivered by the engine, due to the low engine speed. In that case the PMS will find another combination of engines to provide the needed power, as was described in Paragraph 6.3.

Turbocharger

A consequence of not using a dynamic model is the way the turbocharger is simulated. The turbocharger can be seen as a feedback loop where the exhaust gas heat of the current time step is used to calculate the charge pressure of the next time step. Since there is no dynamic model, there are no more time steps. This problem is solved by looping the calculation several times, where the exhaust gas heat of the current calculation is used to determine the charge pressure in the next calculation. Essentially, the time steps are replaced with calculation steps. Figure 37 shows the calculated charge pressure over the calculation loop. It can be seen that after roughly 20 iterations the charge air pressure becomes constant and a stable working point has been reached. For this specific part load condition the final charge pressure is 199277 Pa. For similar conditions the original model reaches a final charge air pressure of 199277 Pa, which matches the new model.

Signatures

The diesel model of the TU Delft does not calculate the temperature of the exhaust gasses. Information from manufacturers shows that the temperature of the exhaust gasses lies around the 330 °Celsius. This average temperature is taken for every engine and working point, even though the actual temperature is dependent on many different variables, including engine type and relative load. The main arguments for this decision are the relatively small differences in temperature between engines and working points (only a few percent) and the amount of assumptions that have to be made in order to increase this precision.

Verification and validation

The new diesel engine model is verified with the use of the existing model. The goal is to have similar results for both models under similar conditions. Figure 38 shows the results of both models. Since the models match perfectly the lines of the models overlap. For this reason markers have been added for some points of the original model. The conditions that are used as input are not representative of actual existing engines. It can be concluded that the verification of the new model is successful.

The new model is validated with data of multiple Wärtsilä engines [29, 30, 31]. For these engines the fuel consumption at different working points is known. Furthermore, most of the input parameters are also given. Figure 39 shows the measurements and the model results for 6 different engine types. It must be noted that Wärtsilä has a 5% tolerance on their stated values. The model results of the 26 and 32 series fit quite well with the given product guide values. The maximal relative differences between the model and these values is 2%. For the 20 series the fit seems to be more poorly, as the maximal difference here is 4%. Given the detail level of the CET, the maximal difference in all three cases is deemed acceptable.

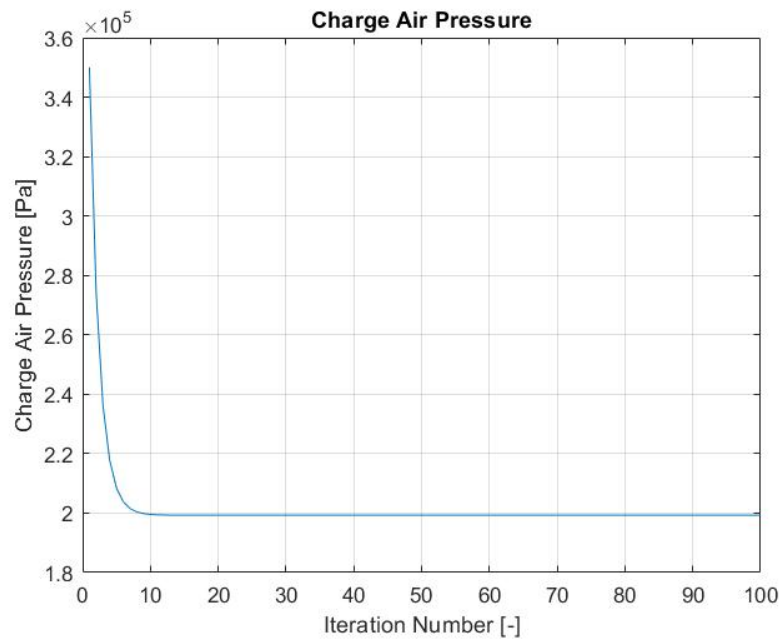


Figure 37: Calculated charge pressure over calculation loop. The starting pressure was set to 3.5 bar. The final pressure is 199277 Pa, which is reached after 19 iterations.

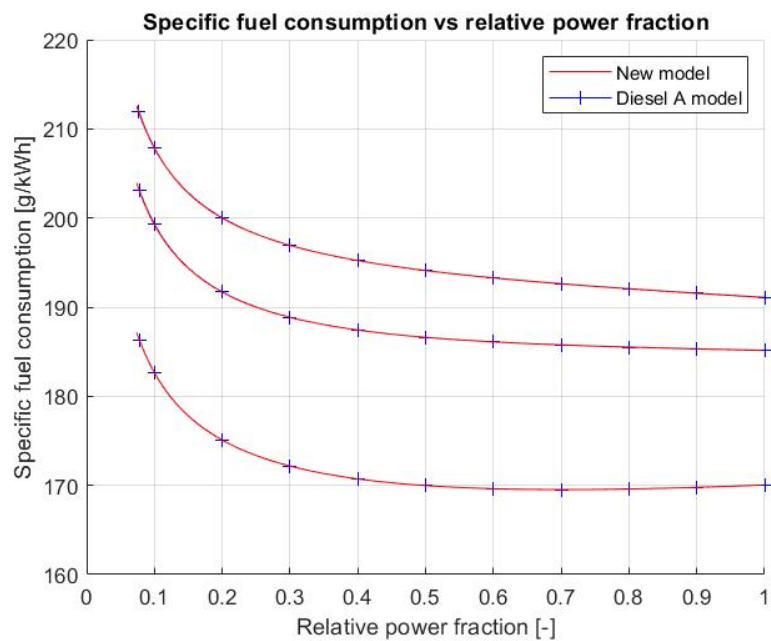


Figure 38: Verification of the new diesel engine model. The results match perfectly, thus the the lines of both models overlap. The given conditions are not representative of existing engines.

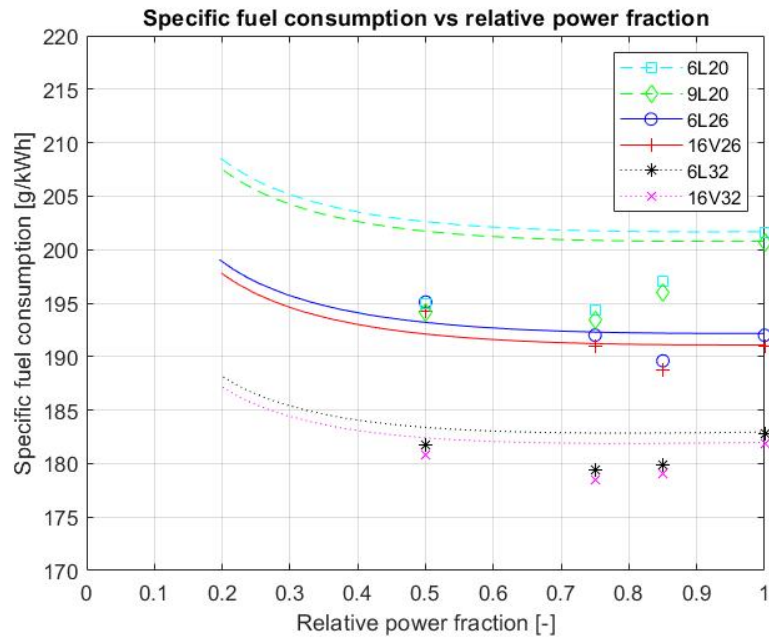


Figure 39: Validation of the new diesel engine model. The measurements are given as markers of the same colour.

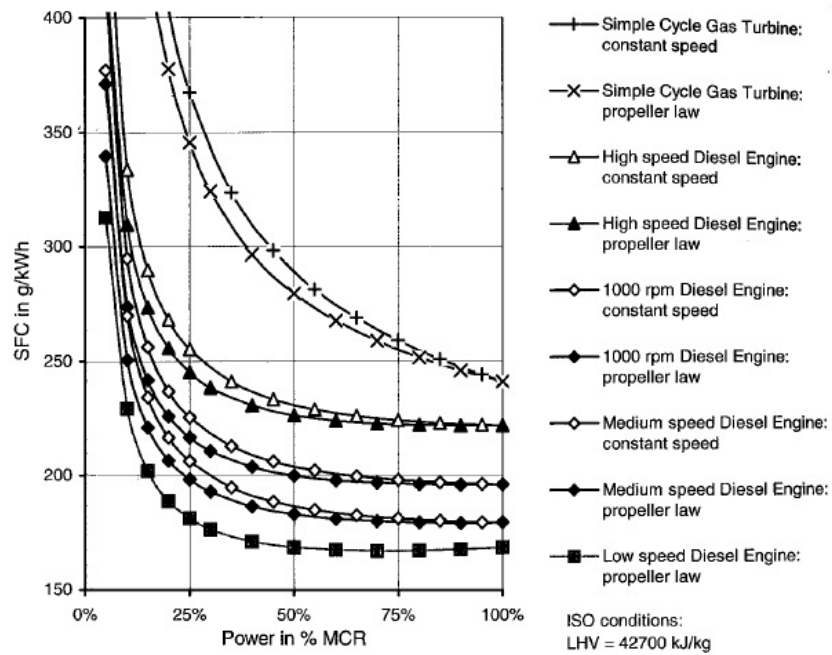


Figure 40: Specific fuel consumption of different engines [34].

Although the differences are acceptable, two drawbacks of the model can be found in the validation. Firstly, at higher power fraction the specific fuel consumption seems to be constant, with the best fuel economy at 100% load. In reality the best fuel economy is often found around 80%, as can be seen in the measurement data. These discrepancies will lead to disadvantages for configurations that work at the ideal working point of the engine. This downside is softened by the fact that the PMS does not look at the actual fuel consumption when distributing power. Hence, all engines are impaired equally, as the PMS tries to get all engines to a working load of 90%.

Secondly, the model often estimates the fuel consumption to be higher than the measured data, since the model takes the 100% load as a base and the fuel consumption always goes up at lower power fractions. This can lead to a general disadvantage of diesel engines compared to a EM and a gas turbine. However, this effect is probably very minor, as the fuel consumption of the three types of engines differs significantly.

When the model output is compared to figure 40, provided by Klein Woud and Stapersma [34], the output of the model matches quite closely. The same constant fuel consumption at higher power fraction can be found and fuel consumption given by Klein Woud and Stapersma is in general even somewhat higher than the output of the model. Though, it must be noted that this figure may be outdated and thus not accurate with current engines. All in all it is concluded that the new diesel model is sufficient for the CET.

8.4.2 Electric motor

The performance model of the electric motor is converted from a dynamic model to a quasi-static model. The choice has been made to not model the working principles of the electric motor, but instead model an efficiency curve. This decision is dictated by the fact that the electric motor has no emissions or signatures, so only the energy conversion is of interest. Moreover, the available research time was limited. The applied efficiency curve is developed by ten Hacken [18] and is based on the dynamic model of a permanent magnet synchronous motor. The curve can be found in Figure 41.

8.4.3 Generators

As mentioned in Paragraph 7.3, the generator-sets are 4-stroke diesel engines. Therefore, the performance of the generator-sets is similar to that of the diesel engines. The only difference is found in the conversion from mechanical to electrical power. The generator has a constant efficiency of 95%. The verification and validation of the generators is analogous to the verification and validation of the diesel engines.

8.4.4 Proton exchange membrane fuel cell

The PEMFC model developed by ten Hacken [18] was based on a submarine application for the fuel cell. This means that the fuel cell was provided with pure pressurised oxygen and hydrogen. Furthermore, the fuel cell was a dead-end configuration, resulting in full fuel utilisation and lower concentration losses. The PEMFC can still be pressurised, but a compressor would be needed. Figure 30 has shown that pressurising a fuel cell with a compressor lead to a net loss in power. This is also true for a PEMFC. Therefore, the operating pressure of the fuel cell is changed to 1 atm. Moreover, the concentration loss coefficient has been changed from 0.01 to 0.06, based on Stapersma and de Vos [26].

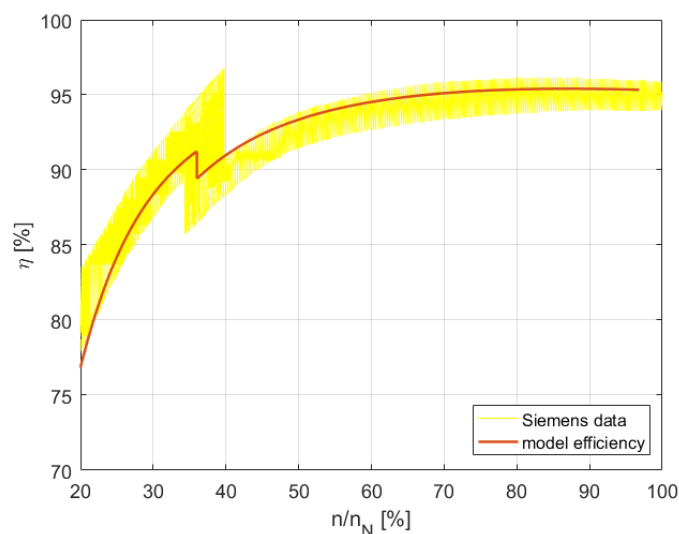


Figure 41: Efficiency curve of the electric motor [18]

9

Robustness

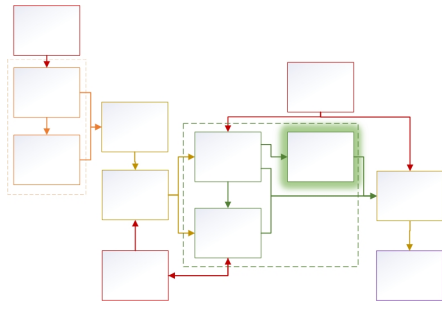


Figure 42: Chapter location within model, based on Figure 5

Robustness is the ability of a system to maintain performance after a failure has occurred. High levels of power plant robustness are advantageous for vessels, as they allow the ship to keep operating and fulfill its mission. This is true for commercial shipping, where internal sources can induce breakdowns, yet even more so for naval vessel, where external sources may try to intentionally harm the ship. Robustness in the context of this thesis is defined as the remaining power output of the power plant in the hurt state. Multiple failures will be simulated to compute an overall robustness score. Figure 42 shows the position of this chapter within the complete model structure. The input of this sub-tool is the actual installed power of every component. The output is passed on to the MCA.

9.1 Quantified definition

Multiple metrics can be developed to assess robustness. The most simplistic measure is to observe if a system is still operating after collapsing. This is useful when the function of a structure is also binary, namely on or off. However, the functioning of a power plant is not binary, since a continuous range of power can be developed. In this case, one could examine the remaining capabilities of the power plant after failure. This idea is used by van Leeuwen [60] in his tool to estimate the vulnerability of a network. De Vos [13] and others [16, 17] have studied the continuous capabilities of a system over time, after a disruption has taken place. A general response curve of a system can be found in Figure 43.

Three states were defined:

- Intact state, the normal state of the system before a failure occurs
- Damage state, the most damaged state shortly after the failure occurs. The capabilities of the system are at their lowest during this state.
- Hurt state, state after some recovery has taken place. After the failure occurred and the system got damaged some capabilities can be regained from the damage state.

The capabilities in the hurt state form an excellent metric for the ability of the vessel to maintain operation, as this is the power capacity the ship will have for the remainder of the mission. Furthermore, it allows the system to deal with a disruption by means of recovery. In the context presented here, recovery is not repairing a failed component, but finding ways for the damaged system to increase performance, while having a damaged part. This can be done for instance by increasing the capacity of other components or

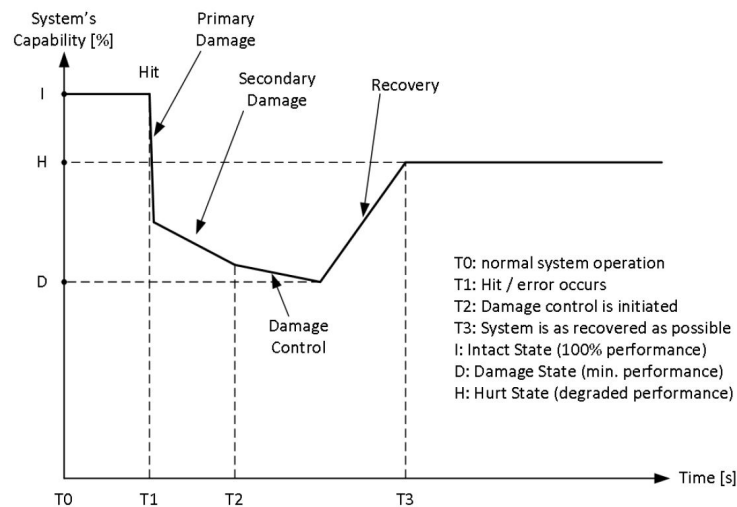


Figure 43: Capabilities over time as a result of a disruption [13]

reconfiguring the connections within the system. Configurations with back-up parts or overcapacity on their components will have a greater measure of recovery, thus a higher level of robustness. This gives the CET motive to install multiple, larger and/or back-up components. As a result, the robustness of a concept is determined with equation 57. It should be noted that the nominal of the operational profile is taken as standard, and not the maximal power of a configuration. The reason for this is that the nominal power is needed to fulfill a mission, so that is the amount of power that should be achieved for a full score on robustness.

$$R = \frac{P_{hurt}}{P_{nom}} \quad (57)$$

9.2 Calculating hurt state power

For the calculation of the power in the hurt state, network theory is being used. A topology of connected systems can be described by a directed network of nodes and edges. The nodes depict the components, while connections are illustrated by the edges. An example can be found in Figure 44, with Table 22 detailing the different nodes and edges. The example is a hybrid configuration with diesel engines, electric motors and generators, as to show all possible connections. The weight of the edges in the figure are equivalent to the maximal power that a component can produce or withstand, as stated in the table. Furthermore, three imaginary nodes (node 1,14 and 15) are added to make calculations possible.

Two notes should be placed. Firstly, it can be argued that the maximal power of a propeller is not infinite. However, since the propeller is not included in the scope of this research, the maximal power is assumed to be infinite. Secondly, the stated maximal power is the absolute maximal power of a component. The CET considers power margins and is capable of designing components with reserve capacity, resulting in a maximal power being higher than the continuous service rating. As robustness becomes relevant in case of emergency, these margins are not longer enforced and the reserve capacity is being called upon.

The power produced by a power plant can be described as a flow from the start (node 1) to either the electrical power drain (node 14) or mechanical power drain (node 15), for electrical and mechanical power respectively. This flow is constraint by the weight of the edges through which the power flows. A failure of a node can be simulated by changing the weight of the outgoing edge to zero, for no power can flow through

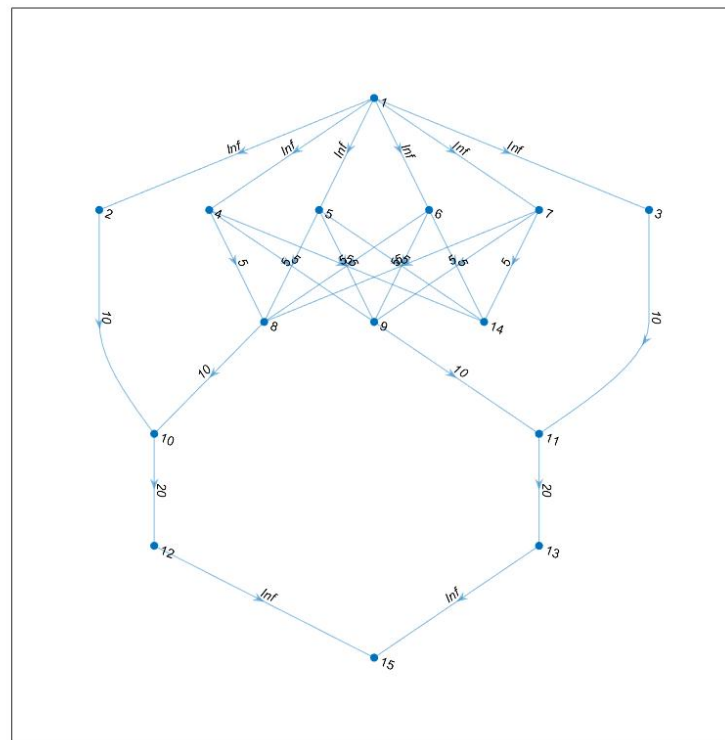


Figure 44: Example of network representation of hybrid configuration

Table 22: Network details

Node	Function	Max Power [MW]
1	Power start	inf
2	Diesel engine	10
3	Diesel engine	10
4	Generator	5
5	Generator	5
6	Generator	5
7	Generator	5
8	Electric motor	10
9	Electric motor	10
10	Gearbox	20
11	Gearbox	20
12	Propeller	inf
13	Propeller	inf
14	Electric power drain	-
15	Mechanical power drain	-

that edge anymore. After a failure is instigated, the resultant flow is equivalent to the maximal power the power plant can produce.

9.3 Simulated failures

In theory, every (combination of) component(s) failure can be simulated. Nonetheless, since only a first indication of the robustness is needed and simulating every breakdown is a costly computational process, three failures are considered. The failures will be studied in separate simulations, so no combined breakdown, and will occur in a gearbox/shaft/propeller, a main engine and a electricity generation system. Within these areas, the component with the highest max power will collapse, as the effects of such failure will be the greatest.

The specific areas of failure are chosen for different reasons. The main engine and electricity generation systems are assumed to be the most likely to deteriorate, because there are often a large number and a substantial amount of heat involved. Furthermore, they can be relatively voluminous, making them a possible target to be hit. The gearbox/shaft/propeller failure is included to differentiate between single shaft and twin-shaft configurations. From practical applications it is known that twin-shaft concepts are more robust and redundant. To show this fact within the CET, this specific failure is included.

The likelihood of failure is not included in this simulation. This would require extensive knowledge of the maintenance cycle of the component for internal failure, as well as the general arrangement of the vessel for external failure. Since both are not included in the CET, all three failures are deemed equally likely to occur. Moreover, other side-effects of the failure, for example risk to personnel, ease of repair, ability to fulfill mission, are not included in the tool.

9.4 Determine robustness score

The final robustness score is build up out of the six separate scores; three failures, with each a score for the mechanical and the electrical robustness. The effect of mechanical and electrical power loss is deemed equally heavy. As a result, the final robustness score is an unweighted average of the six scores. It may occur that the power in the hurt state is greater than the nominal power, as a result of a large power reserve capacity. This would lead to a robustness score greater than one. Since more power than nominal does not lead to extra capabilities of the vessel, the extra power is deemed futile and the robustness score is thus limited to one. This will motivate the CET not to install increasingly large components in order to increase the robustness of the configurations.

9.5 Verification

The robustness model is verified with the tests found in Table 23.

Table 23: Verification tests of robustness model

Test	Outcome	Remark
Network structure	Passed	Both nodes and edges
Edge weights	Passed	Equal to max power component
Failure shaft/propeller	Passed	
Failure main engine	Passed	
Failure EGS	Passed	
Max flow	Passed	
Maximal score	Passed	Equal to 1
Maximal total score	Passed	Average of all scores

Part 3
Model output

*"Computers are incredibly fast, accurate and stupid.
Human beings are incredibly slow, inaccurate and brilliant.
Together they are powerful beyond imagination."*
Unknown

10

Case Studies and Results

A number of case studies have been performed to show the output of the model and the possibilities this output gives to the design process. For each case study a mission profile is defined, along with client preferences. The case studies are based on existing naval vessels, though slightly altered. The sources and actual figures of these vessels are not included, due to confidentiality. Output is given on three different detail levels; concept level, trend level and space level. On the concept level the configurations are described in terms of component selection, component sizing and performance of the KPIs. This allows for detailed examination and comparison of the different concepts. On the trend level the component choice of the best configurations is displayed, in order to find overall trends within the optimal concepts. On the space level the whole design space is presented, which allows for analysis of the whole design space and comparison of the performance of a chosen concept against all other concepts.

Since the design space is multidimensional, it is not possible to display this in a 2D rendering. As a result, three dimensions are compared with each other to get an understanding of the total design space and the position of the optimal concept within this design space. The three chosen dimensions are total efficiency, volume and robustness. These are chosen as they have lowest level of dependency towards each other, i.e. efficiency, emissions and signatures are closely related and volume and mass are closely related. Furthermore, these client preferences are often given priority within the study cases. As a result, these three dimensions provide the best image of the design space. This chapter discusses one design space analysis per case study, the other analyses can be found in Appendix A.

After the case studies, overall trends are discussed and the most evident trend, electric motors and fuels cells, is studied further to find out why this is a dominant combination. Moreover, a sensitivity analysis is performed on the client preferences, to show the influence of this input parameter on the model. Lastly, the results of the entire research will be discussed.

10.1 Case study 1: Frigate

The first case study revolves around a frigate. A frigate is characterised by missions with a potential high level of violence. This results in a higher importance of robustness, signatures and volume, at the expense of efficiency and emissions. The case study is split into two parts. In the first part (case 1A), all possible components are utilised. In the second part (case 1B), the fuel cells are disabled, as they are not yet customary for many navies.

10.1.1 Input

The characteristics of the frigate, including the weight factors for the various KPIs, can be found in table 24. A mission profile is constructed by utilizing constant mission elements, as seen in Table 25. The applied operational profile can be found in Table 26 and Figure 45.

Table 24: Vessel characteristics and weight factors for case study 1A and 1B

Vessel type	Nom power	Nom prop speed	Efficiency	Emissions	Volume	Mass	Signatures	Robustness
-	MW	RPM	-	-	-	-	-	-
Frigate	17.8	210	4	2	8	6	8	10

Table 25: Mission elements of case study 1A and 1B.

Mission element	1	2	3	4	5	6
Mission mode	Anchor	Slow speed	Patrol	Transit	Full speed	Combat
Speed [knts]	0	10	14	18	27	22
Propulsive power [kW]	0	700	1840	3670	17800	7060
Electrical power [kW]	450	760	770	660	770	900

Table 26: Operational profile of case study 1A and 1B.

Mission element	4	3	4	5	3	6	1	2	3	5	6	2	4
Time [hours]	72	72	48	12	24	12	24	24	48	24	12	24	72
Propulsive power [kW]	3670	1840	3670	17800	1840	7060	0	700	1840	17800	7060	700	3670
Electrical power [kW]	660	770	660	770	770	900	450	760	770	770	900	760	660

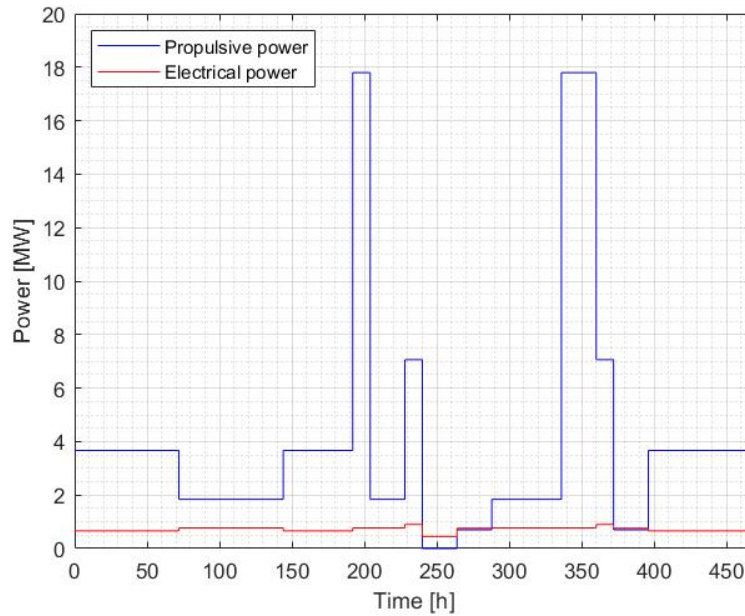


Figure 45: Operational profile of case study 1A and 1B.

10.1.2 Output Concept level

The output of the cases 1A and 1B can be found in Table 27. In case 1A the model chose to implement a geared, twin shaft CPP configuration. Two electric motors, in combination with two SOFCs, were installed to provide the necessary power. No batteries were used a ESS. The diesel engines are running on MDO, while the SOFC are operating on LNG.

The significant importance of robustness has resulted in a significant overcapacity per component for the MPEs and EGSs. In case of a single component failure, the nominal power can almost be met, resulting in minimal robustness losses. On the other hand, the total volume is significantly larger compared to a configuration with internal combustion engines and generator sets. The signatures are kept to a minimum with the application of SOFCs. PEMFCs may be considered to further decrease the signatures, yet this would come at the cost of efficiency and most likely volume and mass. Due to the use of LNG, only CO₂ is emitted.

In case 1B the SOFCs are replaced with diesel generators. As a result, the electric motors are replaced with diesel engines. It is noteworthy that the robustness has increased, even though case 1B is a more constrained version of case 1A. Furthermore, case 1B outperforms case 1A in total volume and mass too. All other metrics are significantly worse.

Trend level

Figures 46 and 47 show the type and number of components used by the best configurations of the respective case studies. This gives an indication about which parts perform well within the given mission profile and client preferences. This global view shows the added value of a CET, as all configurations can be reviewed and global trends can be discovered. The numbers in the labels specify the number of components used in that type of configurations. Moreover, as concepts can combine different components, concepts may be counted double in the histogram. For example, a configuration with 2 DE4s and 1 EM is counted once in the bar of 2 DE4 and once in the bar of 1 EM.

Figure 46 displays a major preference for geared twin-shaft configurations with electric motors. The electric motors are often combined with either PEMFCs or SOFCs. The SOFC is favoured over the PEMFC. Reasons could be the slightly higher efficiency or the ability to use fuels with higher energy densities, leading to smaller volumes and masses. It is notable that gas turbines and generators are hardly or never utilised. This gives a strong indication about the usability of these components in case study 1A. Furthermore, a single shaft concepts is never considered, as can be seen by the use of double propellers, yet a single gearbox does occur.

Table 27: Optimal configuration of case study 1A and 1B, including KPI values

Case 1A	Type	Value	Unit		Value	Unit
Propeller	2x CPP	-	-	Total efficiency	0.62	-
Gearbox	2x	15.6	MW	CO2	574.5	ton
MPE	2x EM	15.6	MW	SOx	0	ton
EGS	3x SOFC	14.0	MW	NOx	0	ton
ESS	-	-	kWh	Total volume	1114	m ³
Fuel	LNG	225	ton	Total mass	741	ton
Average signatures					0.9	MW
Robustness					0.94	-
Case 1B						
Propeller	2x FPP	-	-	Total efficiency	0.41	-
Gearbox	2x	13.8	MW	CO2	1423.4	ton
MPE	4x DE4	6.9	MW	SOx	1.8	ton
EGS	2x DG	0.9	MW	NOx	30.0	ton
ESS	-	-	kWh	Total volume	777	m ³
Fuel	MDO	449	ton	Total mass	727	ton
Average signatures					2.0	MW
Robustness					0.96	-

This means configurations with a direct and geared shaft do make it into the best concepts. Moreover, the use of 2-stroke diesel engines is remarkable, as the priority is given to mass and volume and not efficiency. Therefore, 4-stroke diesel engines would be expected more often. This discrepancy is explained further in Paragraph 10.5. MDO is the most common fuel within the best configurations. This is logical, since every configurations with a reciprocating engine uses either MDO or HFO and MDO is the less polluting variant. The usage of LNG and NH₃ is related to the utilisation of the SOFC, as dual fuel or gas turbines are hardly used.

Figure 47 shows the enforced shift from fuel cells to generators, and the resultant shift from electric motors to internal combustion engines. The use of electric motors is less advantageous when they are not coupled with efficient fuel cells, but they are still the most commonly utilised component. It is noteworthy that a single electric motor is more frequently employed than two electric motors. Since single-shaft concepts did not make it into the top 100, the single electric motor has to be partnered with other engines in a asymmetric topology. This is most likely the result of the priority given to robustness, which motivates the choice to install extra (back-up) engines. For similar reasons, no concept exists with a single generator and 2 identical engine configuration are rare, as multiple engines are presumably combined to enlarge the robustness. The usage of CNG, NH₃ and H₂ has ceased. For hydrogen this is logical, as fuel cells are no longer used and apparently dual fuel engines perform best on LNG.

Space level

Figures 48 and 49 present the total design space in terms of total efficiency versus volume for case study 1A and 1B respectively. The concepts are colour coded based on their overall ranking. The optimal configuration is indicated with a star. The Pareto front for this 2D design space is added as a black line. For case study 1A, the optimal concept lies on the Pareto front, which is to be expected, since volume is given priority and the efficiency influence all other KPIs, as will be discussed in Paragraph 10.5. Similarly, most of the well performing concept are close to the Pareto front, as expected. A small cluster of high ranking concepts can be found between 0.50 and 0.55 efficiency and between 2500 and 3000 m³. This indicates that the other KPIs are influencing the ranking as well. Most of the poor concept can be found at low efficiency and high volume. However, some of the bad configurations can also be found near and around the optimal concept, implying worst performance on the other KPIs. From the position of the optimal concept it can be derived that it is more efficient than almost all other concepts, while being slightly better than the average volume.

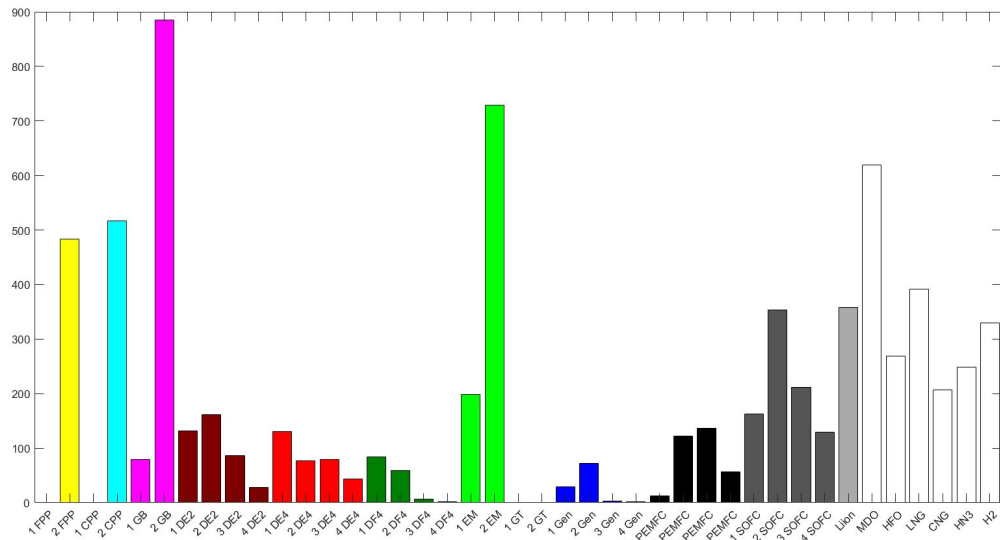


Figure 46: Type and number of components used by the top 1000 configuration of case study 1A. Multiple components can be combined, resulting in a sum of components higher than 1000.

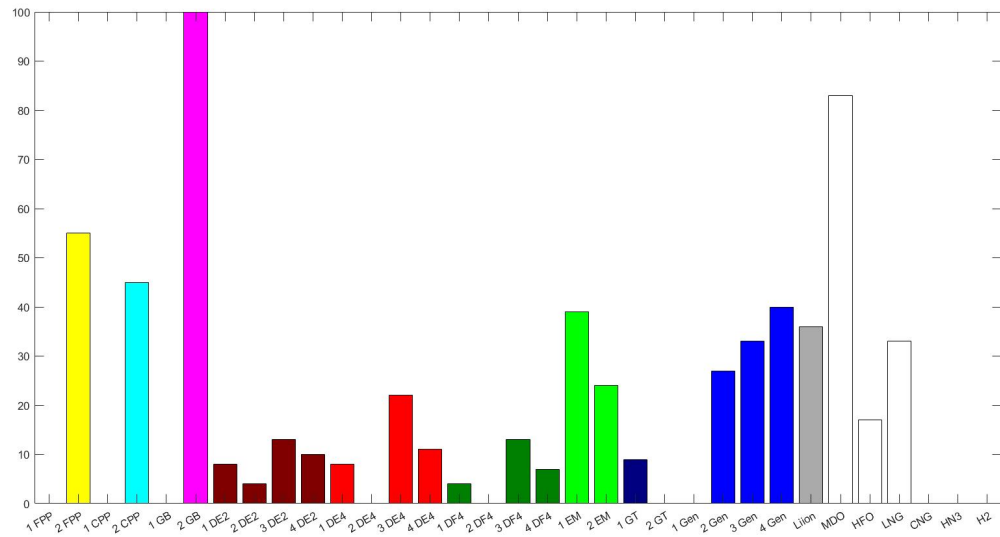


Figure 47: Type and number of components used by the top 100 configuration of case study 1B. Multiple components can be combined, resulting in a sum of components higher than 100.

Furthermore, since the optimal configuration lies on the Pareto front, no performance can be gained on one KPI without losing performance on the other KPI. In case 1B, the optimal configuration does not lie on the Pareto front. In terms of volume, it comes close to the front, but some efficiency could have been gained without compromising on volume. An explanation why the optimal configuration does not lie on the Pareto front can be found in the performance of the other KPIs. Apparently, the optimal concept outperforms the other configurations in these KPIs. The shape of the Pareto front shows that achieving the highest efficiency comes at great cost in terms of volume in this case study.

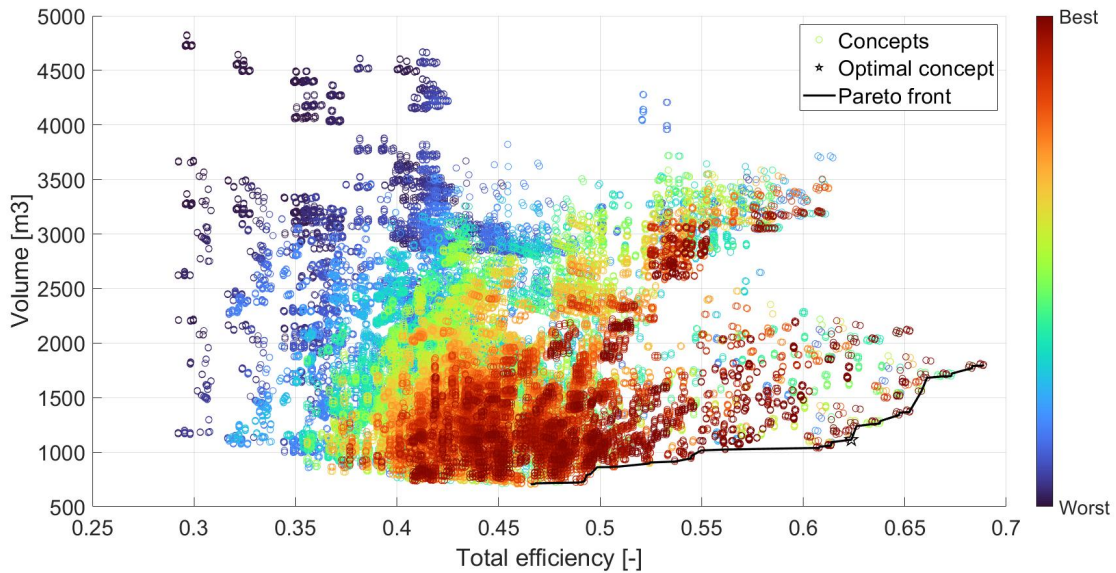


Figure 48: Efficiency-versus-volume design space. All concepts of case study 1A, including the optimal configuration indicated with a star and the Pareto front indicated with a black line. The colour of a concept is based on the overall ranking of the concept from best (red) to worst (blue).

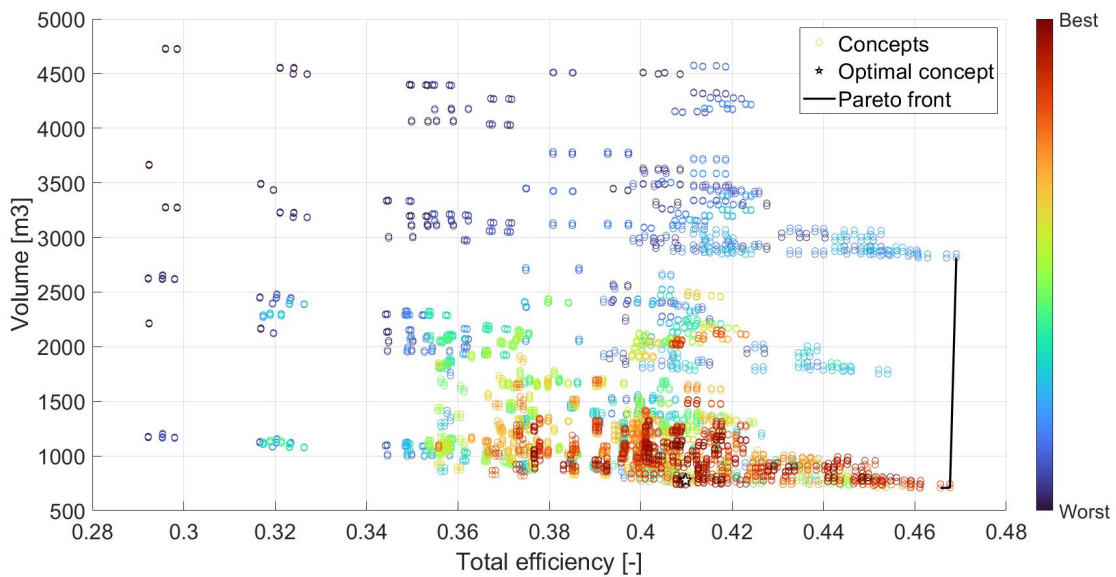


Figure 49: Efficiency-versus-volume design space. All concepts of case study 1B, including the optimal configuration indicated with a star and the Pareto front indicated with a black line. The color of a concept is based on the overall ranking of the concept from best (red) to worst (blue).

10.2 Case study 2: Offshore Patrol Vessel

The second case study is based on an offshore patrol vessel (OPV). The OPV is characterised by missions of a lower level of violence, often closer to shore. This results in a higher importance of efficiency and emissions, at the expense of signatures and robustness. Again the case study is split into two parts; the first one being with all components and the second one with the fuel cells disabled.

10.2.1 Input

The characteristics of the offshore patrol vessel, including the weight factors for the various KPIs, can be found in table 28. The mission elements used to construct the operational profile can be found in Table 29. The applied operational profile is shown in Table 30 and Figure 50.

10.2.2 Output

Concept level

The output of the cases 2A and 2B can be found in Table 31. A direct, twin-shaft, CPP configurations is employed by the model. The high importance of efficiency and emissions resulted in an electric propulsion train, with electric motors and SOFCs. Furthermore, the importance of efficiency led to a direct drive, as there are no gearbox losses and less shaft losses. The SOFC are significantly larger than required, so they can operate at a more efficient lower power fraction. The SOFCs are fueled with NH_3 , as this results in no emissions. A relative large weight of ammonia is required, as the conversion ratio to hydrogen is not particularly high and the molar weight is significant.

Due to the large SOFCs the total mass and volume are noteworthy, especially when compared with case 2B. This drawback is offset by the total efficiency and the lack of emissions. Furthermore, the omission of internal combustion engines leads to a relatively low average signatures. Lastly, the robustness is comparatively small. This is a result of the full electric configuration, since a failure in an EGS will not only result in electric power loss, but also mechanical power loss.

In case 2B the SOFCs are replaced by three diesel generators. The electric motors are also replaced, as the electricity now gets generated by diesel engines. A more environmental friendly options is adopted, namely 4-stroke dual fuel engines. The chosen dual fuel is LNG. The EGSs are naturally smaller, as they no longer have to power the MPEs. The total efficiency and emissions are worse due to the use of internal combustion engines, yet the total volume and mass are better, for the diesel generates don't benefit from overcapacity in the same way the SOFCs do. Since the propulsion train has become mechanical the robustness has increased.

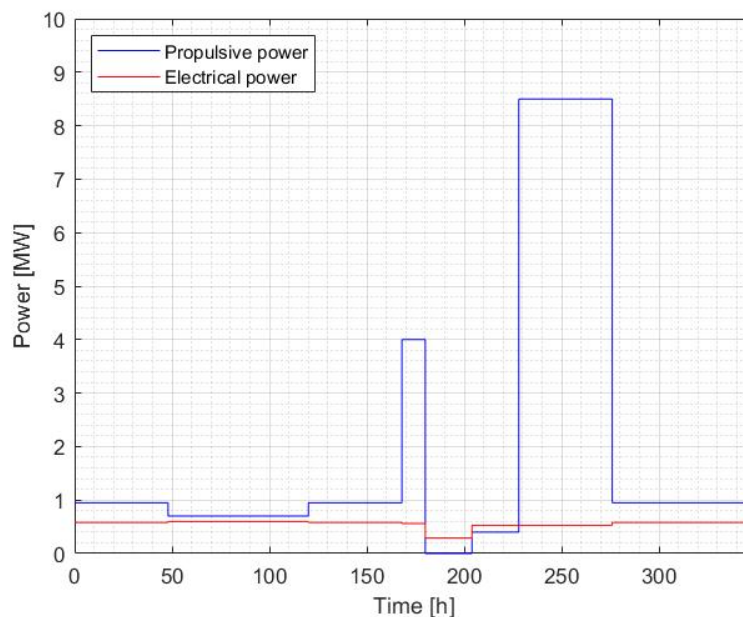


Figure 50: Operational profile of case study 2A and 2B.

Table 28: Vessel characteristics and weight factors for case study 2A and 2B

Vessel type	Nom power	Nom prop speed	Efficiency	Emmissions	Volume	Mass	Signatures	Robustness
-	MW	RPM	-	-	-	-	-	-
OPV	8.5	210	6	7	7	4	3	3

Table 29: Mission elements of case study 2A and 2B.

Mission element	1	2	3	4	5	6
Mission mode	Anchor	Slow speed	Patrol	Transit	Full speed	Combat
Speed [knts]	0	6	10	12	22	18
Propulsive power [kW]	0	400	700	950	8500	4000
Electrical power [kW]	290	530	600	580	530	560

Table 30: Operational profile of case study 2A and 2B.

Mission element	4	3	4	6	1	2	5	4
Time [hours]	48	72	48	12	24	24	48	72
Propulsive power [kW]	950	700	950	4000	0	400	8500	950
Electrical power [kW]	580	600	580	560	290	530	530	580

Table 31: Optimal configuration of case study 2A and 2B, including KPI values

Case 2A	Type	Value	Unit	Value	Unit
Proppeller	2x CPP	-	-	Total efficiency	0.66 -
Gearbox	0x	-	MW	CO2	0 ton
MPE	2x EM	4.8	MW	SOx	0 ton
EGS	2x SOFC	9.2	MW	NOx	0 ton
ESS	-	-	kWh	Total volume	729 m3
Fuel	NH3	256	ton	Total mass	535 ton
				Average signatures	0.5 MW
				Robustness	0.85 -
Case 2B					
Propeller	2x FPP	-	-	Total efficiency	0.42 -
Gearbox	2x	5.8	MW	CO2	409.0 ton
MPE	4x DF4	2.9	MW	SOx	0.1 ton
EGS	3x DG	0.3	MW	NOx	3.9 ton
ESS	-	-	kWh	Total volume	441 m3
Fuel	MDO	43	ton	Total mass	310 ton
	LNG	107		Average signatures	1.9 MW
				Robustness	0.94 -

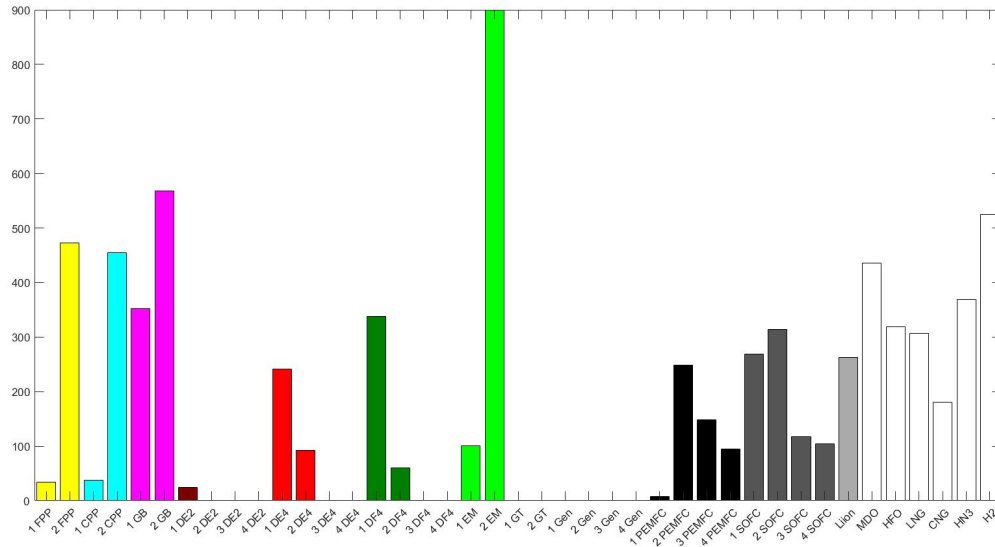


Figure 51: Type and number of components used by the top 1000 configuration of case study 2A. Multiple components can be combined, resulting in a sum of components higher than 1000.

Trend level

Figures 51 and 52 display the component choice of the top configuration in case study 2A and 2B respectively. In case study 2A, every concept in the top 1000 has an electric motor combined with a fuel cell, indicating a definite preference. This choice is a result of the importance of total efficiency and emissions. Since volume and mass are also given priority and robustness is not, the number of internal combustion engines is limited to a maximum of 2 per type. Moreover, within the internal combustion engines, the dual fuel engine is preferred, due to its lower emissions. The gas turbine and 2-stroke diesel engines are hardly or never utilised. Both emit relatively high levels of emissions, while the 2-stroke engine is voluminous and massive and the gas turbine is inefficient, resulting in sub-optimal components within the given client preferences. Furthermore, the SOFC is favoured slightly over the PEMFC, yet not as much as in case 1A. This could be a result of the decrease of importance of volume and mass, whereby the need for energy dense fuels is also decreased. Generators are not considered, most likely due to existence of more efficient and less polluting alternatives. The H_2 is almost solely spend in concepts that employ PEMFCs, meaning that the configurations with merely SOFCs predominantly use either LNG, CNG or NH_3 , showing the advantages of internal reforming versus the use of hydrogen as a fuel.

Figure 52 shows the effect of disabling fuel cells. Again a clear shift from electric motors to internal combustion engines can be witnessed. In this case, the dual fuel engine is favoured over the other engine types, as a result of their reduced emissions. The dual fuel engine is predominantly powered by the combination of MDO and LNG, presumably as this offers the best combination of energy density and pollution. The use of 4-stroke diesel engines is reduced, which is remarkable as one could expect that electric motors would be replaced with diesel engines. Instead, diesel engines are altered to dual fuel engines. A possible explanation is that all diesel engines were used in a hybrid configurations and these concepts are no longer optimal, since the electric motor has lost some of its advantageous. As a result, there is a limited use for 4-stroke diesel engines. Similarly, the usage of battery is sharply decreased. This decline could be caused by the disappearance of hybrid configurations, yet a comparable reduction was not found in case 1.

Space level

Figures 53 and 54 present the total design space in terms of total efficiency versus robustness for case study 2A and 2B respectively. The optimal concept of case study 2A lies on the extreme end in terms of efficiency, but just off the Pareto front. As a result, all other concepts can be found at lower efficiency, but not necessarily at lower levels of robustness. Moreover, a number of concepts with low robustness are still ranked among the best concepts, while a large share of worst concepts can be found at higher levels of robustness. This indicates that robustness is not given priority in the case study, which matches the given client preferences. Furthermore, it can be seen that some of the best and worse concepts exist very near to each other in this 2D design space. Thus, it can be said that the other KPIs are co-determining the result, which is logical

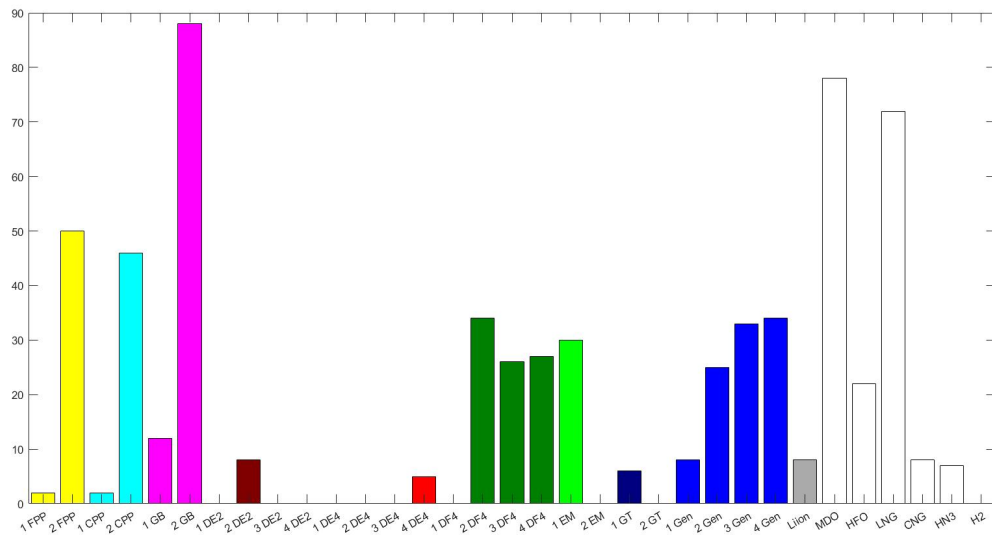


Figure 52: Type and number of components used by the top 1000 configuration of case study 2B. Multiple components can be combined, resulting in a sum of components higher than 100.

if you look at the client preference. The same conclusion can be drawn from Figure 54. In this case, the Pareto front is even formed by concept deemed below average. Moreover, the concepts considered best and worst are rather evenly and randomly spread over this 2D design space. The optimal configuration does achieve the highest robustness, but a significant amount of efficiency could be gained by choosing a different concept. That being said, most of the best concepts have a lower efficiency and robustness than the optimal concepts.

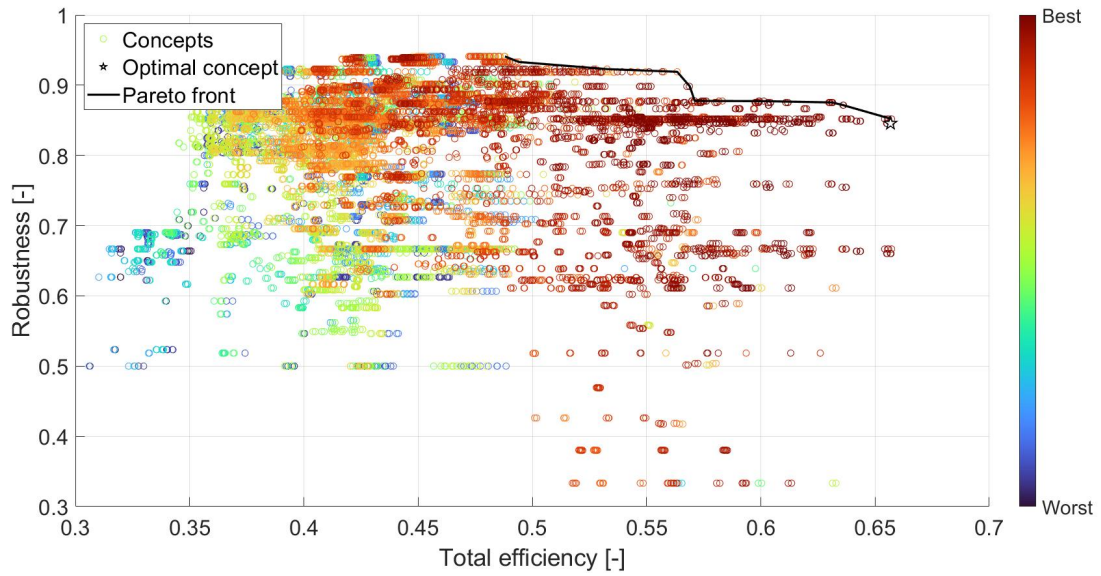


Figure 53: Efficiency-versus-robustness design space. All concepts of case study 2A, including the optimal configuration indicated with a star and the Pareto front indicated with a black line. The colour of a concept is based on the overall ranking of the concept from best (red) to worst (blue).

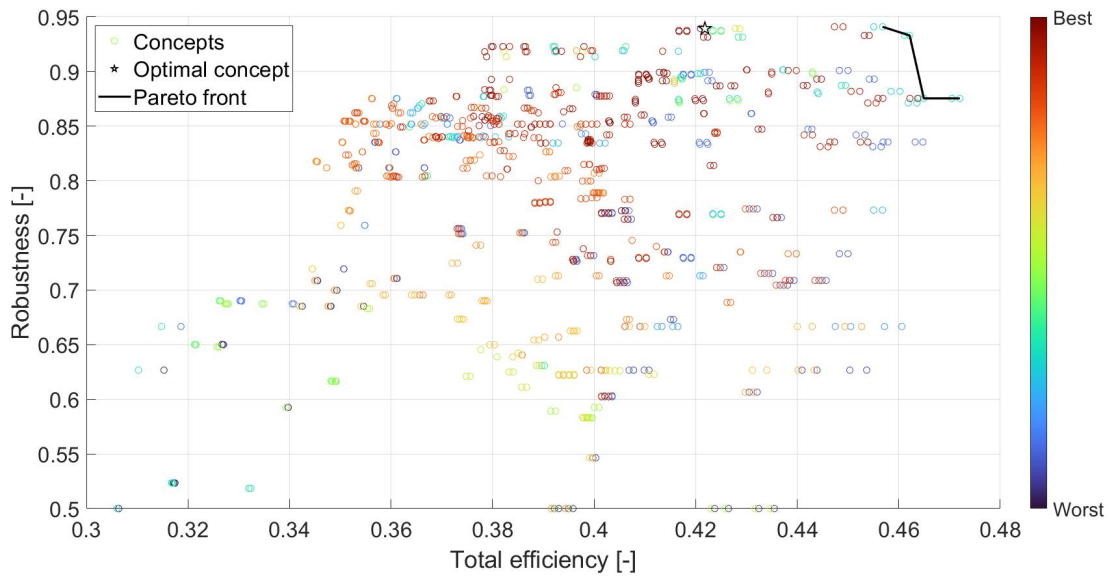


Figure 54: Efficiency-versus-robustness design space. All concepts of case study 2B, including the optimal configuration indicated with a star and the Pareto front indicated with a black line. The color of a concept is based on the overall ranking of the concept from best (red) to worst (blue).

10.3 Case study 3: Fast Offshore Patrol Vessel

The third case study is based on a fast offshore patrol vessel. It differs from the OPV in the previous case study, in terms of the achieved speed and the installed power. The fast OPV is characterised by missions with a low level of violence and the aforementioned achieved speed. This results in a higher importance of volume and mass, at the expense of the other KPIs. Again, the case study is split into two parts. In the first part (case 3A), all possible components are utilised. In the second part (case 3B), the fuel cells are disabled.

10.3.1 Input

The characteristics of the offshore patrol vessel, including the weight factors for the various KPIs, can be found in table 32. The mission elements used to construct the operational profile can be found in Table 33. The applied operational profile is shown in Table 34 and Figure 55.

Table 32: Vessel characteristics and weight factors for case study 3A and 3B

Vessel type	Max power	Max prop speed	Efficiency	Emmissions	Volume	Mass	Signatures	Robustness
-	MW	RPM	-	-	-	-	-	-
FOPV	14	310	4	5	10	8	3	3

Table 33: Mission elements of case study 3A and 3B

Mission element	1	2	3	4	5	6
Mission mode	Anchor	Slow speed	Patrol	Transit	Full speed	Combat
Speed [knts]	0	6	10	15	30	25
Propulsive power [kW]	0	400	1000	2000	14000	10000
Electrical power [kW]	120	220	250	180	280	300

Table 34: Operational profile of case study 3A and 3B.

Mission element	4	3	4	6	1	2	5	4
Time [hours]	48	72	48	12	24	24	48	72
Propulsive power [kW]	2000	1000	2000	10000	0	400	14000	2000
Electrical power [kW]	180	250	180	300	120	220	280	180

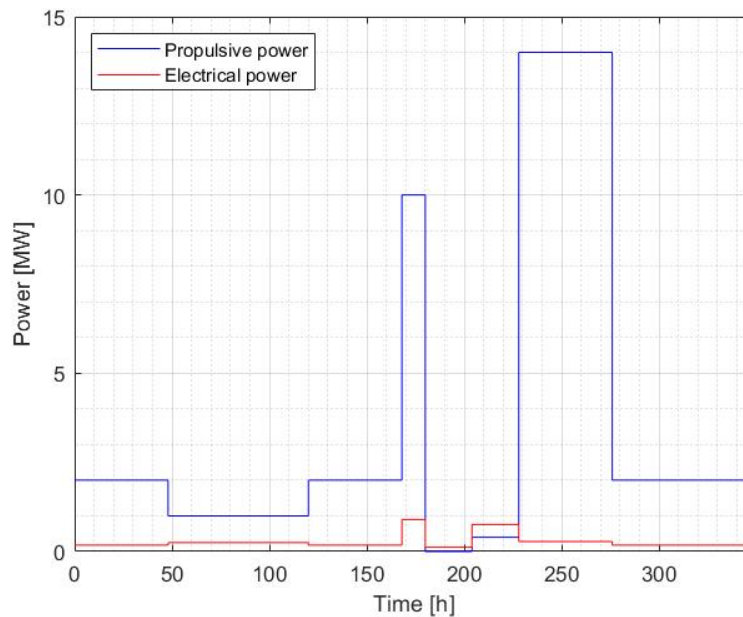


Figure 55: Operational profile of case study 3A and 3B.

10.3.2 Output

Concept level

The output of the cases 3A and 3B can be found in Table 35. Similar to case 2A, a fully electric, geared, twin-shaft, CPP configuration is chosen in case 3A. Due to the importance of volume and mass, the EGSs are no longer overcapacitated. As a result, the SOFC have a less ideal operation point, leading to a lower total efficiency. The SOFCs are fueled with LNG, as this fuel has a superior conversion ratio and molar mass when compared with ammonia, resulting in a lower required fuel weight. All in all, propulsion power can be generated with a comparable volume and mass. A downside is the lower efficiency, the emission of CO₂ and reduction in robustness.

Case 3B is almost identical to case 2B in the applied components. The only difference can be found in the amount of diesel generators. Due to the lower electrical demand and more focus on volume and mass, one diesel engine is deemed unnecessary. Compared with case 2B, the fuel consumption, CO₂ emissions, mass and volume have increased. This is a logical consequence as more power and energy needs to be developed in case 3. The SOx and NOx emissions are lower, since the usage of the diesel generators is reduced. The robustness has decreased slightly, due to the removal of one of the diesel generators.

Trend level

Figure 56 and 57 show the number and type of components in the best configurations of case study 3A and 3B respectively. Similarly to previous case studies, the electric motor in combination with a SOFC is favoured. Unlike previous case studies, the electric motor is not as dominant, while the SOFC is even more dominant. With the emphasis on volume and mass, the SOFC is not the most obvious choice, as it has the lowest power density of all EGSs. However, the high efficiency compensates for the higher volume and mass, through lower fuel consumption. This is analyzed further in Paragraph 10.5. The SOFCs run predominantly on LNG, resulting in it being the preferred fuel. The gas turbine and generator are still hardly used, but their utilisation has increased in comparison with the other case studies. This is a result of the priority that is given to volume and mass. Noteworthy is the occurrence of 2-stroke diesel engine. This most likely follows the same logic as SOFC, where the lower power density is compensated by the higher efficiency.

Table 35: Optimal configuration of case study 3A and 3B, including KPI values

Case 3A	Type	Value	Unit		Value	Unit
Propeller	2x CPP	-	-	Total efficiency	0.53	-
Gearbox	2x	8.1	MW	CO2	402	ton
MPE	2x EM	8.1	MW	SOx	0	ton
EGS	3x SOFC	6.7	MW	NOx	0	ton
ESS	-	-	kWh	Total volume	682	m3
Fuel	LNG	158	ton	Total mass	435	ton
				Average signatures	1.3	MW
				Robustness	0.83	-
Case 3B						
Propeller	2x FPP	-	-	Total efficiency	0.42	-
Gearbox	2x	9	MW	CO2	568.5	ton
MPE	4x DF4	4.5	MW	SOx	0.06	ton
EGS	2x DG	0.3	MW	NOx	3.5	ton
ESS	-	-	kWh	Total volume	706	m3
Fuel	MDO	18	ton	Total mass	463	ton
	LNG	191		Average signatures	1.9	MW
				Robustness	0.92	-

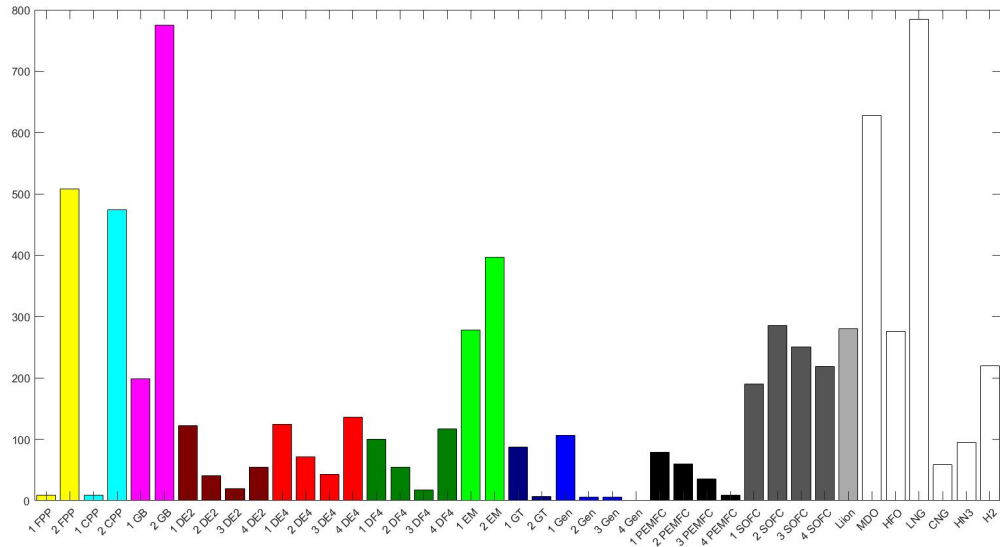


Figure 56: Type and number of components used by the top 1000 configuration of case study 3A. Multiple components can be combined, resulting in a sum of components higher than 1000

In case 3B, the shift from electric motor to internal combustion engine is less than in previous cases. This is mostly down to the lesser employment of electric engines in the first place. Again, the installation of single electric motors can be found, while no single shaft configurations exist in the top 100. As a result, at least half of the concepts are asymmetric. Furthermore, the usage of LNG has decreased with the disappearance of the SOFC, yet it still remains the fuel of choice for dual fuel engines and gas turbines. No clear favoured can be found within the reciprocating engines, while a preference for high speed 4-stroke engine could be expected, due to the importance of mass and volume. The explanation may be found in the same reasoning given in case 3A for the occurrence of 2-stroke diesel engines.

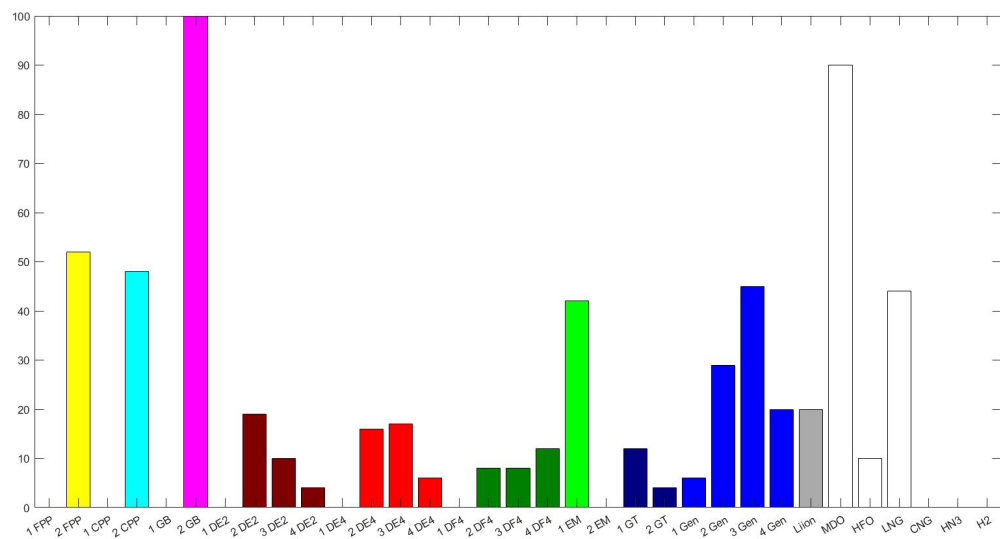


Figure 57: Type and number of components used by the top 100 configuration of case study 3B. Multiple components can be combined, resulting in a sum of components higher than 100

Space level

Figures 58 and 59 present the total design space in terms of total efficiency versus volume for case study 3A and 3B respectively. For case 3A, the optimal concept lies on the Pareto front. It can be seen that in the region of the optimal configuration the Pareto front is relatively flat. This means that a lot of efficiency could be gained, at the cost of relatively little extra volume. However, due to the given client preference, this was not done. This shows a contrast with the client preference of case 2A, where efficiency was more important, leading to optimal configuration having relatively higher efficiency, but also higher volume. Similar to the previous two case studies, most of the concepts are concentrated at lower efficiencies. These concepts are likely not able to achieve higher efficiencies due to their component composition.

In case study 3B, the optimal configurations can not be found on the Pareto front. This is remarkable, as volume is given significant priority over other KPIs. As a result, one would expect that the optimal configuration would lie on the Pareto front that considers volume. Moreover, a small cluster of concepts have achieved significant lower volumes and higher efficiencies. This information can enforce a design team in their decision making. That being said, most of the concepts do have a lower volume, but also a significantly lower efficiency. It is certain that on the other KPIs the optimal concept outperform the other concepts.

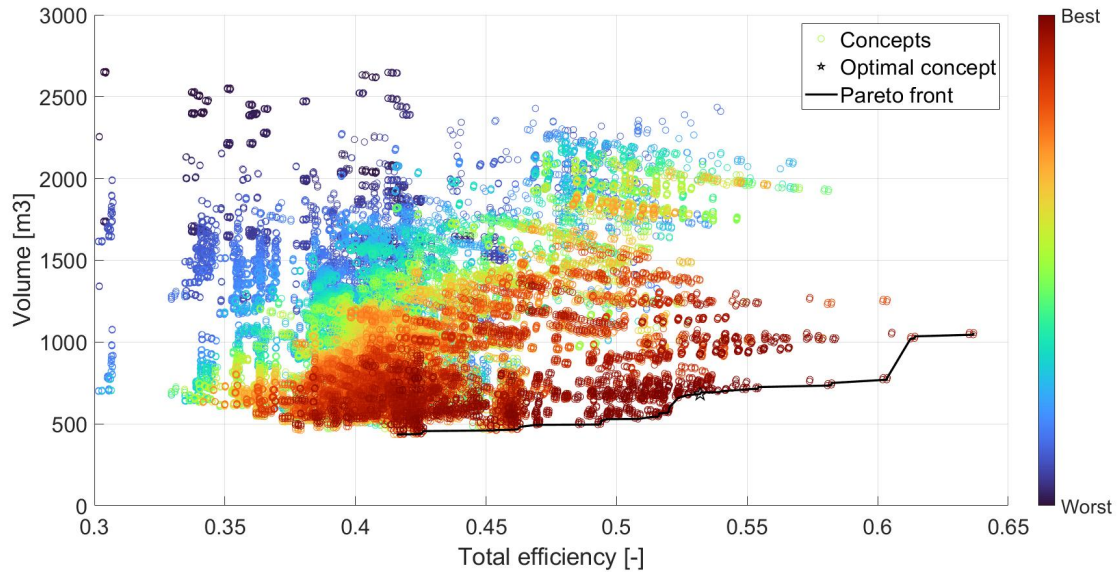


Figure 58: Efficiency-versus-volume design space. All concepts of case study 3A, including the optimal configuration indicated with a star and the Pareto front indicated with a black line. The colour of a concept is based on the overall ranking of the concept from best (red) to worst (blue).

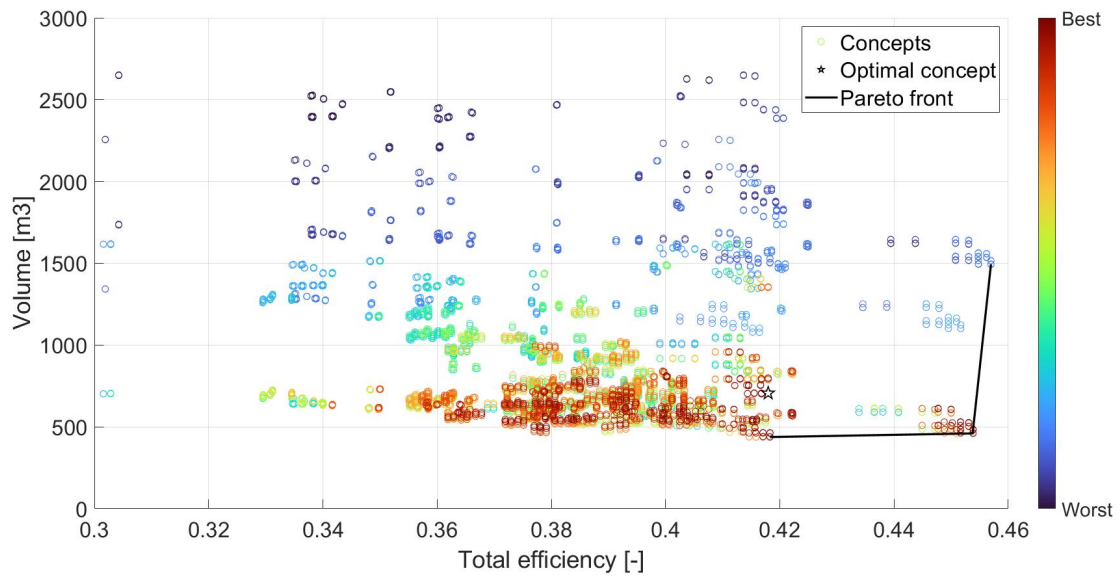


Figure 59: Efficiency-versus-volume design space. All concepts of case study 3B, including the optimal configuration indicated with a star and the Pareto front indicated with a black line. The color of a concept is based on the overall ranking of the concept from best (red) to worst (blue).

10.4 Overall trends

Examining the multiple case studies, certain overall trends can be found. Starting at the propeller, no decisive pick can be made between FPPs and CPPs, although the FPPs are chosen slightly more often. This is most likely a result of the efficiency loss of CPPs in combination with reciprocation engines. In some cases a single shaft configuration is used, but the majority of concepts are twin-shafts. This is logical as the robustness of a single-shaft configuration is generally worst than a twin-shaft composition. Furthermore, these shaft are coupled with a gearbox in most cases, since this gives the opportunity to install multiple engines on one shaft. However, there are cases where a geared drive is combined with a direct drive. This falls within the bigger picture of asymmetric topologies.

The CET is not deterred by asymmetric configurations and occasionally produces asymmetric concepts that lie within the top of a case study. This is a remarkable result, as asymmetric configurations are essentially unused. Practical objections may underlie this, yet the notion is fascinating and shows the potential of a CET in evaluating non-conventional concepts.

The most evident trend that was identified is the utilisation of electric motors, often in unison with fuel cells. The combination of high efficiency over a range of loading conditions and low or no emissions and signatures, ensures a strong configuration. Even when these KPIs are not given the highest priority (case 1 and 3), electric motors and fuel cells are often selected. Within the fuel cell decision, the SOFC is favoured over the PEMFC. Reasons are the higher efficiency and the possibility to use more energy dense fuels. Evidence of this can be found in the fuel consumed by the SOFC, which is natural gas or ammonia in most cases and not hydrogen, which has a lower functional energy density. Since the combination of electric motors and fuels cells is so dominant, extra research is done to find an explanation. This explanation is described in Paragraph 10.5.

When fuel cells are disabled (B cases), a shift is made from electric engines to internal combustion engines. From this it can be concluded that the advantages of the electric motor mostly come from the partnership with fuel cells. Nonetheless, some configurations still have electric motors installed, often in a hybrid form with internal combustion engines. The electric motor is likely employed for part load conditions, in order to increase total efficiency.

The utilisation of batteries is below average. The efficiency improvement is in most cases apparently not enough to offset the extra volume and mass taken up by the batteries. In practice, the more dynamic use of batteries may lead to bigger advantages, but this is not included in the CET.

Lastly, MDO is the most chosen fuel, followed by LNG. The choice for MDO is logical, as every configuration with reciprocating engines consumes either MDO or HFO and MDO is the superior fuel in terms of emissions. LNG is the fuel of choice for dual fuel engines, gas turbine and SOFCs. The combination of energy density, pollution profile and storage methods lead to a fuel that is often optimal.

10.5 Electric motors and fuel cells

The case studies show that the model has a preferences for efficient configurations including electric motors and SOFCs. Even when volume and mass are given priority over efficiency and emissions, this result remains. The explanation can be found in the power and energy density of the different components and fuels.

Table 36 shows the power density of the various main propulsion configurations. These include both direct drive (DD) and geared drive (GD) power trains. The weight and volume of both the gearbox and the engine are included to come to a total power density. The model was instructed to create a power output of 10 MW. It can be seen that for the diesel engines, the actual installed power is higher than the instructed power, due to power created per cylinder and the discreet number of cylinders per engines. Furthermore, the power density of the different engines is as expected, yet the differences in total power density are smaller than anticipated, especially looking at the 4-stroke diesel engine and the gas turbine. The increase in power density of these high speed engines is dampened by the need for a bigger gearbox, leading to only a limited increase in total power density. This is the first reason why other component may not be selected when mass and volume are of importance. The power density of the geared electric motor is significantly larger than the other components, but an electricity generation system is required to let the electric motor operate.

Table 37 displays the power density of various EGS concepts, used to power the electric motor. The components were optimised for both volume and mass (V/M) and for efficiency (Eff). The instructed amount of installed power was 11 MW, but the model was allowed to install a maximum of three times that amount

Table 36: Mass, volume and power density of the various main propulsion configurations. The model was asked to install 10 MW with a shaft speed of 200 rpm. All configurations are optimized for mass and volume, resulting in the highest possible power density.

Component	$P_{installed}$	Mass		Volume		Total power density	
		GB	Engine	GB	Engine	Mass	Volume
	MW	ton	ton	m ³	m ³	kW/ton	kW/m ³
DD DE2	11.8	0	196	0	166	60	71
GD DE2	10.1	8	155	6	132	62	73
GD DE4	10.3	59	80	41	97	74	75
GD DF4	10.8	38	170	26	221	52	44
DD EM	10.0	0	105	0	112	95	89
GD EM	10.0	33	16	23	17	204	250
GD GT	10.0	74	15	52	38	112	111

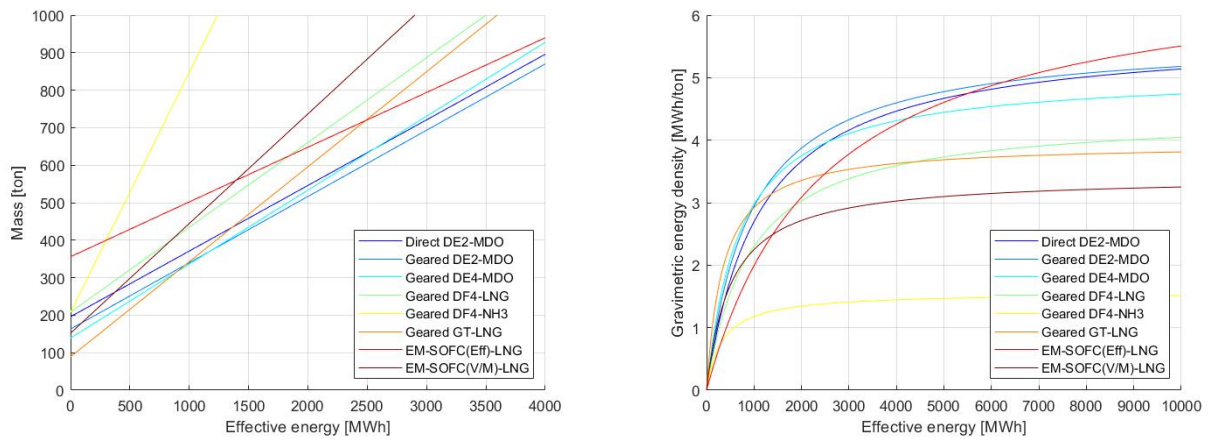
of power. Since larger amounts of power could be installed both the total and functional power densities are calculated. The functional power density is based on the the instructed 11 MW, instead of the actual installed power. It is clear to see that the fuel cells significantly increase in dimensions to operate at a more efficient working point, when the components are optimised for efficiency. The same is done with the generators, which is counter intuitive. The reason for this is a decrease in nominal engine speed, when efficiency is important. Similar to the main engines, the model is not capable of creating generators that exactly match the instructed amount of power. When the EGSs are combined with the electric motor, the overall power density is greatly reduced. This is especially true for the combination of EM and SOFC, yet this remains the optimal configuration in the case studies. An explanation for this can be found in the fuel consumption.

Figures 60 and 61 show the mass and volume of the different main propulsion configurations versus the amount of effective energy that is being produced by the configuration. The effective energy is seen as energy delivered to the propeller. All components operate at the designed 10 MW and it is assumed that the internal combustion engine function at their nominal efficiency, as there are scenarios where the engines are perfectly matched to the power demand. In sub-figures 60a and 61a, the mass and volume of the concepts at 0 energy are equal to the size of all required components, as can be found in Table 36. The slope of the lines are a function of the efficiency of the component, the lower heating value of the fuel and, in case of volume, the density of the fuel. The energy density in sub-figures 60b and 61b increases significantly in the beginning, due to dimensions of the components, after which it settles in the limit. Similarly, the energy density in the limit is a function of the efficiency of the component, the lower heating value of the fuel and, in case of volume, the density of the fuel.

It becomes clear that the combination of electric motor with an efficient SOFC is the heaviest configuration component-wise. However, the high efficiency of this concept, and thus low fuel consumption, compensates

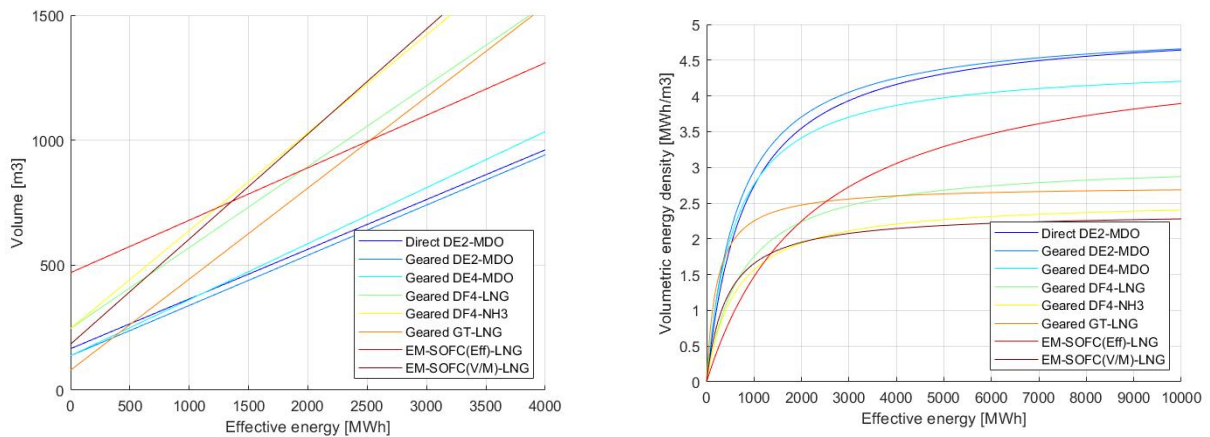
Table 37: Mass, volume and power density of the various electricity generation systems. The model was asked to install 11 MW at 3300V. Configurations are optimised for volume and mass (V/M) and for efficiency (Eff).

	Component	$P_{installed}$	Mass	Volume	Total power density		Functional power density	
					kW/ton	kW/m ³	kW/ton	kW/m ³
		MW	ton	m ³				
V/M	Gen	11.8	117	123	101	96	94	89
	PEMFC	11.1	57	107	195	104	193	103
	SOFC	11.2	103	144	109	78	107	76
Eff	Gen	14.0	185	195	76	72	59	56
	PEMFC	33.1	171	321	194	103	64	34
	SOFC	33.3	307	430	108	77	36	26



(a) Total mass of various concepts, including fuel and tank mass. The mass at 0 energy is equal to the mass of the installed components. (b) Gravimetric energy density of various concepts, including fuel and tank mass. The horizontal axis is extended to show the energy density reaching the limit.

Figure 60: The mass and gravimetric energy density of various main propulsion concepts versus the effective energy delivered to the propeller at 10 MW.



(a) Total volume of various concepts, including fuel volume. The volume at 0 energy is equal to the volume of the installed components. (b) Volumetric energy density of various concepts, including fuel volume. The horizontal axis is extended to show the energy density reaching the limit.

Figure 61: The volume and volumetric energy density of various main propulsion concepts versus the effective energy delivered to the propeller at 10 MW.

Table 38: Mass, volume and power density of the various electricity generation systems. The model was asked to install 1 MW at 690V. Configurations are optimised for volume and mass (V/M) and for efficiency (Eff).

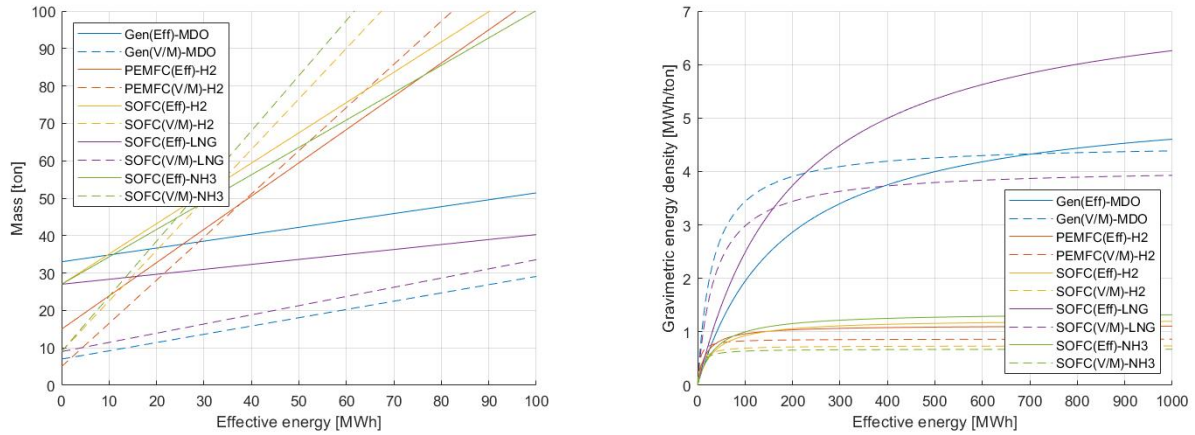
	Component	$P_{installed}$	Mass	Volume	Total power density		Functional power density	
		MW			ton	m ³	kW/ton	kW/m ³
V/M	Gen	1.2	7	7	171	171	143	143
	PEMFC	1.0	5	9	200	111	200	111
	SOFC	1.0	9	13	111	77	111	77
Eff	Gen	1.8	33	31	55	58	30	32
	PEMFC	3.0	15	28	200	107	67	36
	SOFC	3.0	27	38	111	79	37	26

for this fact. As a result, the energy density of this configuration is reasonably favourable when the amount of required energy is large enough. Furthermore, the figures are based on calculations assuming a constant nominal power demand. If the power demand decreases, the efficiency of all internal combustion engines will also decrease, yet the efficiency of the SOFC will increase. Thus, the energy density of the internal combustion engine will be reduced, whereas the energy density of the electric motor and SOFC will be enlarged. All in all, the dimensions and energy density of a SOFC configurations are not as bad as one would expect when solely looking at the components. Moreover, the results on the other KPIs are generally better than when compared to other main propulsive concepts.

Other notable findings are the low gravimetric energy density of a dual fuel engine running on ammonia and the gas turbine. For the dual fuel engine, this is a result of the relatively low lower heating value of the fuel. When examining the volumetric energy density, this fact is offset by a relatively high density. The gas turbine suffers from the lowest nominal efficiency of all components. However, the intended application of a gas turbine does appear in all figures, namely providing a large amount of power for a short amount of time. The energy density of the gas turbine is the highest at small amounts of effective energy. Moreover, all components are sized to 10 MW, whereas gas turbines are often larger. When larger amounts of power are required, the higher power density of the gas turbine becomes more relevant. Lastly, an interesting comparison can be made between the two variations of the SOFC. Even though the V/M SOFC is significantly lighter and smaller than the efficient SOFC, this effect is rapidly diminished by the higher fuel consumption. This explains why, depending on the operational profile and the client preference, the size of the SOFCs will vary between cases.

A similar comparison based on energy density can be made for detached EGS. Table 38 displays the mass, volume and power density for various EGS concepts. The instructed power demand is 1 MW at 690V and the model was allowed to install a maximum of three times that power. Again, the model is not capable of creating generators that exactly match the instructed amount of power and the size of the generators increases when efficiency becomes a priority, due to the lower engine speed. As a result, not only the functional, but also the total power density decreases when the components are optimised for efficiency. In the case of efficiency optimisation, the size of the fuel cells is once more maximized, leading to a sharp decrease in functional power density. The power density of the SOFC is the lowest, yet it is selected in the optimal power plant configuration.

Figures 62 and 63 display the mass, volume and energy density of various electricity generation configurations. Both the version optimised for volume and mass (V/M), as the version optimised for efficiency (Eff) are shown. All components operate at the design power of 1 MW and it is assumed that the generators perform at their nominal efficiency, as there are scenarios where the installed power matches perfectly with the required power. In sub-figures 62a and 63a, the mass and volume at 0 energy are equal to the size of the installed components. The slope of these lines are a function on the efficiency of the component, energy density of the fuel and, in the case of volume, the density of the fuel. The energy density in sub-figures 62b and 63b increases significantly in the beginning, due to dimensions of the components, after which it settles in the limit. Similarly, the energy density in the limit is a function of the efficiency of the component, the lower heating value of the fuel and, in case of volume, the density of the fuel.

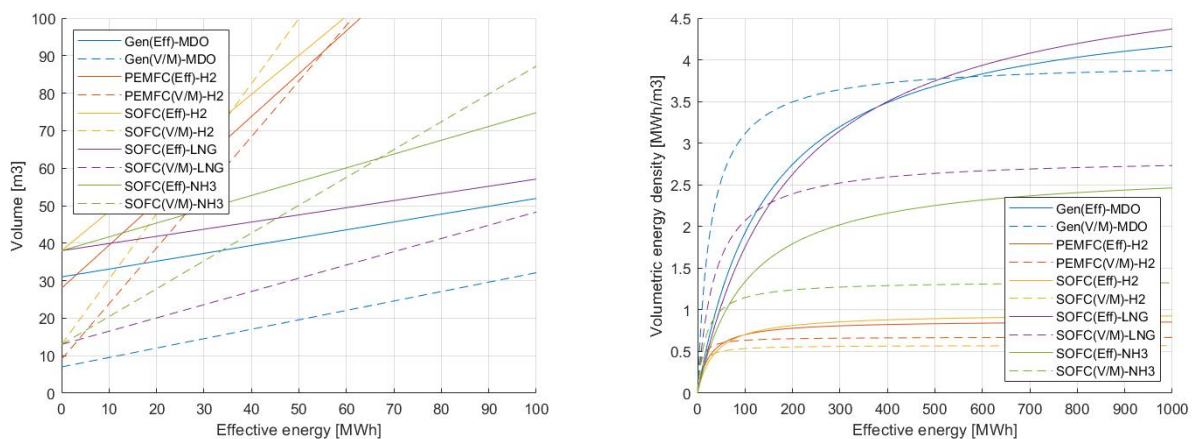


(a) Total mass of various concepts, including fuel and tank mass. The mass at 0 energy is equal to the mass of the installed components.

(b) Gravimetric energy density of various concepts, including fuel and tank mass. The horizontal axis is extended to show the energy density reaching the limit.

Figure 62: The mass and gravimetric energy density of various electric generation concepts versus the effective energy delivered to the electric grid at 1 MW.

The highest energy density is achieved by the SOFC, when enough energy is required. This is due to the high efficiency of the SOFC. For lower energy demands, small generators are optimal, due to their high power density and relatively good fuel consumption. It becomes clear that components running on hydrogen perform very poorly. This is a result of the relatively low density and the storage method. 17.5 kilograms of tank is needed, resulting in a very low functional energy density [18]. Similarly, ammonia suffers from a low energy density and relatively high specific tank mass. It becomes clear that the SOFC only outperforms the generators, if it is fueled with LNG. A calculation example of this can also be found in Table 39. Furthermore, the efficient components seem to quite quickly outperform their smaller counterparts. The exception to this are the generators, which is logical as the gain in efficiency is not as large as with fuel cells and the dimension increase significantly.



(a) Total volume of various concepts, including fuel volume. The volume at 0 energy is equal to the volume of the installed components.

(b) Volumetric energy density of various concepts, including fuel volume. The horizontal axis is extended to show the energy density reaching the limit.

Figure 63: The volume and volumetric energy density of various electric generation concepts versus the effective energy delivered to the electric grid at 1 MW.

Table 39: Calculation example of a 2 MW SOFC producing 1 MW of electric power with different fuels.

	Unit	H2	LNG	NH3
Electric power produced	MW	1	1	1
Molar flow electron	kmol/h	47.0	47.7	48.0
Fuel utilisation	-	0.9	0.9	0.9
Molar flow H2	kmol/h	26.1	26.5	26.7
Reaction equilibrium	mol/mol	1	3.927	1.495
Molar flow fuel	kmol/h	26.1	6.7	17.8
Molar mass fuel	g/mol	2.018	16.04	17.03
Mass flow fuel	kg/h	52.7	108.2	303.8
Specific tank mass	kg/kg	17.5	0.48	1.91
Mass flow tank	kg/h	922.1	52.0	580.2
Density fuel	kg/m ³	42	470	683
Volume flow fuel	m ³ /h	1.25	0.23	0.44
Lower heating value	MJ/kg	120	55	18.6
Chemical power fuel	MJ/h	6323	5953	5650
Chemical power fuel	MW	1.76	1.65	1.57
Efficiency	-	0.57	0.60	0.64
Total mass flow	kg/h	974.8	160.2	884.0
Total volume flow	m ³ /h	1.25	0.23	0.44

Table 39 shows an calculation example of a 2 MW SOFC producing 1 MW of electric energy with different fuels. The calculation runs from the top of the table to the bottom. Some notable points have been highlighted. The required molar flow of the electrons is slightly higher for LNG and NH₃, as the SOFC is slightly less efficient with these fuels. The needed mass flow of hydrogen is actual lower than the other fuels, due to the small molar mass. However, the specific tank mass nullifies this advantage, since the mass of the tank is relatively large. The mass flow of an actual tank may seem odd, yet it perfectly shows how much tank must be added for one hour of operation. It also shows why hydrogen, and NH₃ to a lesser degree, have a relatively small gravimetric energy density. Similarly, the low density of hydrogen causes a low volumetric energy density. The chemical power of the fuel is computed with the use of the lower heating value, as if the fuel would be burned, since this is how the model calculates the overall efficiency when processing all the results. The resulting efficiency shows a remarkable result; even though the electrochemical efficiency of the SOFC is higher with hydrogen, the overall efficiency is higher with the other fuels. This extra efficiency can be found in the internal reforming process, which is endothermic. Essentially, waste heat is used to reform the fuels, adding extra chemical energy to the end product. This can be seen as a waste heat recovery process, adding efficiency to the total energy production. All in all, LNG is the fuel with the highest energy density and even has an positive effect on the total efficiency of the fuel cell.

Altogether, it can be concluded that the high mass and volume of the SOFC is compensated by its higher efficiency, resulting in a competitive energy density. When large amounts of energy are required, the SOFC might even be the most optimal choice in terms of mass and volume. This fact, combined with the performance on the other KPIs, clarify why the SOFC is preferred by the model in most, if not all, case studies.

10.6 Sensitivity analysis client preference

A sensitivity analysis is performed on the client preferences. The model is executed with a different set of client preference for every run. By changing the client preferences, the model will make different decision, both in the internal optimisation as well as in the final MCA. As a result, the values of the KPIs of the optimal configuration will change. In some cases different components will be selected, as they are now seen as optimal.

For every case study, both A and B, this sensitivity analysis is performed. The input and output can be found in appendix B. Set 1 is the base case study, from where the deviations are computed. Table 40 shows the overall absolute deviations from the base case studies. For the calculations of the emissions sensitivity a slight change has been made to the calculation. Since the emissions can be zero in the base case study, any increase in emissions in subsequent case study would be an infinite deviation. This would result in an infinite total average, which does not hold much information. Therefore, the choice has been made to compute the emissions sensitivity based on case studies B, where there are always emissions in the base case study. For the cases with an infinite increase in emissions, it is best to study the absolute inflation and examine if this increase is acceptable to the design team.

The most noteworthy deviation can be found with SO_x. This deviation is the consequence of set 5 of client preferences, where the importance of emissions is set to 0. As a result, the CET switches from MDO to HFO. This drastically increases the SO_x emissions. As long as the client preference of emissions is not set to 0, this change will almost never occur. Similar behaviour can be found with the NO_x emissions, where the change is often either non or very significant. This is likely caused by a change in components, leading to a different NO_x emissions rate. Small changes in emissions are the result of different sizing and usage of the same components.

The behaviour of the signature sensitivity is comparable to that of the emissions, where significant deviations can be found, when different components are chosen. It is noteworthy that both signatures and emissions show considerable deviations when their respective client preference is kept constant. This indicates that in most cases these KPIs are the result of choice made based on other KPIs. Even when signature is given a high importance (case 1), this is true.

The other KPIs show more moderate behaviour, with the largest deviations found when their respective KPI is set to an extreme. However, this can be misleading, as efficiency and robustness are relative values in and of itself. Most of the values for efficiency can be found between 0.4 and 0.6 and for robustness between 0.6 and 1.0. This means that the maximal deviation is limited. Therefore, it is good to also examine if changes in the client preferences lead to different component composition.

In 31% of the sensitivity analysis cases, the component compositions did not change. In all other cases one or more parts were exchanged. This component replacement can be found over the whole spectrum of client preference changes. However, in every case that robustness changed, the configuration was modified. From this perspective, one could conclude that all client preferences, but especially robustness, are sensitive.

All in all, it can be said that variations in client preferences almost always lead to different output. In a majority of the cases, the component composition differed from the base case study, resulting in another optimal concept. In the other cases, the sizing or usage of the components were altered. Only in certain rare cases, nothing internally changed in the optimal configuration. It is hard to quantify the sensitivity to the client preferences, as changes express themselves both qualitatively and quantitatively and on varying scales. However, it is probably fair to conclude that the client preferences have a major effect on the outcome of the CET. Therefore, it is important to have a good understanding of the wishes of the client and the knowledge on how to convert these wishes to quantified weight factors. Moreover, it is best not to look at the single optimal concept as the output of the tool, but rather also look at the given trends of the top concepts and the visualisation of the total design space.

Table 40: Total absolute average deviations from the base case studies.

Efficiency	CO ₂	SO _x	NO _x	Volume	Mass	Signatures	Robustness
3%	8%	851%	44%	14%	9%	37%	4%

10.7 Research results

The results of the research are separated from the outcome of the case studies. This is done, since the main research question is about a design methodology and not about the optimal configuration itself. Therefore, this paragraph highlights the results of the research into the made concept exploration tool.

The made CET is capable of generating and evaluating thousands of varying concepts and choose an optimal configuration based on the preference of the client. This is done with an modified brute-forcing algorithm. The computational speed of the model is increased with a factor 200 to 500 compared to the previous version. As a result, case studies can be run in minutes instead of hours, as can be seen in Table 41. The table also shows the number of considered concepts and mission elements per case study. For the larger case studies A, a run takes several minutes. When the case is more constraint in version B, the run time is brought back to a couple dozens of seconds. This speed is unmatched by any human design team and can enable such teams to expand their search range. Furthermore, the effect of changes to the constraints, mission profile or client preferences can quickly be computed, resulting in a faster conversation between designer and client.

However, this CET also showed that a number of constraints have to be implemented to keep the size of the design space manageable, even though a computer is utilised. These constraints can both be a prior constraints or the use of an IDEA. In this perspective the tool failed in exploring a fully unconstrained design space. It can be argued that this would be impossible to start with for such a complex design space, yet with a better model structure and the evolution of computer hardware, a more unconstrained design space may be explored in the future. A design team may make the decision to increase the acceptable run time to enlarge the number of feasible concept. Extrapolating from the data found in Table 41, roughly 15 to 20 million concepts can be generated and evaluated within 24 hours.

The model produces output on three different detail levels, as was shown in the case studies. These levels (concept, trend and space level), can be exploited for varying means. Firstly, on concept levels all details of every component in every configuration are given. This goes as far as cylinder diameters for internal combustion engines and number of cells for batteries and fuel cells. Furthermore, the dimensions and performance per mission element of all components are provided. This information can be used for detailed comparison between multiple components or configurations and as input for future design steps, such as 3D modelling.

Secondly, the trend level shows which components are employed by the best concepts. This allows the design team to look for certain combinations of components that work well, within the given mission profile and client preferences. An advantage of this methodology is that it takes some of the sensitivity of the client preferences out of the equation. This output can be used to determine global design directions, such as number of shafts, hybridisation of the power plant or the usage of certain fuels. Furthermore, it shows how trends and optimal combinations change, if the input and constraints are altered.

Thirdly, the space level present the complete design space, the position and ranking of any concept within that space and the Pareto front. This visualisation of the design space is not often used by maritime engineers. However, this representation can support the design process in multiple ways. First of all, it shows the size of the complete design space, both in the number of possible concepts as well as in the range of KPI values these concepts lay in. Having an understanding of this size might inform designers about all the possibilities and make them look beyond the well known configurations. Furthermore, it can display certain trends found shared between all concepts, as concepts have both a position and ranking within the

Table 41: Number of concepts, number of elements and run time in seconds per case study

Case	Concepts	Mission elements	Time [s]
1A	62872	13	417
2A	67848	8	292
3A	55656	8	208
1B	4296	13	87
2B	4840	8	40
3B	3896	8	38

design space. Some of these trends may seem logical, but this visualisation may enforce the logic behind these trends. Other trends may not have occurred to a design team and may be the start of further study into these concepts. Moreover, the location a concept has with respect to other concepts and the Pareto front gives valuable information about the possibilities to increase the performance of a certain KPI. This can be done by either changing to a different concept or tweaking the existing concept towards other concepts. By extension, possible promising outliers can easily be identified. This can be a single concept or a cluster of possible concepts. Examples of this can be found in Figure 53, where both volume and robustness are sacrificed for efficiency to produce the optimal concept, or in Figure 48, where a cluster of promising concepts lies away from the majority of concepts at a higher volume.

Furthermore, the three detail levels do not only support design teams, they also allow for a first low detail study into new technologies. Apart from calculating the performance, the CET enables the integration of the new technology into existing configuration. Moreover, a comparison between new and existing technology is possible and can be visualised on different detail levels. In this thesis, this was done for the SOFC. In the case studies it was shown that the SOFC is a very promising technology and performs well in comparison with other technology. It must be said that this comparison is on a low detail level and a number of disadvantages of SOFCs is not included in the CET. However, this result may be the start of future feasibility studies and more detailed research into the new technology.

11

**Conclusion and
Discussion**

11.1 Conclusion

A concept exploration tool is developed to explore the concept design space of power plants of naval surface vessels. The tool combines various components into all possible combinations and evaluates these configurations. Based on the input given by the client, a ranking of all concepts is produced, designating the optimal power plant configuration. Essentially, the tool enables the user to form a first idea within minutes. Such a tool is needed, as the design space is ever expanding, yet the resources of a human design team are limited.

The input provided to the program consists of client preferences, in the form of weight factors, and a propulsive and electrical mission profile. Since the tool is to be used in the first stage of the design process, the input is often of low detail. This plays into the modelling choice of the modes, for a quasi-static modelling method is applied, in order to decrease the computational time. A detailed output is delivered by the model, with sizing and performance of every configuration on component level. This detailed output may be built on by a design team in future design steps.

As optimal is a subjective term, client preferences are utilised. The client preferences are based on the key performance indices that can quantify the overall performance of a power plant. These KPIs are studied in the first sub-research question:

What are the KPIs of a naval vessel on which to evaluate power plant concepts?

Van Dijk established four KPIs, namely fuel consumption, emissions, volume and mass. In this research fuel consumption was changed to total efficiency, as this is a more indicative figure and it takes the heating values of the different fuels into account. Furthermore, two new KPIs were added. These KPIs, signatures and robustness, signify the naval aspect of the power plants and endorse the usage of the tool for naval purposes. Signatures are of importance as being undetected is the first line of defence in a combat situation. The literature study showed that the heat signature of the exhaust gasses is the predominant signature when it comes to power plants. Thus, the heat of the exhaust gasses is adopted as a KPI. Robustness is essential, since a naval ship possibly faces hostile environments and needs to be able to fulfill its mission even after a failure has occurred. The robustness of a vessel is defined as the power capabilities of the power plant after a failure has occurred.

The other input to the tool is a potential mission profile of the vessel in terms of needed power. The maximal demanded power and energy requirements have a significant influence on power plant configuration, which leads to the second sub-question:

What are the mission profile and ship characteristics per naval vessel?

Three mission profiles and ship characteristics for three different vessels are depicted in the study cases in Chapter 10. The profiles sketched in the study cases are based on actual vessels and their power demands, thus fairly accurate. However, the low computational time of the program made an accurate operational profile of less importance. Since the tool takes merely minutes to run, multiple different operational profiles can be investigated in a short amount of time. Therefore, more global trends can be studied instead of one specific case study, which diminishes the need for a single highly accurate mission profile.

The tool created in this research is based on the model of van Dijk, which has its focus on commercial shipping. For this reason certain components commonly found on naval vessels, but not on commercial ships, were not modelled. The most prominent missing components were the controllable pitch propeller and the gas turbine. Thus, these components were added in this program. The modelling method is the basis for the following sub-question:

How can a controllable pitch propeller and a gas turbine be modelled?

The controllable pitch propeller is modelled with a standard constant combinator curve, as is shown in Paragraph 8.3. The actual pitch is not modelled, only the effect on the propeller speed and thus the engine speed. The results should be evaluated critically, as most of the advantages of a CPP are not taken into account. Furthermore, the way the CPP model and the engine models interact can be counter-intuitive, as performance may degrade where better performance is expected.

The gas turbine model is centered around the Rolls-Royce MT-30 simple cycle gas turbine. This is a commonly used gas turbine on American and British vessels. The sizing of the gas turbine is based on the method of van Es, which is corrected for the Rolls-Royce MT-30. The performance is simulated with the

use of the thermodynamical principles. First all variables are computed in the nominal working point, after which they are extrapolated to the desired part load condition.

The focus of navies has shifted more towards economical and sustainable sailing. Therefore, the CET should be able to accommodate these preferences of clients by featuring so called alternative components. As research and computational time is limited, only promising technologies should be considered for the tool:

What new alternative power plant components could be considered for a power plant of a naval vessel?

Four categories were considered; a main propulsive engine, an electricity generation system, an energy storage system and a new fuel type. For the main propulsive engine a permanent magnet synchronous motor is already available, so no new MPE was analysed. The literature study concluded that the best ESS was a lithium-ion battery, which is already included in the model. Furthermore, NaBH_4 is deemed a promising fuel and would thus be implemented into the CET. However, research time turned out to be a limiting factor, resulting in the omission of this fuel. For the EGS studies showed that the solid oxide fuel cell is recognized as the most upcoming technology. Therefore, the SOFC is implemented in the program. The modelling method is the basis for the next sub-question:

How can these alternative power plant components be modelled?

The performance of the SOFC is modelled with the use of a polarization curve. This method gives a high enough detail level, while being computationally light. The operating temperature of the SOFC is made dependent on the variability on the mission profile, so more dynamic profiles will lead to lower design operating temperatures and vice versa. Internal reforming is enabled within the model, meaning not only hydrogen, but also natural gas and ammonia can be used to fuel the SOFC. Fuel utilisation and conversion ratios are included for all fuels. The subsequent changes in open circuit voltages when using different fuels are taken into account. An overcapacitated fuel cell can be installed, as this not only increases the robustness of the configurations, but may also increase the total efficiency of the SOFC.

A significant point of improvement of the tool by van Dijk is the computational time. From a scientific point of view, this may not have the highest priority. However, from a usability standpoint, the computational time partially determines whether the tool can be applied for real life purposes. Therefore, a sub-question was dedicated to this subject:

What model structures can be used to ensure limited computational time?

By using a quasi-static modelling structure, the dynamical performance simulation applied by van Dijk can be eliminated. This dynamical simulation was the most computationally heavy part and removing it drastically reduced the computational time. The resultant model is estimated to be 200 to 500 times faster than the original model, depending on the input. A drawback of the quasi-static modelling is the reduced level of detail, especially in transitional areas of the mission profile. Since the CET is used in the first phase of design process, the level of detail is predicted to be low, so a loss in detail is deemed acceptable.

The last sub-question entails the search for an overarching trend between different input parameters:

What is the optimal power plant configuration for a naval surface vessel given multiple ship types, multiple mission profiles and multiple client preferences?

The case studies showed a dominant combination of CPPs, EM and SOFC. The combination of a CPP and a EM stems from the efficiency gain at lower load ratios. The combination of EM and SOFC was further studied in the case studies. It was shown that the higher efficiency of this configurations ultimately outweighs the initial mass and volume deficit. When enough energy is produced, it may even occur that the energy density of the SOFC and its fuel becomes higher than other concepts.

Lastly, the main research question will be answered:

How can the optimal power plant configuration for a naval surface vessel be determined given the mission profile and client preferences?

The proposed solution of a concept exploration tool has been studied and described in this thesis. It is able to generate and evaluate thousands of varying concepts and choose an optimal configuration based on the preference of the client. In addition, the CET can give an insight in the design space the design team is working in. This visualisation may be of added value to the design team when searching for trends, outliers or comparable concepts. The solutions found in the study cases show usable and mostly expected results.

Furthermore, the influence of both the mission profile and client preference can be found in the output of the model. This indicates that the tool is flexible enough to not produce the same optimal concept every time. Moreover, the output in terms of KPI values gives a design team a starting point for the rest of the design process and facilitates the comparison between different configurations based on quantified calculations. This may empower the human design team in their decision making for the rest of the design process.

That being said, a critical note must be placed on the size of the explored design space. A number of constrained were implemented to keep the design space manageable. This research showed that, even though computers are utilised, the limits of a workable design space can quickly be reached, especially when the run time must be minimised for practical applications. All in all, it can be concluded that a CET enables design teams to explore larger power plant design spaces within a practical time frame. However, constraints must still be implemented to keep the size of the design space manageable.

11.2 Discussion

As the quote on part 1 states: "All models are wrong, but some are useful", this model is no different. No model can perfectly simulate the real world, as assumptions and internal decision have to be made. These assumptions affect the output of the model, in one way or another. Therefore, a discussion will be held about the developed CET. First a discussion will be held on the model structure. Next, the assumptions and shortcomings of the model operations itself will be debated. Lastly, the output will be reviewed.

11.2.1 Model structure

The first major decision made in the creation of the CET was stepping away from the dynamic modelling done by van Dijk and converting it to a quasi-static model structure. This decision was made to increase the usability of the tool. From a scientific point it can be argued that this adjustment only deteriorates the model, as precision is exchanged for computational speed. Science may have little interest in the speed of the model, it is the outcome that matters. To counter this argument a philosophical engineering question must be asked:

What is the value of a tool, if it is left unused?

This question is left for the reader to answer, as there may be no correct answer. However, the implication of the question is that the usability of the tool gives it its right to exist. The essential function of a CET is to aid in human decision making. When a CET is not accessible, it won't be utilised and therefore have no function. This small query is part of a much larger scientific and philosophical debate on why assumptions are made in the first place, and thus won't be elaborated on further.

The effects of the quasi-static modelling on the detail level are mainly reflected in the transitional areas of the mission profile and the inability to model peak loads and other fluctuations in the power demand. The transient areas are insignificantly small when compared with the rest of the operational profile, yet their effect on the components may last longer. Similarly, peak loads may be of short duration, but have strenuous effects on the equipment. An attempt has been made to ensure that all components, and especially the SOFC, are within a operating window where they could properly react to changes in the required power. For the detail level of the concept phase, the taken measures are deemed acceptable, as the CET mainly shows the optimal combination of components, not the detailed usage of these components. Nonetheless, the output should be reviewed critically and in later design stages more detailed calculation are needed.

Next, the chosen KPIs determine to which vessels and missions the tool is applicable. Furthermore, it can steer the output of the model into certain directions. The selected KPIs provide a good first estimation of the performance of the power plant and are quantifiable. The latter is important, since a computer model has to calculate the values of the elected KPIs. It can be reasoned that other or more KPIs should have been included, such as manoeuvrability and easy of installation/maintenance. Although these KPI do indeed give a more complete picture, they are difficult to quantify and are therefore not used within the model. Other KPIs that are quantifiable, for example magnetic signatures, were not added due to limited research time. In the end, a balance had to be found between the added value of a KPI and the research time it would take to implement it.

The previous discussion signifies a larger debate: certain intangible knowledge and experience can not be captured in variables and values. An advanced artificial neural network with enough training data might be able to succeed in uncovering all the underlying presumptions. However, this amount of training data might not be available and a the network has to be trained again when new technologies arrive. Thus, at this moment, there is no possibility to capture all the expertise of maritime engineers in a computer controlled

design process. Therefore, the tool should always be seen as an aid to humans, not as a replacement of humans.

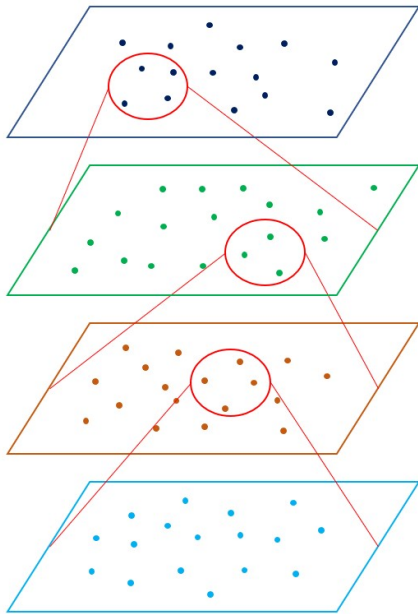


Figure 64: Diagram of a multi-stage exploration tool

A brute force search algorithm is applied to explore the design space. This algorithm is known as an exhaustive search algorithm, since it exhaust all possible options to find the optimal solution. A disadvantage of such an algorithm is that the number of possibilities can quickly grow beyond manageable proportions, this phenomenon is known as a combinatorial explosion. In this research the number of possible options was limited by a priori feasibility constraints, as the number of concepts was too large. However, reality has proven that a combinatorial explosion may still occur, due to internal design choices. Therefore, the algorithm was modified with the introduction of the IDeA. Consequently, the algorithm is no longer exhaustive, since not every options is evaluated. Unevaluated gaps will appear in the design space. An example can be found in the assignment of power by the PMS, where only one power allocation per concept is considered, while other power distributions may turn out to be more optimal. Essentially, a problem occurs when multiple different choices or dimensions are explored at the same time, due to excessive number of possible combinations.

A solution to this problem may be found in a multi-stage exploration tool, for which a diagram can be found in Figure 64. A multi-stage exploration tool makes every dimension or design choice into its own design space. After a stage is completed, the best concepts are taken to the next stage where a new dimensions is added. For example, in the first stage the type and number of components is determined, but the power is kept equal for every part. The best concepts are

taken to the next stage, where the power of the MPEs is varied. Instead of one power allocation per concept, multiple power distribution per configuration can be evaluated, as the number of concepts has been reduced in the previous stage. Later stages may involve the power distribution of the EGSs, the sizing of components and the usage of all parts. Even external exploration tools, such as the network exploration of de Vos [13], may be added as a stage. This may sound similar to recursive algorithms, such as genetic algorithms. However, a significant difference is the addition of dimensions per stage. Furthermore, for every stage a different exploration algorithm may be used, as long as a number of optimal configurations is outputted. A disadvantage of this method is that it too is not an exhaustive search of the total design space, but rather an exhaustive search of a design sub-space. This comes back to the discussion of local versus global optimum. Moreover, the computational time of tool is likely to increase, which contradicts all previous attempts to decrease this.

A final remark on the structure of the model is the internal programming style. The model is soft coded, meaning the tool does not have to be changed when the input changes. However, if new components or KPIs are to be added in the future, the code has to be severely altered. An underlying thought of the model was that new components could be easily implemented in the future, essentially creating a plug-and-play CET. This level of coding was not achieved, resulting in a code that is not as future-proof as was desired.

11.2.2 Model operation

Moving towards the actual model itself, the first choices are made within the concept generation, namely which components to model. Again, a balance must be found between the research and programming time on one hand and added value on the other. The gas turbine and CPP were implemented to make a fair comparison possible between existing vessels and model output. The realisation of a SOFC model is more questionable, since fuel cells are not common practice on naval vessels, let alone high temperature fuel cells. A shaft engine/motor with all its applications maybe would have been a more valuable addition to the tool. However, the employment of the SOFC can be seen as a test case, both for the model and the fuel cell itself. It shows that the model is able to handle non conventional equipment, while also demonstrating the potential of the SOFC. Clients that do not wish to consider a SOFC, or any other component for that matter, have the option to disable that single component.

Within the CET the most influential assumptions are made in the power management strategy, for the PMS dictates the size and usage of all other components. Furthermore, where most components are variable, the PMS is kept constant. This is the result of giving the PMS a heuristic rule based approach. The set of rules needs to be applicable to every configurations, thus also every non standard exemption. Defining such a set of rules, that is efficient and elegant too, proved to be difficult. Therefore, the decision was made to implement a single set of rules, instead of defining multiple sets of rules for various situations. The applied rule set is formulated on practical trends, yet opinions may differ over what the optimal real world practice is. This all results in a PMS that is fairly simple, robust and computational light, yet does not generate all feasible solutions or include the subtleties of real world power management strategies.

A clear improvement that can be made to the power usage PMS is the selection of the optimal engine combination. The PMS chooses the engines that combine to a power output closest to the required power. However, this may not always result in the most efficient engine choice. For example, an electric motor at a 40% load ratio combined with a generator at a 90 % load ratio might be more efficient than a diesel engine at 60 % load ratio. The PMS will choose the latter as the power output of the diesel engine lies closer to the power output compared to the electric motor. All in all, the usage PMS focuses on achieving the most efficient load ratio for all components, while it should be focusing on achieving the highest overall efficiency, which is not the same. A solution that was contemplated, but not implemented, is finding the combination of components with the least losses. This would automatically be the combination with the highest overall efficiency.

The effects of the propeller choice on the MPEs have already been discussed in Paragraph 8.3. As said, the outcome of the propeller choice should be critically evaluated. When a certain propeller is desired by the client, the choice could be made to disable the other propeller, so no confusion can arise.

The model does not consider the practical limits of certain components. It can construct gas turbine of a few kilowatts, but also fuel cells of multiple mega watts. From a physics stand point this is not a problem, yet it is uncertain if the same performance models are still valid at such a scale. Furthermore, these components will most likely not be available in real life, making the output potentially inapplicable. A solution could be to gather existing devices in a database and have the CET select from this database. This would ensure practical feasibility, but constraint the design space. Moreover, it can prove difficult to find characteristics of all the numerous components.

Mainly the main components of a power plant are modelled within the CET. In a real power plant, many other sub-components and systems can be found, all with their own volume and mass. A number of these sub-components are main component specific, for example heat exchangers on a SOFC. The consistency with which these sub-systems are included could be improved upon. The difficulty of sub-components is twofold. Firstly, determining to which sub-layer components should be incorporated and consistently applying this layer over all components. Secondly, the modelling of the components themselves. For sub-components less literature and dimensioning methods are available, so modelling them may prove to be challenging. The biggest inconsistency in the current CET may be found in the SOFC and the gas turbine. With the SOFC, the heat exchangers are not included, while they are essential for the operation of the fuel cell. With the gas turbine, the sizing is based on a packaged gas turbine, as delivered by Rolls-Royce. This package may included many sub-systems that are not included in other main components, making the gas turbine relatively heavier. This may explain why the SOFC is favoured by the CET and the gas turbine is not.

To continue on the previous point, the detail level of the different main components is not as consistent as could be. Since various parts are modelled by various authors, the detail level varies between these components. This discrepancy in detail level may make certain component seem more favourable than other, even though each component is validated. This inconsistency is probably the greatest with the performance of electric motor and the sizing of the gas turbine. The electric motor is modelled as an efficiency curve dependent on the engine speed, while other components are modelled on their first principles. The dimensions of the gas turbine are established with a fit function, while other components are sized based on calculations of their expected performance and the workings of individual inner parts.

11.2.3 Model output

The multi-criteria analysis looks at the relative performance of a configuration compared to other configurations. As a result, the presence of an excessively worse performing concept has an influence on the scores of the other configurations, as they are now performing relatively well. Subsequently, the KPI on which the poor score is recorded has become less relevant on the total score, since almost all concepts score well on

this KPI. Furthermore, the weights given to the different KPIs have no meaning in and of itself. A weight factor that is twice as high as another weight factor does not necessarily make that KPI twice as important within the model. This problem is rooted in every multi-criteria analysis, as it attempts to quantify importance.

Moreover, the different KPIs show a certain underlying dependency. The most obvious example of this is the effect of total efficiency on the other KPIs. A configuration that is more efficient consumes less fuel, therefore generally emits less emission and has less fuel on board in terms of weight and volume. It could even be argued that the signatures decrease when the efficiency increases, since less heat is lost to the exhaust gasses. As a result, developing a highly efficient concept is advantageous, even when efficiency is not important. This is one of the reasons why an efficient SOFC is often chosen, even though the power density of the component itself is worse than a generator or a PEMFC.

A final remark is made about the output of the model. As mentioned in the case study and the conclusion, the found optimal configurations are logical and as expected. From this, the question arises:

Is a concept exploration tool needed, if it produces predictable output?

The aim of a concept exploration tool is to evaluate the total design space, in order to find the optimal solution. It seems that humans have been able to find the optimal solution without considering all of the options. However, this does not implicate that a CET has no function, as is appealed in the following arguments.

Firstly, the presented case studies were of conventional naval vessels, with conventional propulsion trains. When non traditional case studies are tried, humans may have more difficulty finding the optimal solutions, as there are no previous examples. A CET does not consider how typical a vessel or mission profile is. Thus, a CET may have added value in eccentric projects. Building on this argument, humankind has decades of experience in modern marine engineering. It had time to develop knowledge about the existing technologies and how to optimise its potential. Nowadays, technologies are evolving faster than ever and it could be questioned if humans can keep up or if the human factor will limit the implementation of new technologies in marine engineering. A CET does not face this same problem, due to its computing power and its unconstrained design approach.

Secondly, the CET, as presented in this thesis, is quite limited in the number of (sub-)components and systems. When an increasing number of parts is taking into a single optimisation problem, the more complex this problem becomes. A more complex problem often leads to more constraints to simplify the problem to a manageable size. With a CET, these constraints can be omitted and more complex problems can be tackled. This is shown in the case study, where the number of components is increased in case A in comparison with case B. The computational does increase, but a more optimal solution is eventually found.

Thirdly, the speed with which the CET evaluates all possible solution is unmatched by humans. In the minutes it takes the CET to perform a run, a human could hardly finish the evaluation of a single configurations. It must be noted that the input of the CET must be created by a human, so it is not a completely fair comparison. However, even with the extra preparation time, the CET is significantly faster. The practical implications are shorter design iterations and faster feedback to the client.

Fourthly, it can reassure or empower a design team in its decision making, as it can be backed with objective calculations. Furthermore, it may also give a design team food for thought, by giving alternatives and providing reasoning why certain configurations would work and why others would not. These calculations and alternatives can be generated without spending a lot of resources.

Lastly, the CET does not only explore the design space, but essentially does a first iteration of the concept design. The output of the tool can be used by the design team in future design steps, or by other modelling tools to further the design process. Even when a predictable outcome is obtained, the characteristic of the propulsion train will have been computed.

All in all, a concept exploration tool has a function, even when it presents predictable results. In the future, when this area of research has been further developed, the advantages of such a tool will only grow. Nonetheless, a CET may always live in a paradox: When it cultivates predictable result, its added value is questioned. When it cultivates unexpected results, its output is questioned.

12

Recommendations

A number of recommendations result from this thesis and specifically the discussion. The recommendations are not aimed particularly at improving this exact tool, but rather on advancing the research area of concept exploration tools and optimisation in design processes in general. The recommendations can be categorized in three groups: The structure of the model, the operation of the model and the output of the model.

12.1 Model structure

The model is quite rigid, meaning that it may be difficult to add new model parts in the future. The code would have to be partially rewritten. A more modular model structure may prevent this problem, making the code more future prove. This would allow the tool to grow, be updated to the state of the art and accommodate multiple authors working in parallel or in succession.

The topology is kept constant to limit the amount of configuration. The computational time has decreased to such extent that the possibility might arise to start experimenting with variable topologies in combinations with variable component selection. This could be in multiple successive models or, in a more distant future, a single combined model.

To extend the previous point, a study into multi-stage exploration might be very interesting. This type of exploration method may lead to a more exhaustive search of parts of the design space by limiting the constraints put on the problem by the user. Furthermore, the model becomes more modular, as separate stages can be integrated in to the tool at later moments. To go one step further, more fundamental research into digitised design method for marine engineering may lay a broader foundation for this area of research to develop and might result in more unconstrained exploration tools.

12.2 Model operation

The client preferences are a quantified measure of the importance of a certain KPI. More research is needed into the underlying relevance of each KPI and their internal relationship. A qualitative inquiry is required to link the values of the weight factors to the level of importance a client expresses. This would make the model more user friendly and the output better explainable to clients.

Once the client preferences have been given to the CET, they are kept constant throughout the whole model. In reality, the wishes of the client may differ from mission element to mission element. During transit the importance may lie on efficiency and emissions, while during combat, none of that matters and robustness and signatures are given the highest priority. The goal was to incorporate this feature into the existing CETm but research time did not allow for this. The model is set-up to evaluate the mission elements separately, so only the final step of an element-wise comparison has to be taken.

As mentioned in the discussion, the most influential modelling assumptions are made in the power management strategy. A simple improvement was already brought up, yet further improvement is possible. A limiting factor of the PMS is the fact that it is rule based. These rules have to be applicable to every configuration, independent of the type and number of components that is being used. Therefore, simple rules are applied, which are not always the best. The PMS should be seen as an optimisation problem of itself and it would be interesting to unleash optimisation and network theory on the PMS. The aim should be to create a more flexible PMS, that is applicable to many different configurations, while also considering the potential missions and wishes of a client. Eventually a PMS could be created that chooses the components that should be installed, instead of brute-forcing every possibility.

The sizing of the gas turbine is done on the basis of fit functions. Furthermore, certain sub-systems are included in the dimensions of the gas turbine, as it gets installed as a package. A dedicated dimensioning method on centered around the first principles is needed to increase to accuracy of the tool. In a broader sense, the dimensioning of continuous flow machines is not widely elaborated in scientific literature. If this gap gets filled, it does not only increase the accuracy of the sizing tool, but may also constitute to a better understanding of the inner workings of a gas turbine. Therefore, the performance simulation might be improved.

New components could be added to the tool to further increase the explored design space. The most obvious one is a shaft engine/generator to function as a PTI/PTO. An electric engine is already modelled, yet the PMS does not allow this engine to be used as a generator. Furthermore, a lot of smaller sub-systems should be modelled to increase the accuracy of the tool. Moreover, combinations of sub-components and main components could be made and an optimisation challenge could be stated on component level. An example of such combined components is a combined turbo charged SOFC gas turbine.

A first step was made to include the robustness of a network into a bigger optimisation tool. The utilised robustness model works decent, yet further improvements could be made. More detailed robustness models already exist and could be integrated in a CET. Furthermore, it would be interesting to include the likelihood of failure, especially for naval vessel. As external sources could induce failure, the spacial design of a vessel has an influence on this likelihood. Adding this aspect to the robustness model would lift the whole CET to a new level, as the arrangement of the vessel is incorporated.

12.3 Model output

The output of the model show certain intriguing results. The model seems to prefer SOFCs in most situation. Reason for this are mentioned in the discussion, yet the first estimations by the CET suggest that it could be a promising technology on board of vessels. A feasibility study could be conducted into the practical applications of SOFCs. This research can focus not only on the theoretical performance of the fuel cell, but also on the functional challenge that come with a high-temperature fuel cell. These challenge could be found in a marine engineering perspective, but it may even be more interesting to look at the challenge of integrating a SOFC from a ship design perspective. Questions that should be answered involve the cooling of the fuel cell, placement within the vessel, required sub-systems, mass flow towards and from the fuel cell and, of course, response to dynamic behaviour.

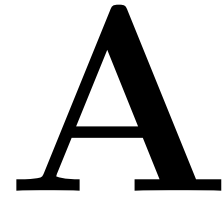
Another notable result that gives a possibility for future research is the combination of electric motor, gearbox and controllable pitch propeller. The CET highlights the added efficiency of this combination. It shows that in mission profile where the engines operate at a low load ratio for a majority of the time, this configuration type outperforms other concepts. However, an equally interesting subject may be the operational envelope and mission usability of such a configuration. As mentioned, the high torque at low rpm results in great manoeuvrability and the adaptability of the CPP and the electric motor leads to a configuration that can be applied to many different situations. Further research into these practical advantages, as well as the disadvantages of such a combination may be interesting.

References

- [1] Cengiz Deniz and Burak Zincir. Environmental and economical assessment of alternative marine fuels. *Journal of Cleaner Production*, 113:438–449, 2016.
- [2] Anh Tuan Hoang and Van Viet Pham. A REVIEW ON FUELS USED FOR MARINE DIESEL ENGINES. *Journal of Mechanical Engineering Research and Developments*, 41(4):22–32, nov 2018.
- [3] L. van Biert, M. Godjevac, K. Visser, and P.V. Aravind. A review of fuel cell systems for maritime applications. *Journal of Power Sources*, 327:345–364, 2016.
- [4] R.D. Geertsma, R.R. Negenborn, K. Visser, and J.J. Hopman. Design and control of hybrid power and propulsion systems for smart ships: A review of developments. *Applied Energy*, 194:30–54, 2017.
- [5] B R Clayton. Wind-assisted ship propulsion. *Physics in Technology*, 18(2):53–60, mar 1987.
- [6] Ruihua Lu and Jonas W. Ringsberg. Ship energy performance study of three wind-assisted ship propulsion technologies including a parametric study of the flettner rotor technology. *Ships and Offshore Structures*, 15(3):249–258, may 2019.
- [7] Council of the European Union. ENVIRONMENTAL PROTECTION AND ENERGY EFFICIENCY FOR EU-LED MILITARY OPERATIONS. 2012.
- [8] Ministerie van Defensie. Operationele Energiestrategie. 2015.
- [9] Ministerie van Defensie. Defensie Energie en Omgeving Strategie 2019-2022. 2019.
- [10] Svein Gunnar Sjøtun. A ferry making waves: A demonstration project ‘doing’ institutional work in a greening maritime industry. *Norsk Geografisk Tidsskrift - Norwegian Journal of Geography*, 73(1):16–28, oct 2018.
- [11] P. de Vos and D. Stapersma. Automatic topology generation for early design of on-board energy distribution systems. *Ocean Engineering*, 170:55–73, 2018.
- [12] Jitte van Dijk. Automatic selection of an optimal power plant configuration. Master’s thesis, Delft University of Technology, 2018.
- [13] Peter de Vos. *On early-stage design of vital distribution systems on board ships*. PhD thesis, Delft University of Technology, 2018.
- [14] Tom de van der Schueren. Power plant configuration selection based on mission profile and client preferences. Literature report, Delft University of Technology, 2021.
- [15] J Thompson, D Vaitekunas, and AM Birk. Ir signature suppression of modern naval ships. In *ASNE 21st century combatant technology symposium*, volume 1, pages 27–30, 1998.
- [16] Alexander Spyro Piperakis. *An Integrated Approach to Naval Ship Survivability in Preliminary Ship Design*. PhD thesis, University College London, 2013.
- [17] Henry H. Willis and Kathleen Loa. *Measuring the Resilience of Energy Distribution Systems*. RAND Corporation, Santa Monica, CA, 2015.
- [18] Marjolein ten Hacken. Optimization of a submarine propulsion system by implementing a pem fuel cell and a pmsm in a first principle model. Master’s thesis, Delft University of Technology, 2017.
- [19] Rolls-Royce. Rolls-royce completes factory acceptance test for first gas turbine for royal navy’s type 26 global combat ship. Press Release, February 2016.
- [20] Rolls-Royce. Rolls-royce completes delivery of power and propulsion systems package for future uss zumwalt (ddg 1000) multi mission destroyer. Press Releas, July 2015.

- [21] Frank van Es. Designing and evaluating propulsion concepts of surface combatants. Master's thesis, TU Delft, 2011.
- [22] Rolls-Royce. Principle dimensions mt-30. Website.
- [23] Gurbinder Kaur. *Solid Oxide Fuel Cell Components*. Springer, 2016.
- [24] Wei Jiang, Ruixian Fang, Jamil A. Khan, and Roger A. Dougal. Parameter setting and analysis of a dynamic tubular sofc model. *Journal of Power Sources*, 162(1):316–326, 2006.
- [25] Ryan O'Hayre, Suk-Won Cha, Whitney Colella, and Fritz B. Prinz. *Fuel Cell Fundamentals*. John Wiley & Sons, 3rd edition, June 2016.
- [26] Stapersma and de Vos. Dimension prediction models of ship system components based on first principles. In *Proc. of 12th Int. Marine Design Conference (IMDC)*, 2015.
- [27] Shuai Ma, Meng Lin, Tzu-En Lin, Tian Lan, Xun Liao, François Maréchal, Jan Van herle, Yongping Yang, Changqing Dong, and Ligang Wang. Fuel cell-battery hybrid systems for mobility and off-grid applications: A review. *Renewable and Sustainable Energy Reviews*, 135:110119, 2021.
- [28] Heide Budde-Meiwes, Julia Drillkens, Benedikt Lunz, Jens Muennix, Susanne Rothgang, Julia Kowal, and Dirk Uwe Sauer. A review of current automotive battery technology and future prospects. *Proceedings of the Institution of Mechanical Engineers, Part D: Journal of Automobile Engineering*, 227(5):761–776, apr 2013.
- [29] Wärtsilä Marine Solutions. Wärtsilä 20 Product Guide, 2020.
- [30] Wärtsilä Marine Solutions. Wärtsilä 26 Product Guide, 2018.
- [31] Wärtsilä Marine Solutions. Wärtsilä 32 Product Guide, 2021.
- [32] ABB. Abb central inverters. Technical report, 2011.
- [33] R.D. Geertsma, R.R. Negenborn, K. Visser, M.A. Loonstijn, and J.J. Hopman. Pitch control for ships with diesel mechanical and hybrid propulsion: Modelling, validation and performance quantification. *Applied Energy*, 206:1609–1631, nov 2017.
- [34] Hans Klein Woud and Douwe Stapersma. *Design of Propulsion and Electric Power Generation Systems*. IMarEST, 2012.
- [35] General Electric. Datasheet 25mw marine gas turbine, 2018.
- [36] Jerzy Herdzik and Romuald Cwilewicz. Remarks on utilization of marine trent 30 gas turbine as prime mover on vessels. *Journal of KONES*, 2017.
- [37] Janusz Kotowicz, Marcin Job, Mateusz Brzeczek, Krzysztof Nawrat, and Janusz Medrych. The methodology of the gas turbine efficiency calculation. *Archives of Thermodynamics*, 37(4):19–35, dec 2016.
- [38] Philip P Walsh and Paul Fletcher. *Gas turbine performance*. John Wiley & Sons, 2004.
- [39] James Larminie. *Fuel cell systems explained*. J. Wiley, Chichester, West Sussex, 2003.
- [40] L. van Biert. *Solid oxide fuel cells for ships: System integration concepts with reforming and thermal cycles*. PhD thesis, Delft University of Technology, 2020.
- [41] G. Chiodelli and L. Malavasi. Electrochemical open circuit voltage (OCV) characterization of SOFC materials. *Ionics*, 19(8):1135–1144, jan 2013.
- [42] Andrew L. Dicks, David A. J. Rand. *Fuel Cell Systems Explained, Third Edition*. John Wiley & Sons Ltd., 2018.
- [43] A. Sorce, A. Greco, L. Magistri, and P. Costamagna. Fdi oriented modeling of an experimental sofc system, model validation and simulation of faulty states. *Applied Energy*, 136:894–908, 2014.
- [44] Caisheng Wang and M.H. Nehrir. A physically based dynamic model for solid oxide fuel cells. *IEEE Transactions on Energy Conversion*, 22(4):887–897, dec 2007.
- [45] L. van Biert, M. Godjevac, K. Visser, and P.V. Aravind. A review of fuel cell systems for maritime applications. *Journal of Power Sources*, 327:345–364, sep 2016.

- [46] Biao Huang, Yutong Qi, and Monjur Murshed. Solid oxide fuel cell: Perspective of dynamic modeling and control. *Journal of Process Control*, 21(10):1426–1437, 2011.
- [47] Paul Boldrin and Nigel P. Brandon. Progress and outlook for solid oxide fuel cells for transportation applications. *Nature Catalysis*, 2(7):571–577, jul 2019.
- [48] M. Abdus Salam, Md Shehan Habib, Paroma Arefin, Kawsar Ahmed, Md Sahab Uddin, Tareq Hossain, and Nasrin Papri. Effect of temperature on the performance factors and durability of proton exchange membrane of hydrogen fuel cell: A narrative review. *Material Science Research India*, 17(2):179–191, aug 2020.
- [49] Peter de Vos and H.T. Grimmeliuss. Dynamic modeling of propulsion systems for inland ships using different fuels and fuel cells. In *Environment-Friendly Inland Shipping*. International Symposium on Marine Engineering, 2009.
- [50] Dhruv Kler, Kanwar P. S. Rana, and Vineet Kumar. Parameter extraction of fuel cells using hybrid interior search algorithm. *International Journal of Energy Research*, 43(7):2854–2880, may 2019.
- [51] Kevin Huang. Fuel utilization and fuel sensitivity of solid oxide fuel cells. *Journal of Power Sources*, 196(5):2763–2767, 2011.
- [52] A.H. Fakeeha, F.A. Abd El Aleem, and H.M. Ettouney. The internal reforming fuel cells as a clean energy system for natural gas utilization in the kingdom. *Journal of King Saud University - Engineering Sciences*, 7:171–188, 1995.
- [53] Noureddine Hajjaji, Marie-Noëlle Pons, Ammar Houas, and Viviane Renaudin. Exergy analysis: An efficient tool for understanding and improving hydrogen production via the steam methane reforming process. *Energy Policy*, 42:392–399, mar 2012.
- [54] Kazunari Miyazaki, Hiroki Muroyama, Toshiaki Matsui, and Koichi Eguchi. Impact of the ammonia decomposition reaction over an anode on direct ammonia-fueled protonic ceramic fuel cells. *Sustainable Energy & Fuels*, 4(10):5238–5246, 2020.
- [55] Denver Cheddie. Ammonia as a hydrogen source for fuel cells: A review. In *Hydrogen Energy - Challenges and Perspectives*. InTech, oct 2012.
- [56] A Vrijdag, D Stapersma, and T van Terwisga. Control of propeller cavitation in operational conditions. *Journal of Marine Engineering & Technology*, 9(1):15–26, jan 2010.
- [57] F. De Luca & C. Pensa F. Balsamo. A new logic for controllable pitch propeller management. *Sustainable Maritime Transportation and Exploitation of Sea Resources*, 2012.
- [58] Antonio Bacciaglia, Alessandro Ceruti, and Alfredo Liverani. Controllable pitch propeller optimization through meta-heuristic algorithm. *Engineering with Computers*, jan 2020.
- [59] R.D. Geertsma, K. Visser, and R.R. Negenborn. Adaptive pitch control for ships with diesel mechanical and hybrid propulsion. *Applied Energy*, 228:2490–2509, 2018.
- [60] S.P. van Leeuwen. Estimating the vulnerability of ship distributed system topologies. Master’s thesis, Delft University of Technology, 2017.



Design space analysis

The analysis of the other design space images of case study 1, 2 and 3.

A.1 Case study 1

Figures 65 and 66 show the total design space in terms of total efficiency versus robustness for case study 1A and 1B respectively. It can be clearly seen that robustness is given the highest priority as lower levels of robustness directly lead to lower ranking concepts in both case studies. In case study 1A, the optimal concept lies near, but not on, the Pareto front. This is noteworthy, since the robustness could apparently be enlarged without damaging the efficiency. However, this would most likely compromise other KPIs, resulting in a less optimal configuration. Some level of discretisation can be found in terms of robustness, which is logical, as failing components are a discreet event. The position of the optimal concepts versus all other concepts shows again that the optimal configuration is more efficient than the vast majority and has some of the highest levels of robustness.

In case 1B, the optimal configurations lies further away from the Pareto front than in case 1A. More noticeable is the position of the position of the optimal concept versus the rest of the concepts. A significant number of concepts is both more efficient and more robust than the optimal configuration. As a result, a concept with a more robustness or efficiency could be chosen by the human design team, if that would be desirable. The optimal concept seemingly outperform the other concepts in terms of the other KPIs. Similarly to case 1A, some level of discretisation can be found for the same reason.

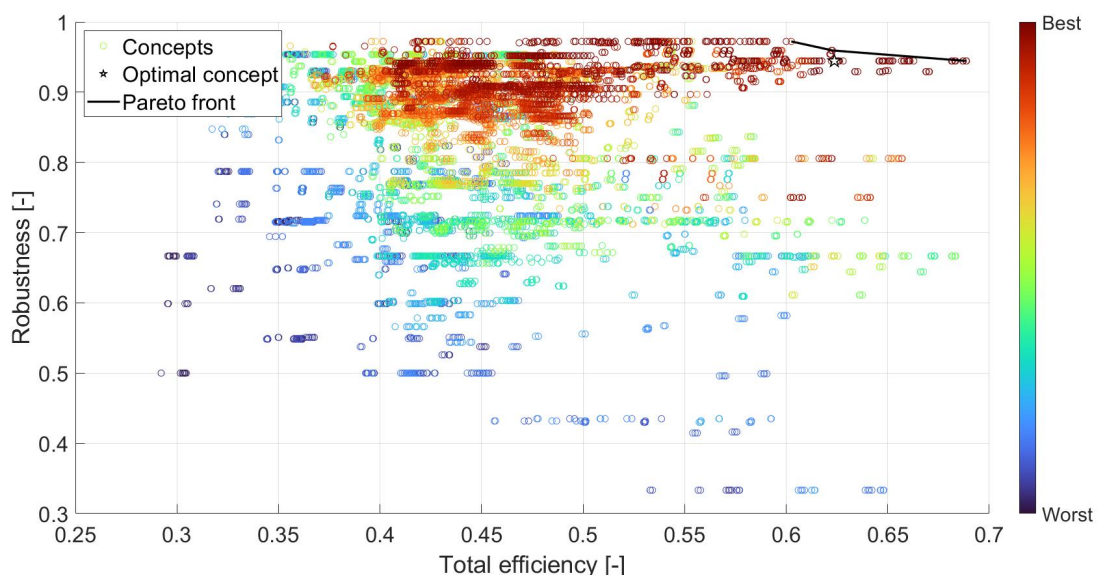


Figure 65: Efficiency-versus-robustness design space. All concepts of case study 1A, including the optimal configuration indicated with a star and the Pareto front indicated with a black line. The colour of a concept is based on the overall ranking of the concept from best (red) to worst (blue).

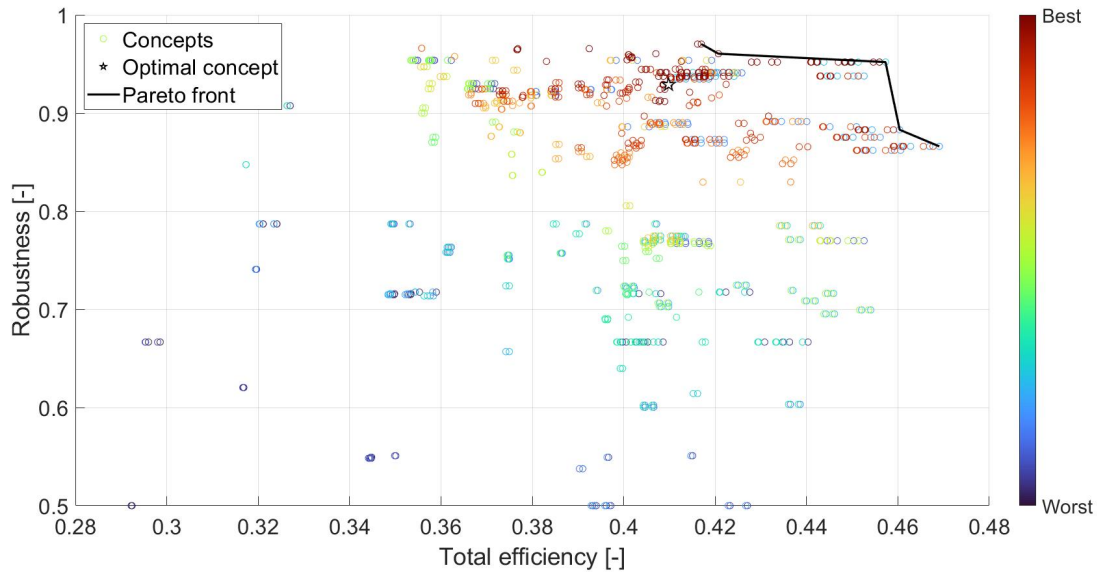


Figure 66: Efficiency-versus-robustness design space. All concepts of case study 1B, including the optimal configuration indicated with a star and the Pareto front indicated with a black line. The color of a concept is based on the overall ranking of the concept from best (red) to worst (blue).

Figures 67 and 68 display the total design space in terms of volume versus robustness for case study 1A and 1B respectively. In case study 1A, the highest concentration of concepts can be found near the Pareto front, including the optimal configuration. This reflects the importance of both volume and robustness, since most concepts are internally optimised towards these two KPIs. Meanwhile, it is noteworthy to see that the most optimal concept does not lie on or even close to the Pareto front. In the two previous renders of the design space the optimal configuration did lie on the Pareto front. Being on other Pareto fronts does not guarantee being on this front as well, but as these KPIs were given the highest importance, one could expect the optimal concept to be near or on the Pareto front. This does give the design team the flexibility to choose another concept nearer to the front, if desirable.

In case study 1B, the optimal concept lies closer to the Pareto front than in case 1A. Better yet, one could argue that the optimal configurations of case study 1B outperforms the optimal configuration of case study 1A in this aspect. This is remarkable as case study B is a more constraint version of case study A. Similar to case study 1A, most of the concepts can be found near the Pareto front, indication internal optimisation towards these KPIs. The optimal concept of case study 1B never lies on a 2D Pareto front, meaning it can always be improved on one KPI while not impeding the other KPI. However, in the multidimensional design space, it must lie on the total Pareto front, being the optimal combination of all KPIs.

A.2 Case study 2

Figures 69 and 70 present the total design space in terms of total efficiency versus volume for case study 2A and 2B respectively. For case study 2A the optimal concept lies on the Pareto front, which is to be expected, since efficiency and volume are given priority in this case study. The location of the optimal configuration shows that the second highest efficiency has been achieved. The significant volumetric cost of reaching the highest efficiency has made the CET settle for this concept. A noticeable gradient from red to blue can be observed when moving away from the Pareto front. This indicates that this 2D front heavily influences the overall Pareto front and the subsequent ranking. That being said, the majority of concept is not found near the Pareto front. This means that either the concepts were not internally optimised towards these KPIs or, more likely, are not capable of achieving better scores on these KPIs, due to component selection.

In case 2B, the optimal configuration almost has the lowest volume, yet the efficiency could be improvement upon when comparing it to the other concepts. This is noteworthy, as both volume and efficiency are of high importance in this case study. Furthermore, in case study 2A the optimal concepts did lie on the Pareto front. That being said, most other concepts have a lower efficiency and a higher volume. A design team

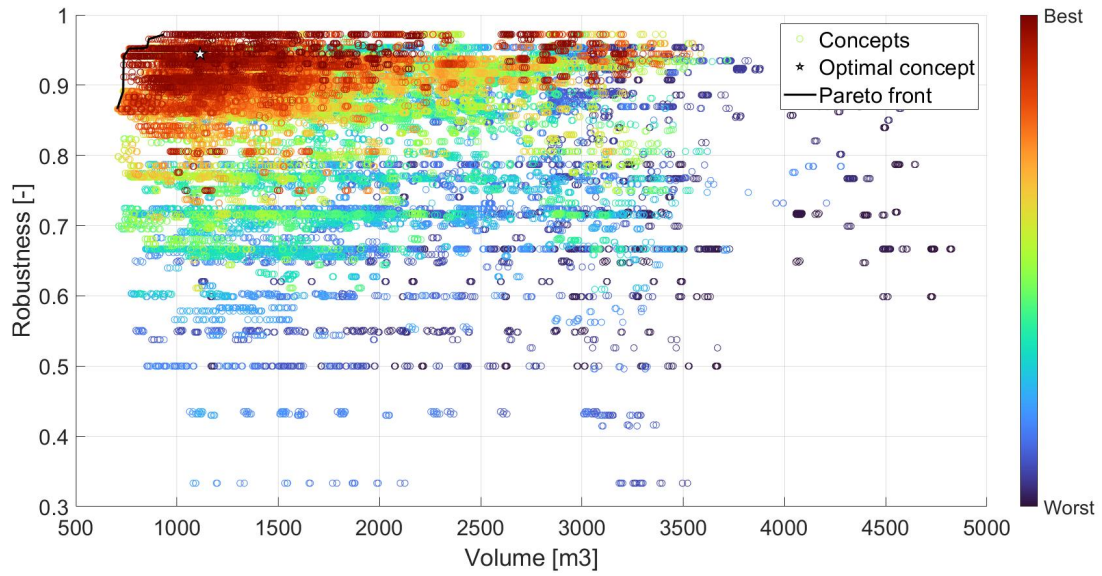


Figure 67: Volume-versus-robustness design space. All concepts of case study 1A, including the optimal configuration indicated with a star and the Pareto front indicated with a black line. The colour of a concept is based on the overall ranking of the concept from best (red) to worst (blue).

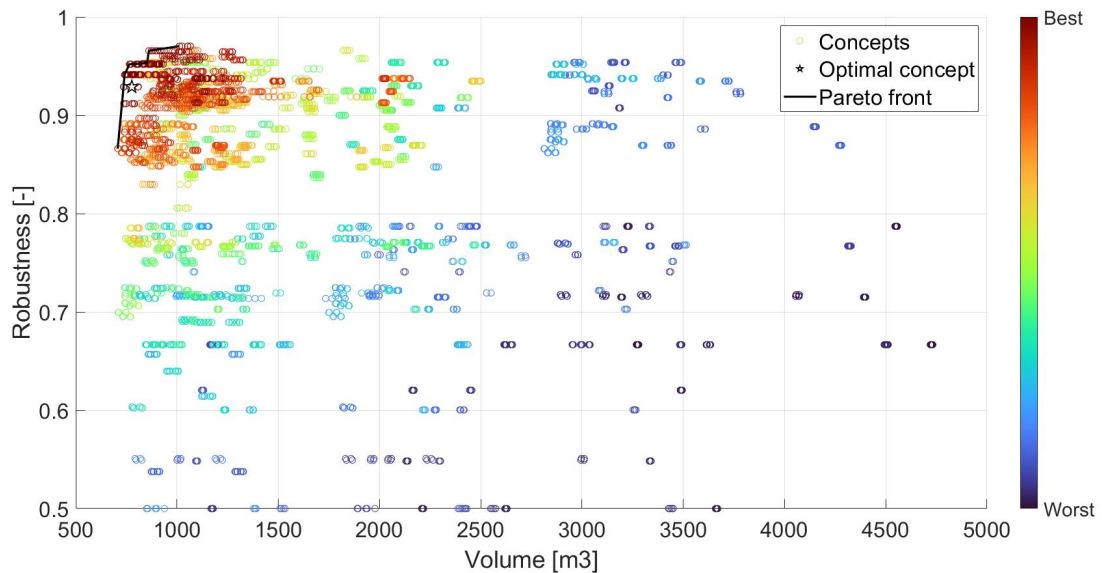


Figure 68: Volume-versus-robustness design space. All concepts of case study 1B, including the optimal configuration indicated with a star and the Pareto front indicated with a black line. The color of a concept is based on the overall ranking of the concept from best (red) to worst (blue).

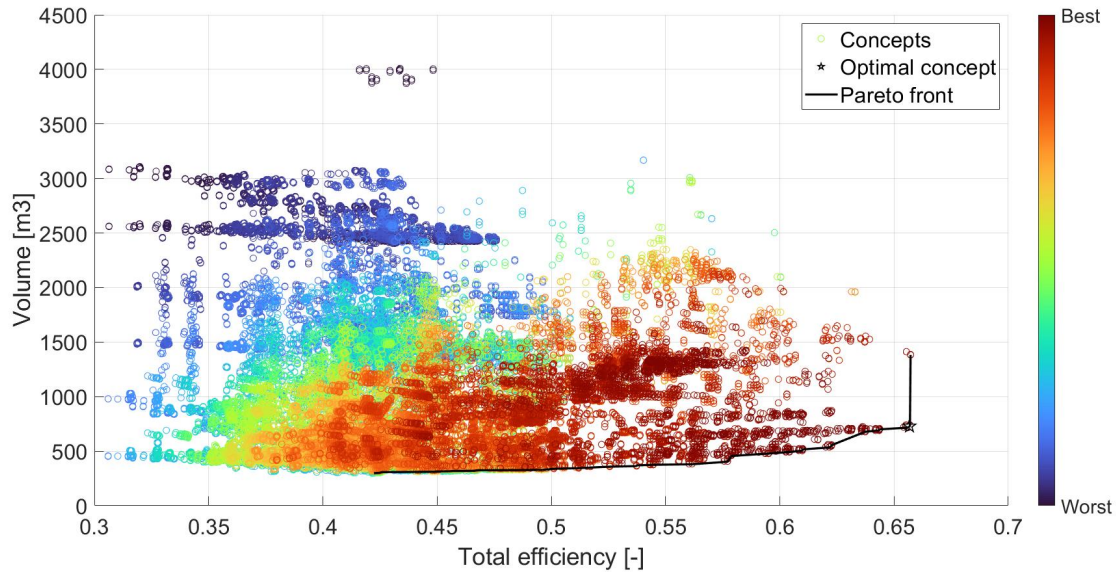


Figure 69: Efficiency-versus-volume design space. All concepts of case study 2A, including the optimal configuration indicated with a star and the Pareto front indicated with a black line. The colour of a concept is based on the overall ranking of the concept from best (red) to worst (blue).

could make the decision of going with a concept with a higher efficiency without compromising on fuel, yet this would certainly damage the performance of the other KPI.

Figures 71 and 72 present the total design space in terms of total efficiency versus robustness for case study 2A and 2B respectively. In case 2A, the optimal configuration lies quite far from the Pareto front in the middle of the majority of concepts. A more definite gradient from red to blue can be observed than in the previous design space representation, supporting the conclusion that volume is a more decisive KPI than efficiency. That being said, a distinct line of well performing concepts can be found around 1300 tons. These concepts most likely have hydrogen fuel cells installed, resulting in no emissions, which is the other KPI that is given priority. Thus, these concepts perform well, without having the lowest volume. The position of the optimal configuration shows that both in terms of volume and robustness a significant improvement can be made by choosing a different concept. Furthermore, in this 2D design space, there is nothing that makes the optimal concept stand out between the other concepts. This leads to an interesting conclusion; even though volume is the most decisive KPI, the optimal concept has optimised efficiency over volume, making it somewhat of an outsider.

In case 2B, the optimal concept does lie near the Pareto front, as it almost achieves the highest robustness. In terms of volume a significant number of concepts score better, all be it just slightly. Again a clear gradient is visible along the volume axis, indicating the decisiveness of this KPI. Unlike case 2A, the optimal configuration of case 2B has optimised volume over efficiency. This follows the expected logic formulated previously.

A.3 Case study 3

Figures 73 and 74 display the total design space in terms of total efficiency versus robustness for case study 3A and 3B respectively. The optimal concept lies away from the Pareto front, yet not many configuration exist between the optimal one and the Pareto front. The majority of the of the concepts, both best and worst, are found at a lower efficiency, but higher robustness. The blue worst concepts are not clearly visible, as they are overlapped by the red best concepts. Similar to case 2, it is evident that robustness is not given priority. Unlike case 2, efficiency is now also of less importance, resulting of a shift of concepts from high efficiency to lower efficiency. Furthermore, also more of the best concepts can now be found at lower efficiencies.

Figure 73 shows similarities with Figure 54, in that the Pareto front is formed by sub-optimal concepts and that a number of the worst concepts are spread between the best concepts. The optimal configuration has

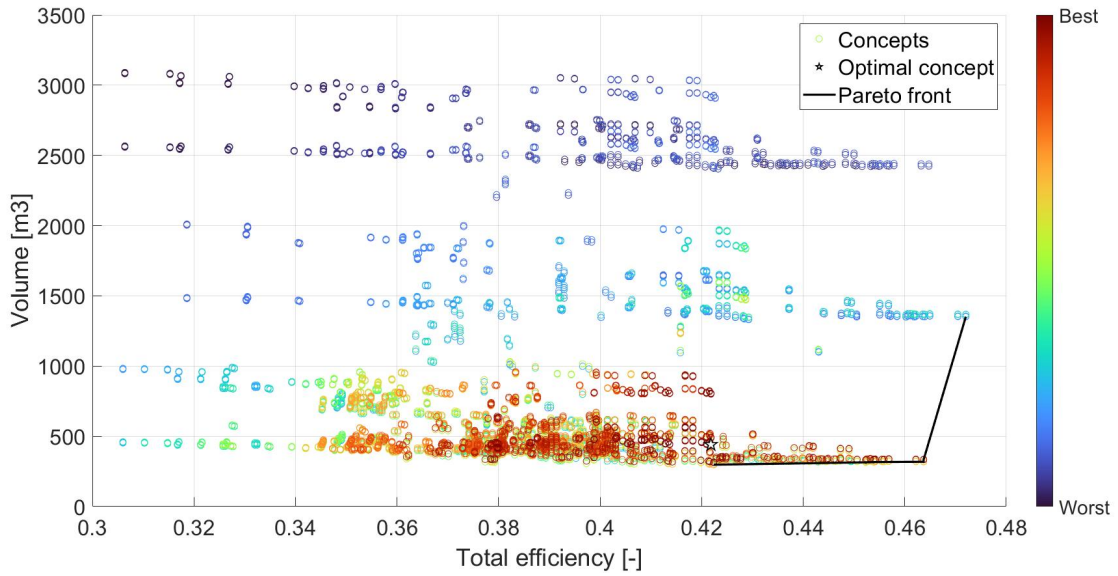


Figure 70: Efficiency-versus-volume design space. All concepts of case study 2B, including the optimal configuration indicated with a star and the Pareto front indicated with a black line. The color of a concept is based on the overall ranking of the concept from best (red) to worst (blue).

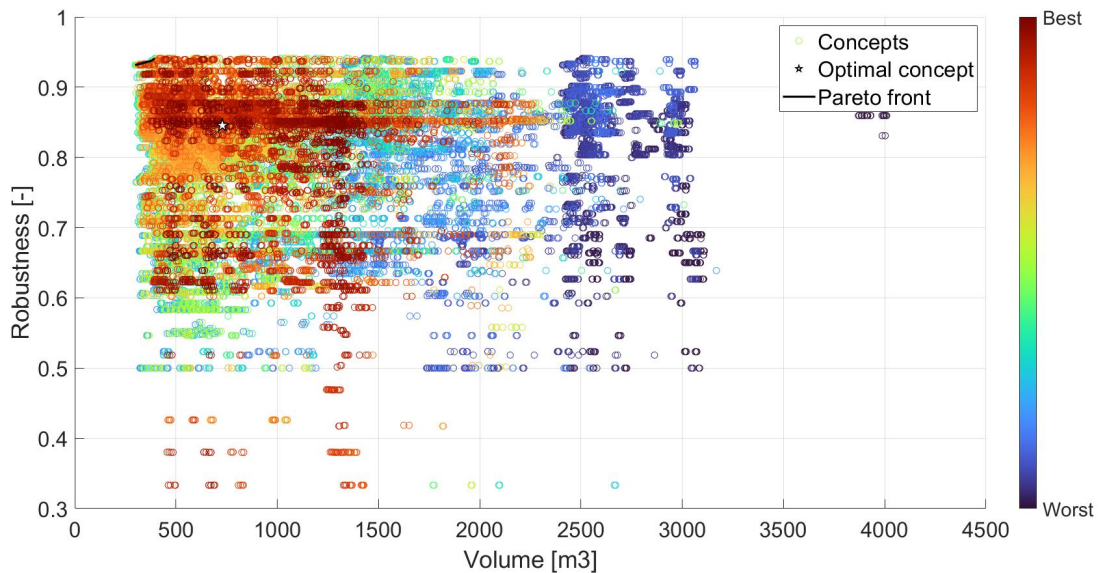


Figure 71: Volume-versus-robustness design space. All concepts of case study 2A, including the optimal configuration indicated with a star and the Pareto front indicated with a black line. The colour of a concept is based on the overall ranking of the concept from best (red) to worst (blue).

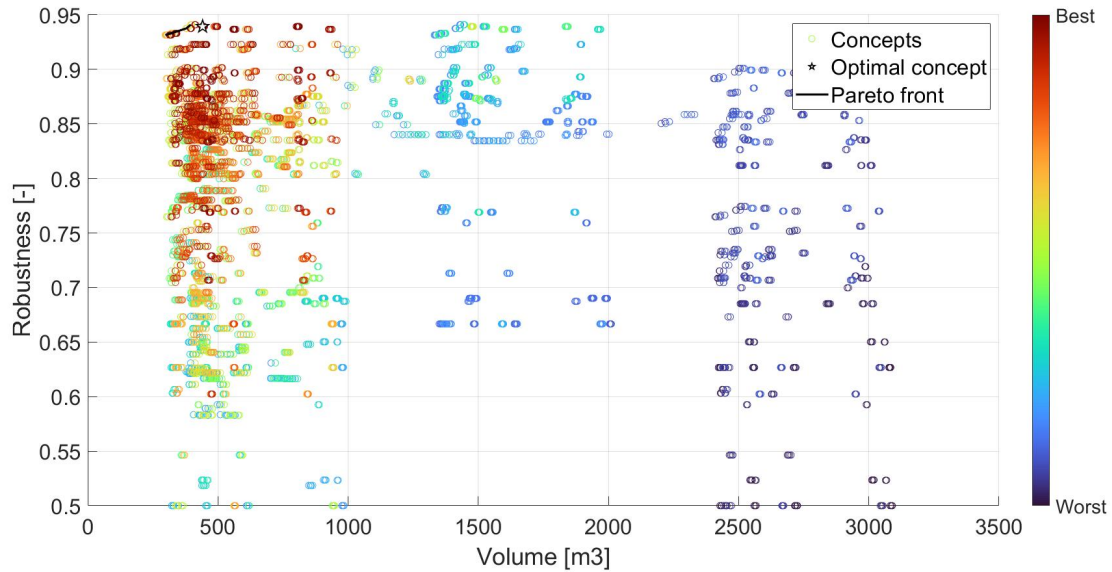


Figure 72: Volume-versus-robustness design space. All concepts of case study 2B, including the optimal configuration indicated with a star and the Pareto front indicated with a black line. The color of a concept is based on the overall ranking of the concept from best (red) to worst (blue).

a high level of robustness and efficiency when compared with most other concept. However, a significant increase in efficiency is possible when choosing a different concept.

Figures 75 and 76 represent the total design space in terms of volume versus robustness for case study 3A and 3B respectively. It could be expected that a higher level of robustness may come at the cost of a higher volume, as multiple or overcapacitated components are applied. However, both figures show that most concepts are able to achieve a high level of robustness at a relatively low volume. In case study 3A, the optimal concept lies quite a bit away from the Pareto front, which is remarkable as volume is given priority. Improvement of either volume or robustness will likely reduce the efficiency of the concept, resulting in a less optimal configuration. Similar conclusions can be drawn for case study 3B in Figure 76. In both figures the importance of volume over robustness can be found in the fact that colour gradient runs along the volume axis.

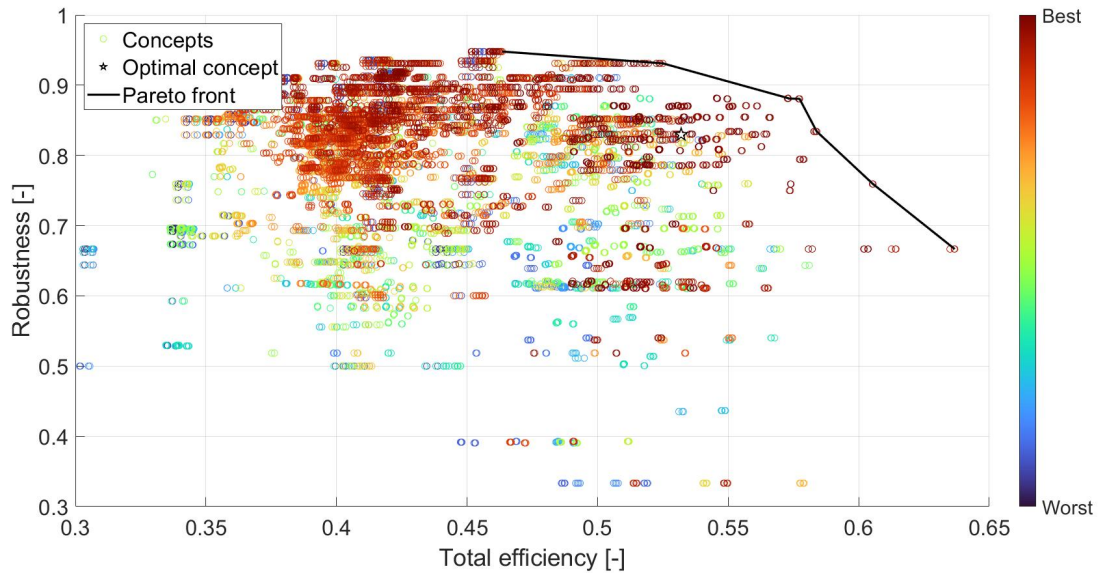


Figure 73: Efficiency-versus-robustness design space. All concepts of case study 3A, including the optimal configuration indicated with a star and the Pareto front indicated with a black line. The colour of a concept is based on the overall ranking of the concept from best (red) to worst (blue).

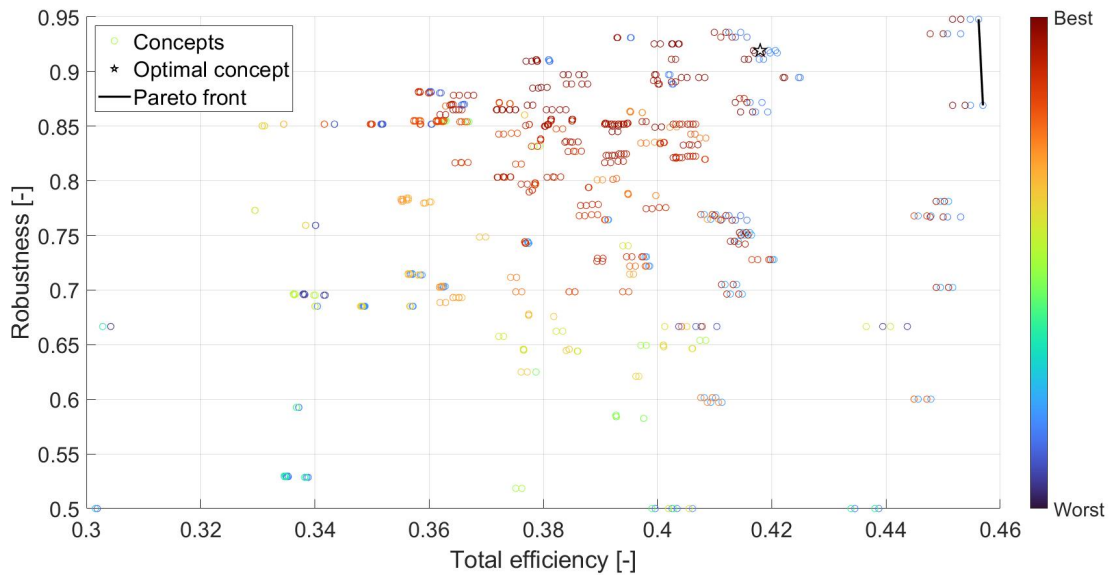


Figure 74: Efficiency-versus-robustness design space. All concepts of case study 3B, including the optimal configuration indicated with a star and the Pareto front indicated with a black line. The color of a concept is based on the overall ranking of the concept from best (red) to worst (blue).

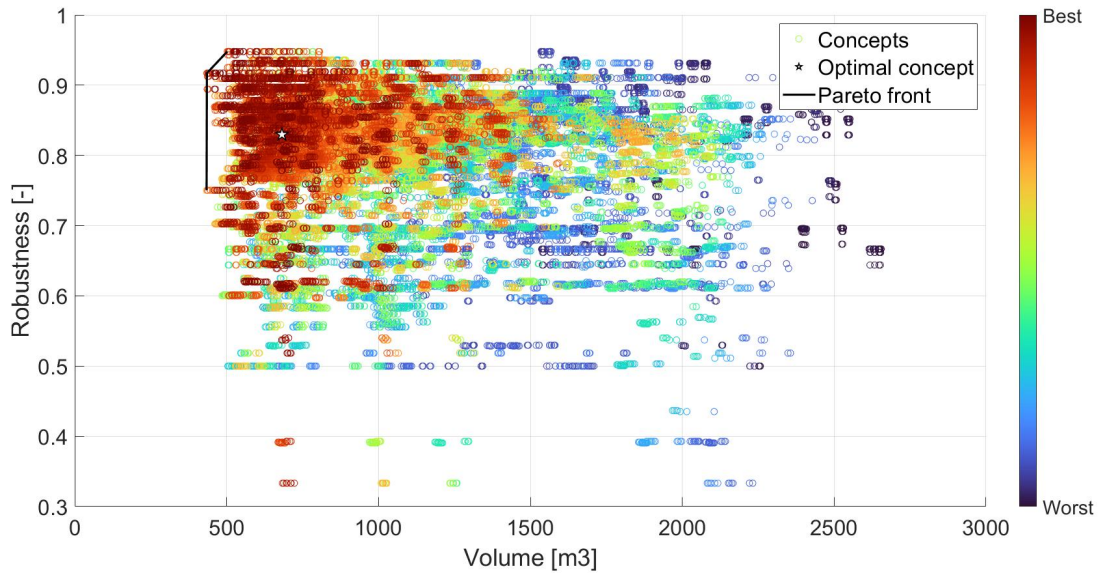


Figure 75: Volume-versus-robustness design space. All concepts of case study 3A, including the optimal configuration indicated with a star and the Pareto front indicated with a black line. The colour of a concept is based on the overall ranking of the concept from best (red) to worst (blue).

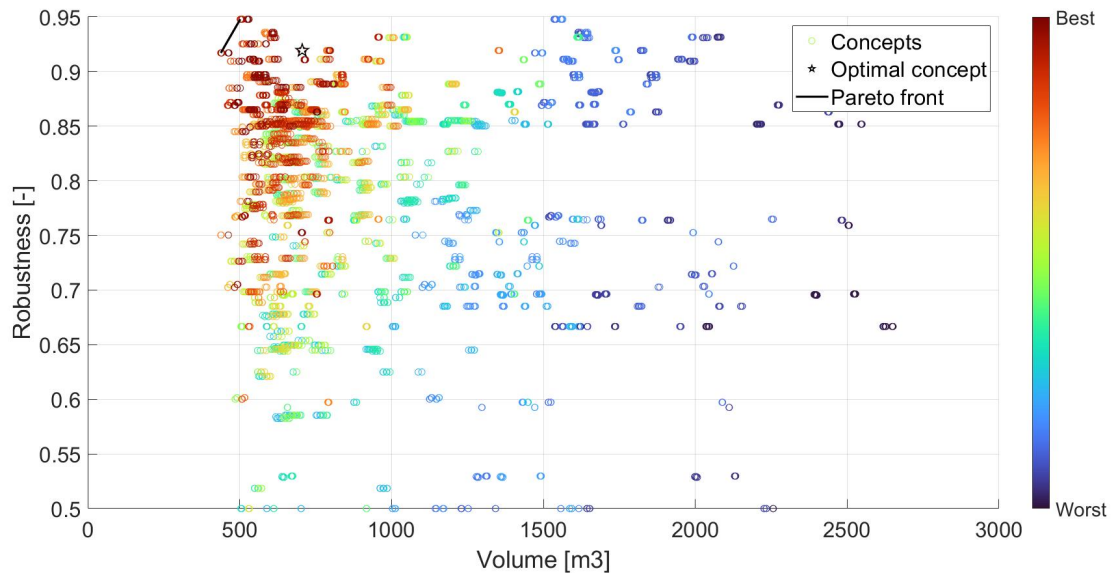


Figure 76: Volume-versus-robustness design space. All concepts of case study 3B, including the optimal configuration indicated with a star and the Pareto front indicated with a black line. The color of a concept is based on the overall ranking of the concept from best (red) to worst (blue).

B

Client preferences

The client preferences of sensitivity analysis of the case studies can be found in Tables 42, 43 and 44. The first set is the normal set of client preferences as used in the case study.

Table 42: Client preference sets of case study 1A and 1B.

Set	Efficiency	Emission	Volume	Mass	Signatures	Robustness
1	4	2	8	6	8	10
2	0	2	8	6	8	10
3	6	2	8	6	8	10
4	10	2	8	6	8	10
5	4	0	8	6	8	10
6	4	6	8	6	8	10
7	4	10	8	6	8	10
8	4	2	0	6	8	10
9	4	2	3	6	8	10
10	4	2	10	6	8	10
11	4	2	8	0	8	10
12	4	2	8	3	8	10
13	4	2	8	10	8	10
14	4	2	8	6	0	10
15	4	2	8	6	3	10
16	4	2	8	6	10	10
17	4	2	8	6	8	0
18	4	2	8	6	8	3
19	4	2	8	6	8	6

Table 43: Client preference sets of case study 2A and 2B.

Set	Efficiency	Emission	Volume	Mass	Signatures	Robustness
1	6	7	7	4	3	3
2	0	7	7	4	3	3
3	3	7	7	4	3	3
4	10	7	7	4	3	3
5	6	0	7	4	3	3
6	6	3	7	4	3	3
7	6	10	7	4	3	3
8	6	7	0	4	3	3
9	6	7	3	4	3	3
10	6	7	10	4	3	3
11	6	7	7	0	3	3
12	6	7	7	6	3	3
13	6	7	7	10	3	3
14	6	7	7	4	0	3
15	6	7	7	4	6	3
16	6	7	7	4	10	3
17	6	7	7	4	3	0
18	6	7	7	4	3	6
19	6	7	7	4	3	10

Table 44: Client preference sets of case study 3A and 3B

Set	Efficiency	Emission	Volume	Mass	Signatures	Robustness
1	4	5	10	8	3	3
2	0	5	10	8	3	3
3	6	5	10	8	3	3
4	10	5	10	8	3	3
5	4	0	10	8	3	3
6	4	3	10	8	3	3
7	4	10	10	8	3	3
8	4	5	0	8	3	3
9	4	5	3	8	3	3
10	4	5	6	8	3	3
11	4	5	10	0	3	3
12	4	5	10	3	3	3
13	4	5	10	10	3	3
14	4	5	10	8	0	3
15	4	5	10	8	6	3
16	4	5	10	8	10	3
17	4	5	10	8	3	0
18	4	5	10	8	3	6
19	4	5	10	8	3	10

Table 45: Sensitivity analysis of client preferences in case study 1A

Set	Efficiency	CO2	SOx	NOx	Volume	Mass	Signatures	Robustness
1	0%	0%	0%	0%	0%	0%	0%	0%
2	-2%	2%	0%	0%	-5%	-6%	-23%	-2%
3	0%	0%	0%	0%	4%	7%	-25%	-1%
4	4%	-4%	0%	0%	21%	29%	-36%	0%
5	0%	0%	0%	0%	0%	0%	0%	0%
6	0%	0%	0%	0%	4%	7%	-25%	-1%
7	6%	-100%	0%	0%	44%	63%	-24%	-1%
8	-1%	-100%	0%	0%	190%	-14%	-100%	6%
9	4%	-4%	0%	0%	26%	37%	-36%	6%
10	-2%	2%	0%	0%	-5%	-5%	-23%	-4%
11	4%	-4%	0%	0%	24%	32%	-29%	6%
12	0%	0%	0%	0%	5%	9%	-25%	3%
13	-2%	2%	0%	0%	-5%	-6%	-23%	-6%
14	-15%	20%	0%	inf	-20%	-26%	474%	0%
15	0%	0%	0%	0%	0%	0%	0%	0%
16	0%	0%	0%	0%	-1%	0%	-33%	0%
17	-3%	3%	0%	0%	-8%	-11%	-59%	-35%
18	-2%	2%	0%	0%	-6%	-8%	-23%	-11%
19	-2%	2%	0%	0%	-6%	-8%	-23%	-9%

Table 46: Sensitivity analysis of client preferences in case study 1B

Set	Efficiency	CO2	SOx	NOx	Volume	Mass	Signatures	Robustness
1	0%	0%	0%	0%	0%	0%	0%	0%
2	1%	-1%	-1%	8%	8%	5%	37%	3%
3	0%	0%	0%	0%	0%	0%	0%	0%
4	10%	-9%	-9%	44%	4%	13%	51%	2%
5	1%	5%	1720%	14%	2%	8%	37%	3%
6	0%	-26%	-78%	-71%	42%	5%	11%	1%
7	0%	-26%	-78%	-71%	42%	5%	11%	1%
8	9%	-8%	-8%	1%	11%	18%	58%	6%
9	-4%	-14%	-50%	-36%	51%	30%	34%	8%
10	8%	-7%	-7%	-7%	-4%	2%	15%	1%
11	1%	-1%	-1%	10%	26%	32%	36%	8%
12	10%	-9%	-9%	-1%	8%	18%	53%	4%
13	8%	-7%	-7%	-7%	-4%	2%	15%	1%
14	2%	-16%	-44%	-33%	9%	-10%	335%	4%
15	2%	-2%	-2%	5%	1%	0%	34%	1%
16	0%	0%	0%	0%	0%	0%	0%	0%
17	0%	0%	0%	1%	-1%	-1%	2%	-18%
18	10%	-9%	-9%	-3%	-1%	7%	49%	2%
19	10%	-9%	-9%	-3%	-1%	7%	49%	2%

Table 47: Sensitivity analysis of client preferences in case study 2A

Set	Efficiency	CO2	SOx	NOx	Volume	Mass	Signatures	Robustness
1	0%	0%	0%	0%	0%	0%	0%	0%
2	-7%	inf	inf	inf	-7%	-7%	40%	0%
3	-4%	inf	inf	inf	-6%	-5%	103%	4%
4	2%	0%	0%	0%	3%	3%	31%	1%
5	-8%	inf	inf	inf	-29%	-35%	1%	3%
6	-2%	0%	0%	0%	-5%	-6%	2%	0%
7	0%	0%	0%	0%	0%	0%	0%	0%
8	4%	0%	0%	0%	17%	18%	-36%	12%
9	0%	0%	0%	0%	3%	3%	0%	3%
10	0%	0%	0%	0%	-1%	-1%	100%	1%
11	0%	0%	0%	0%	3%	4%	0%	3%
12	0%	0%	0%	0%	-1%	-1%	100%	1%
13	-3%	0%	0%	0%	-7%	-7%	106%	1%
14	-6%	0%	0%	0%	-9%	-10%	323%	1%
15	-1%	inf	inf	inf	-1%	-1%	0%	4%
16	0%	0%	0%	0%	2%	2%	0%	1%
17	-7%	0%	0%	0%	-8%	-7%	-39%	-39%
18	-3%	inf	inf	inf	-2%	-1%	2%	10%
19	-2%	0%	0%	0%	-2%	-1%	2%	16%

Table 48: Sensitivity analysis of client preferences in case study 2B

Set	Efficiency	CO2	SOx	NOx	Volume	Mass	Signatures	Robustness
1	0%	0%	0%	0%	0%	0%	0%	0%
2	0%	0%	0%	0%	0%	0%	0%	0%
3	0%	0%	0%	0%	0%	0%	0%	0%
4	0%	0%	0%	0%	0%	0%	0%	0%
5	1%	42%	8434%	236%	-27%	12%	-51%	-6%
6	0%	0%	0%	0%	0%	0%	0%	0%
7	0%	0%	0%	0%	0%	0%	0%	0%
8	-3%	6%	41%	23%	2%	6%	-51%	0%
9	0%	0%	0%	0%	0%	0%	0%	0%
10	0%	0%	0%	0%	0%	0%	0%	0%
11	0%	0%	0%	0%	0%	0%	0%	0%
12	0%	0%	0%	0%	0%	0%	0%	0%
13	0%	0%	0%	0%	0%	0%	0%	0%
14	0%	0%	0%	0%	0%	0%	0%	0%
15	-2%	3%	9%	7%	1%	1%	-26%	-4%
16	-4%	5%	18%	-7%	1%	2%	-51%	-18%
17	-3%	5%	18%	-7%	-2%	-2%	-52%	-20%
18	-5%	9%	51%	3%	-3%	-1%	-52%	0%
19	0%	0%	0%	1%	4%	4%	1%	1%

Table 49: Sensitivity analysis of client preferences in case study 3A

Set	Efficiency	CO2	SOx	NOx	Volume	Mass	Signatures	Robustness
1	0%	0%	0%	0%	0%	0%	0%	0%
2	-12%	28%	inf	inf	-16%	-16%	-31%	-5%
3	5%	-5%	0%	0%	4%	6%	-29%	-2%
4	12%	-11%	0%	0%	12%	15%	-47%	0%
5	-20%	111%	inf	inf	-36%	-1%	0%	11%
6	0%	0%	0%	0%	0%	0%	0%	0%
7	10%	-100%	0%	0%	49%	69%	-3%	1%
8	6%	-100%	0%	0%	188%	-31%	-100%	5%
9	6%	-100%	0%	0%	186%	-34%	-100%	3%
10	9%	-9%	0%	0%	8%	11%	-31%	3%
11	19%	-100%	0%	0%	52%	74%	-46%	0%
12	9%	-9%	0%	0%	8%	11%	-31%	3%
13	0%	0%	0%	0%	0%	0%	0%	0%
14	-12%	28%	inf	inf	-16%	-16%	251%	5%
15	9%	-9%	0%	0%	8%	11%	-31%	3%
16	9%	-8%	0%	0%	9%	12%	-45%	0%
17	-3%	3%	0%	0%	-1%	-2%	-61%	-26%
18	9%	-9%	0%	0%	8%	11%	-31%	3%
19	9%	-9%	0%	0%	10%	15%	-31%	9%

Table 50: Sensitivity analysis of client preferences in case study 3B

Set	Efficiency	CO2	SOx	NOx	Volume	Mass	Signatures	Robustness
1	0%	0%	0%	0%	0%	0%	0%	0%
2	0%	0%	0%	0%	0%	0%	0%	0%
3	0%	0%	0%	0%	0%	0%	0%	0%
4	8%	34%	1416%	372%	-26%	17%	6%	3%
5	0%	55%	30195%	423%	-38%	-5%	-9%	0%
6	0%	45%	1541%	396%	-35%	-8%	-9%	0%
7	0%	0%	0%	0%	0%	0%	0%	0%
8	0%	0%	0%	2%	5%	6%	2%	3%
9	0%	0%	0%	2%	5%	6%	2%	3%
10	0%	0%	0%	0%	0%	0%	0%	0%
11	0%	0%	0%	2%	5%	6%	2%	3%
12	0%	0%	0%	0%	0%	0%	0%	0%
13	0%	0%	0%	0%	0%	0%	0%	0%
14	-1%	20%	652%	187%	-23%	-14%	136%	-1%
15	0%	0%	0%	0%	0%	0%	0%	0%
16	0%	0%	0%	0%	0%	0%	0%	0%
17	-1%	1%	10%	5%	0%	0%	-10%	-18%
18	0%	0%	0%	2%	5%	6%	2%	3%
19	-1%	46%	1559%	402%	-32%	-4%	-13%	3%